12-2023

Biochemical and Kinetic Analysis of Phosphofructokinase in the Eukaryotic Human Pathogen Entamoeba histolytica

Jin Cho
jinc@g.clemson.edu

BIOCHEMICAL AND KINETIC ANALYSIS OF PHOSPHOFRUCTOKINASE IN THE EUKARYOTIC HUMAN PATHOGEN *ENTAMOEBA HISTOLYTICA*

A Dissertation
Presented to
the Graduate School of
Clemson University

In Partial Fulfillment
of the Requirements for the Degree
Doctor of Philosophy
Biochemistry and Molecular Biology

---

by
Jin Cho
December 2023

Accepted by:
Cheryl Ingram-Smith, Committee Chair
Lukasz Kozubowski
Kerry Smith
Lesly Temesvari

ABSTRACT

Entamoeba histolytica is a water- and food-borne intestinal parasite that causes amoebiasis and liver abscess in ~100 million people each year leading to ~100,000 deaths. This amitochondriate parasite lacks many metabolic pathways including the tricarboxylic acid cycle and oxidative phosphorylation, and cannot synthesize purines, pyrimidines, or most amino acids. As a result, *E. histolytica* is presumed to rely on its modified pyrophosphate (PP_i)-dependent glycolytic pathway for ATP production during growth on glucose. This pathway relies on a PP_i-dependent rather than ATP-dependent phosphofructokinase (PFK) and thus has a net production of three ATP per glucose. However, in addition to the one PP_i-dependent PFK, the *E. histolytica* genome encodes three putative ATP-dependent PFKs, (designated as EhPFK1, EhPFK2, and EhPFK3). I have recombinantly produced and purified EhPFK2 and EhPFK3 to analyze their enzymatic activities and regulation. Both enzymes displayed cooperative kinetics instead of Michaelis-Menten kinetics with respect to the two substrates fructose 6-phosphate (F6P) and ATP. Kinetic analysis showed that EhPFK2 is the more efficient enzyme compared to EhPFK3. Various ligands such as AMP that have been shown to regulate PFKs in other organisms have been tested to analyze their effects on *E. histolytica* PFK activities. Specifically, I identified phosphoenolpyruvate (PEP), PP_i, and citrate as inhibitors, with PEP being the most potent, and CoA is a potent activator, differentiating EhPFK2 and EhPFK3 from the canonical PFK. I have shown experimentally and through structural model predictions that PEP, PP_i, and citrate each bind at different allosteric sites. In addition, these inhibitors had different effects with respect to F6P and ATP

substrate binding. The gene encoding PP_i-dependent PFK is highly expressed during standard trophozoite growth in *E. histolytica* as well as in the reptile pathogen *Entamoeba invadens*. RNAseq studies in *E. invadens* indicate that one of its two genes encoding putative ATP-dependent PFK is strongly upregulated during excystation. The differences in enzymatic activity and regulation suggest that the four PFKs play different metabolic roles.

DEDICATION

I would like to dedicate this to my family: My dad, mom, and my two brothers, Jin Soo and Sam. Without you guys, I would not have been able to come this far. Thank you guys so much for all the love and support!

ACKNOWLEDGEMENTS

First, I would like to thank my advisor Dr. Cheryl Ingram-Smith. You are an amazing advisor, teacher, friend, and lab mom. Through your guidance and help, I was able to grow as a scientist. But more importantly, I was able to grow as a person through the way you treated people with respect and kindness. I was so lucky to have been able to join your lab in Clemson and even if I were to go back in time, I would not change my mind. Thank you so much for everything you have done for me!

I would also like to thank my committee members. Dr. Kerry Smith, thank you so much for being a great lab father and all the knowledge and expertise you shared with me during lab meetings on metabolism. Dr. Lukasz Kozubowski, thank you so much for your insightful questions, advice on future careers, and for including me in group gatherings. Dr. Lesly Temesvari, thank you so much for helping me build a strong foundation in *E. histolytica* through your knowledge and expertise and showing me cool stuff under the microscope!

I would also like to thank Dr. Kimberly Metris for being my teaching mentor during my teaching assistantship. Working under your guidance and help made me realize just how much I like teaching and where my passion lies.

I would like to thank everyone in Ingram-Smith and Smith lab: Dr. Irem Bastuzel for being my first friend in Clemson since I came in 2017 and continuing to be my Best Friend Forever; Dr. Matthew Angel, Dr. Oly Ahmed, and Rodrigo Catalan-Hurtado for being my brothers; Dr. Jordan Wesel for teaching me about *Entamoeba histolytica* culture when I first joined the lab; Dr. Perry Kezh for being an awesome roommate over

summer; Arohi Singhal for always listening to my concerns and introducing me to spicy food; Will Betsill for all the fun newspaper talks and helping me with tech stuff; Claudia Gonzalez and Jack Talledo for the valuable friendship despite short time we got to know each other, I really wish that I could stay longer to spend more time with you guys; I would also like to thank Stephani Martinez and Kristina Parman for being awesome friends the whole time I have been at Clemson. My experience in Clemson would have been very different if I did not get to know such great friends.

Finally, I would like to thank all the faculty and staff members of Genetics and Biochemistry. Especially Rick Moseley for always being such an awesome person and helping me out with literally everything.

TABLE OF CONTENTS

Page

LIST OF TABLES

LIST OF FIGURES

CHAPTER I

LITERATURE REVIEW

Introduction

Entamoeba histolytica is an intestinal parasite that is water and food borne. It can cause amebiasis and liver abscess and is prevalent in regions with poor sanitation, including large areas within Africa and Asia (Figure 1.1) (Stanley, 2003). In 2010, the World Health Organization reported ~1.85 billion cases of diarrheal illness per year worldwide in which ~ 820 million cases were from bacteria (44%), ~647 million were from viruses (35%), and ~342 million were from parasites (19%) (World Health Organization, 2015). From the parasitic cases, ~100 million cases were due to *E. histolytica* infection (World Health Organization, 2015). Infection by *E. histolytica* may approach as many as 1 billion people per year though as only 10% of cases are symptomatic (Baxt and Singh, 2008). Common symptoms of amebiasis include bloody diarrhea, abdominal pain, and vomiting (Stanley, 2003). Treatments are available, such as paromomycin for non-symptomatic infections and metronidazole for symptomatic infections. However, there are some side effects associated with these drugs, such as nausea, loss of appetite, and headaches (Carrero et al., 2020). Due to many side effects as well as poor efficacy, new drugs need to be developed.

The purpose of this review is to provide an overview of *E. histolytica*'s life cycle and metabolism, with a focus on the glycolytic pathway as this modified pathway is

thought to be the main player for energy generation. Gaining deeper insight into *E. histolytica's* metabolism is essential for identifying new targets for drug discovery.

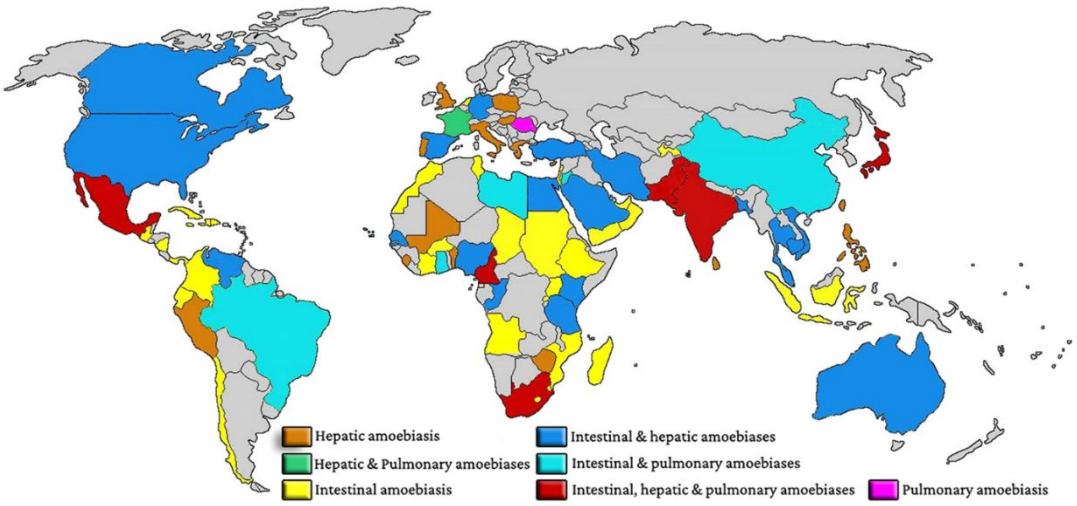

Figure 1.1. Global distribution of diverse clinical forms of amebiasis. Figure obtained from Nasrallah et al., 2022. https://doi.org/10.1016/j.jiph.2022.08.013. Permission granted through Elsevier and Creative Commons CC-BY-NC-ND license. https://creativecommons.org/licenses/by-nc-nd/4.0/.

Entamoeba histolytica **Genome**

In 2005, *E. histolytica* strain HM-1: IMSS was sequenced via the whole-genome shotgun method to generate the first *E. histolytica* genome (Loftus et al., 2005). The genome size was about 24 million base pairs with 9,938 predicted protein coding genes, which made up 49% of the genome. The annotated genome revealed that one-quarter of these genes were predicted to contain introns, in which 6% of the genes contained multiple introns. The number of chromosomes could not be determined due to length variability between different isolates as well as uncertainty in ploidy (Loftus et al., 2005).

The *E. histolytica* genome published in 2005 was error prone due to a solely automated approach to genome analysis. To gain more accurate genome information, the *E. histolytica* genome was reassembled and reannotated in 2010 using both automated and manual methods (Lorenzi et al., 2010). By incorporating the manual method, the new genome assembly reduced the overestimation of genes present in the published genome caused by tandem duplications and genes present within repetitive regions. As a result, the size of the newly assembled genome was reduced to ~20 million base pairs and 8,201 predicted protein coding genes. Several predicted genes from the old genome assembly that were annotated as hypothetical protein coding genes did not map to the new genome assembly. In addition, 36% of the genes that mapped to the new genome assembly had structural changes compared to the old genome assembly (Lorenzi et al., 2010).

Virulence, Infection, and Diagnosis

Life Cycle of *Entamoeba histolytica*

E. histolytica has two stages in its life cycle, the dormant cyst and motile trophozoite forms (Figure 1.2). Tetra-nucleate cysts are protected by a chitin wall, which allows them to survive in the environment from stresses such as osmotic shock and stomach acid (Samuelson and Robbins, 2011). Cysts are round and range in size from 10-16 μm in diameter, while trophozoites are pleomorphic in shape and range from 20-40 μm (Figure 1.3) (Lohia, 2003; Stanley, 2003). Transmission occurs via an oral-fecal route which begins when *E. histolytica* cysts are shed from the host into the environment (Wesel et al., 2021). Once the infectious cysts are ingested through contaminated water or food, they undergo excystation to the disease-causing motile trophozoite form in the small intestine. They then travel to the large intestine and colonize (Wesel et al., 2021). In the large intestine, trophozoites feed on bacteria and residual food from the host, divide via binary fission, and undergo encystation (Stanley, 2003). The cycle continues as both cysts and trophozoites are shed into the environment through the stool (Huston et al., 1999). However, trophozoites cannot survive outside of the host in the environment as they lack the chitin wall that provides protection against various stresses (Stanley, 2003).

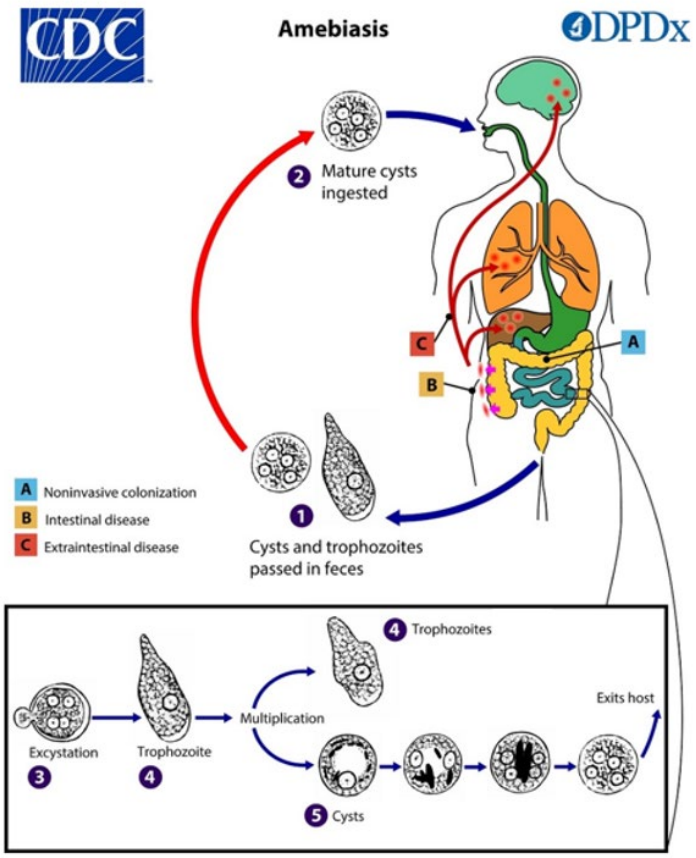

Figure 1.2. Life cycle of *E. histolytica*. 1) *E. histolytica* cysts and trophozoites are released into the environment through stool. **2)** Mature cysts are ingested via contaminated water or food. **3)** Cysts undergo excystation to trophozoites in the small intestine. **4)** Motile trophozoites colonize the large intestine **5)** Some trophozoites undergo encystation and both cysts and trophozoites are shed into the environment to continue the infection cycle. Figure obtained and modified from the CDC website ("CDC - DPDx - Amebiasis," 2019).

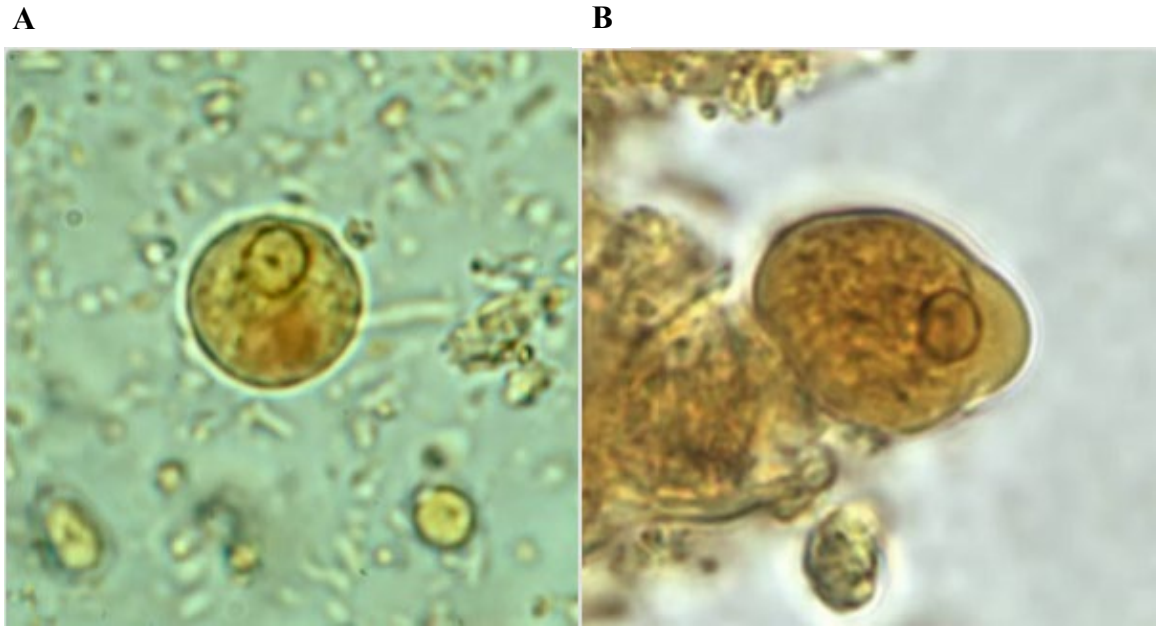

Figure 1.3. Morphology of *E. histolytica* cyst and trophozoite. **A)** *E. histolytica* cyst stained with iodine. **B)** *E. histolytica* trophozoites stained with iodine. Figure obtained from the CDC website ("CDC - DPDx - Amebiasis," 2019).

Other common protozoan parasites that cause diarrheal diseases are *Giardia lamblia* and *Cryptosporidium parvum* (Hemphill et al., 2019). A study on prevalence of intestinal parasites in 293 young children in Ecuador showed that 57.1% of the children had *E. histolytica*, 21.1% had *G. lamblia*, and 8.9% had *C. parvum* (Jacobsen et al., 2007). *G. lamblia* and *C. parvum* also infect the human intestinal tract and cause giardiasis and cryptosporidiosis, respectively (Haque, 2007). For *G. lamblia*, infection occurs upon ingestion of cysts, which undergo excystation to trophozoites that adhere to epithelial cells (Hemphill et al., 2019). For *C. parvum*, infection occurs upon ingestion of oocysts that contain sporozoites, which will then enter intestinal epithelial cells. Once

sporozoites enter epithelial cells, they can develop into either Type I or Type II merozoites to undergo asexual proliferation and sexual development (Hemphill et al., 2019). Although transmission of *G. lamblia* and *C. parvum* occurs via an oral-fecal route just like *E. histolytica*, they colonize the ileum, duodenum, and jejunum of the small intestine instead of colon (Hemphill et al., 2019; Kucik et al., 2004).

Virulence Factors

Lectins on the surface of *E. histolytica* trophozoites allow the parasite to adhere to the mucin layer as they have high affinity for galactose (Gal) and N-acetyl-D-galactosamine oligosaccharides (GalNAc) on host mucin proteins (Marie and Petri, 2014). Gal/GalNAc lectin is a heterodimer that is composed of transmembrane heavy subunit (Hgl) and glycosylphosphatidylinositol-anchored light subunit (Lgl) (Verma and Datta, 2017). Hgl provides specificity for Gal and GalNAc as it has a carbohydrate recognition domain and inhibition of this subunit prevents adherence (Petri et al., 2002; Verma and Datta, 2017). In the case of *E. histolytica*, Gal/GalNAc lectin binds to Mucin-2 protein (MUC2) (Cornick et al., 2017). It was shown that MUC2 acts as a barrier against *E. histolytica* infection as MUC2-deficient mice showed greater secretory and pro-inflammatory responses (Kissoon-Singh et al., 2013). If mucins are absent, lectins will bind to Gal and GalNAc on the surface of epithelial cells instead (Marie and Petri, 2014).

Cysteine proteinases, which are nucleophilic proteolytic enzymes containing cysteine residues in the enzymatic domain, have also been shown to be involved in *E.*

histolytica invasion as lysates of *E. histolytica* produced and released 10- to 1,000-fold more proteinases compared to noninvasive *E. dispar*(Que and Reed, 2000; Yang et al., 2023). They play an important role in the parasite's invasion by cleaving collagen, fibrinogen, laminin, and elastin, which are major components of extracellular matrix (Keene et al., 1986). They also degrade immunoglobulin A (IgA) as well as C3a and C5a anaphylatoxins to bypass host immune system (Reed et al., 1995). In addition, cysteine proteinases disrupt MUC2's barrier function by cleaving the C-terminal domain of the mucin (Lidell et al., 2006). Fifty genes which could encode for cysteine proteinases have been identified in *E. histolytica* and EhCP1, EhCP2, and EhCP5 make up 90% of total proteinase activity in the axenic trophozoite culture (He et al., 2010). Silencing of EhCP5 prevented invasion of epithelium by the parasite even though mucin proteins were degraded (Serrano-Luna et al., 2013).

Symptoms, Diagnosis, and Treatments

Individuals infected by *E. histolytica* can be asymptomatic carriers as trophozoites are confined to intestinal lumen ("CDC - DPDx - Amebiasis," 2019). However, trophozoites can sometimes invade the mucosa, the inner-most layer of the gastrointestinal tract that surrounds the lumen, to cause amebiasis (Carrero et al., 2020). Common symptoms of amebiasis include abdominal pain, weight loss, and bloody diarrhea (Chou and Austin, 2023). Trophozoites can also enter the bloodstream and infect brain, lungs, and liver to cause amoebic liver abscess (ALA), which is fatal if left untreated (Carrero et al., 2020). Some common symptoms of ALA are fever and

abdominal pain (Chou and Austin, 2023). Patients with ALA also show leukocytosis (elevated white blood cell count) and high levels of alkaline phosphatase (Tanyuksel and Petri, 2003). Interestingly, patients with ALA often do not show any symptoms for amebiasis and show no sign of cysts and trophozoites in the stool (Stanley, 2003). Both amoebic brain abscess and pleuropulmonary amebiasis can occur along with ALA. Symptoms of amoebic brain abscess include headache, vomiting, and seizures, while patients with pleuropulmonary amebiasis show chest pain, cough, and respiratory distress. Since patients can develop pleuropulmonary amebiasis along with ALA, abscesses can sometimes rupture into the pericardium to cause cardiac tamponade (fatal drop in blood pressure) or pericarditis (shortness of breath and increase in heart beat) (Stanley, 2003).

There are several methods of diagnosis for *E. histolytica* infection, one of which is examination of stool samples through a microscope (Tanyuksel and Petri, 2003). However, this method poses challenges due to poor sensitivity and the difficulty in morphologically distinguishing *E. histolytica* from other nonpathogenic *Entamoeba* species, such as *E. dispar and E. moshkovskii* (Tanyuksel and Petri, 2003). It is possible to distinguish *E. histolytica* from *E. moshkovskii* through culture methods due to *E. moshkovskii* having different growth characteristics, but there are still limitations, such as contamination in the samples with other species of *Entamoeba*, *Iodamoeba*, and *Endolimax* ("CDC - DPDx - Amebiasis," 2019; Hamzah et al., 2006).

Immunodiagnostic methods, such as enzyme-linked immunosorbent assay (ELISA), can be used to distinguish *E. histolytica* from *E. dispar*, however these methods

are not readily available in developing countries where infection is endemic (Stanley, 2003). Antibody detection through blood test is useful for patients with ALA as cysts and trophozoites are not generally found in the stool sample ("CDC - DPDx - Amebiasis," 2019). However, this assay is not useful for patients from high endemic areas as they most likely have already been exposed to the parasite (Tanyuksel and Petri, 2003). Antigen detection methods and molecular methods such as PCR provide highest sensitivity and specificity, with the latter showing 92%-100% sensitivity and 89%-100% specificity (Chou and Austin, 2023).

Infected individuals are typically treated with nitroimidazole derivative drugs, such as metronidazole and tinidazole, as they are highly effective against invading trophozoites (Shirley et al., 2018; Stanley, 2003). Metronidazole is typically used as it is more effective at clearing trophozoites, despite tinidazole having longer half-life and being better tolerated (Gonzales et al., 2019). High dose of metronidazole is required to reach the lumen of the colon as drug is generally absorbed in the small intestine and it is prone to degradation by the acidic pH of the stomach and various degradative enzymes (Oliveira et al., 2022; Pritt and Clark, 2008). However, there are side effects associated with metronidazole, such as nausea, headache, vomiting, and dry mouth (Petri, 2003). In addition, use of high concentration of metronidazole can produce off target effects, where high concentration of drugs are also found in the liver, kidney, and bladder (Dingsdag and Hunter, 2018). In mice and rats, administration of metronidazole for long period of time has found to be carcinogenic ("Metronidazole," 2012). There has not been a report of clinical resistance to metronidazole yet, however successful induction of

metronidazole resistance in an axenic strain of *E. histolytica* has been shown (Samarawickrema, 1997). Demonstration of different drug sensitivity among *E. histolytica* strains as well as reports of metronidazole treatment failure indicate the possibility that *E. histolytica* might develop resistance to anti-amoebic drugs in the future (Bansal et al., 2004; Burchard and Mirelman, 1988). Nitroimidazole drugs are not effective against cysts, so luminal drugs such as paromomycin and diloxanide furoate must be used as well (Stanley, 2003). These luminal agents can also cause side effects such as diarrhea and nausea, so they should be administered to patients after they have gone through the nitroimidazole treatment (Shirley et al., 2018).

Currently, there are no vaccines for amebiasis, although there are several potential targets for vaccine development. The first target is Gal lectin, which allows the parasite to adhere to the mucin layer (Quach et al., 2014). Gal lectin became the primary focus of vaccine development when a study involving Bangladeshi children revealed that presence of IgA Gal lectin specific antibodies correlated with 64% lower reinfection rates (Haque et al., 2001). Both native and recombinant Gal lectin vaccines showed protection against amebic colitis (AC) and ALA in the gerbil model (Petri and Ravdin, 1991; Quach et al., 2014). Other vaccine targets include serine-rich *E. histolytica* protein (SREHP) and 29-kDa antigen (Eh29), which play a role in adhesion and detoxification of reactive oxygen species secreted by the microflora or immune cells, respectively (Quach et al., 2014). Vaccines targeting these two proteins using several animal models, such as gerbil, mice, hamster, and guinea pig, demonstrated high protection against AC and ALA as well (Quach et al., 2014). Despite seeing success of vaccines using various animal models,

these animal models do not mimic the entire life cycle of *E. histolytica* (Tsutsumi and Shibayama, 2006). As such, clinical trials will need to be carried out to test efficacy in humans.

Energy Metabolism

E. histolytica has unique aspects to its metabolism that differ from that of a typical eukaryotic organism. It is an amitochondriate protozoan parasite that lacks a functional citric acid cycle and oxidative phosphorylation (Clark et al., 2007). In addition, it is unable to synthesize purines, pyrimidines, and amino acids other than cysteine and serine (Loftus et al., 2005). Therefore, it has been presumed to rely on glycolysis as its major way of generating energy. However, *E. histolytica* encounters many different environments, such as nutrient deprivation, during invasion (Tovy et al., 2011). As a result, *E. histolytica* must obtain nutrients through the host or by other means to survive.

E. histolytica is able to acquire nutrients, such as amino acids, carbohydrates, and lipids, through constitutive endocytosis (Marie and Petri, 2014; Meza and Clarke, 2004). It can take in fluids and small molecules through pinocytosis and when larger particles are present, it can phagocytose bacteria and other unicellular organisms (Meza and Clarke, 2004; Somlata and Bhattacharya, 2015). Phagocytosis has been shown to play an important role in pathogenesis as a phagocytosis-defective mutant cell line showed decreased virulence and growth defects (Somlata and Bhattacharya, 2015). The human gut microbiome is made up of numerous microbial species and the composition can vary from one person to another, and it has been shown that composition of the microbiota can affect pathogen behavior and virulence (Marie and Petri, 2014). Guinea pigs who were administered different species of bacteria four hours after amebic inoculation showed different percentages of amebic lesion development in the cecum as well as differences in mortality rate. Inoculation with *Clostridium perfringens* and *Lactobacillus acidophilus*

resulted in the highest percentage of guinea pigs that developed amebic lesions at 67%, while inoculation with *Escherichia coli* resulted in only 26% with lesions (Phillips and Gorstein, 1966). Another study showed that *Lactobacillus ruminis* was the most preferred bacterial species to be phagocytosed by *E. histolytica* (Iyer et al., 2019). Interestingly, a study involving patients from Cote d'Ivoire showed that intestinal parasites, such as *E. histolytica* and *Blastocystis hominis*, can induce alteration in the gut microbiota (Burgess et al., 2017). These results demonstrate the importance of interactions between *E. histolytica* and bacteria.

Amino acid catabolism has been suggested as a means for *E. histolytica* to generate energy as it was shown that the parasite consumed several amino acids, such as asparagine and aspartate, both in the presence and absence of glucose (Coombs, 1991). In addition, phylogenetic analysis of *E. histolytica* genes related to amino acid catabolism suggests they have been acquired through lateral gene transfer (LGT) from bacteria (Loftus et al., 2005). The ability of other protists, such as *G. lamblia*, to degrade amino acids to use as a fuel also reinforces the idea that amino acid catabolism may be an important energy pathway in *E. histolytica* (Knodler et al., 1995). The presence of genes encoding fructokinase and galactokinase suggests that *E. histolytica* may be able to utilize other sugars such as fructose and galactose (Loftus et al., 2005).

Glycogen metabolism is another way in which *E. histolytica* is able to adapt to low glucose environment, such as large intestine (Wesel and Ingram-Smith, 2023). Glycogen granules have been detected in trophozoites through electron microscopy and glycogen is thought to play a role in chitin synthesis (Rosenbaum and Wittner, 1970;

Samanta and Ghosh, 2012). A recent study has shown that the cellular glycogen level was reduced when *E. histolytica* trophozoites were transferred from glucose-rich media to glucose-poor media. On the other hand, glycogen accumulation was observed going from glucose-poor media to glucose-rich media, suggesting that *E. histolytica* utilizes glycogen as a source of energy (Wesel and Ingram-Smith, 2023).

Glycolytic Pathway

Glycolysis is an important metabolic pathway that breaks down glucose to generate energy. Although the glycolytic pathway is present in *E. histolytica*, there are several differences compared to the typical eukaryotic glycolytic pathway (Figure 1.4). The conversion of fructose 6-phosphate to fructose 1,6-bisphosphate is catalyzed by inorganic pyrophosphate-dependent phosphofructokinase (PP_i-PFK), instead of ATP-dependent PFK (ATP-PFK) (Reeves et al., 1976). Since ATP is not consumed in this step, there is a net yield of three ATP molecules from glycolysis instead of the typical two. Another difference in this modified glycolysis is that the conversion of phosphoenolpyruvate to pyruvate is catalyzed by PP_i-dependent pyruvate phosphate dikinase (PPDK) instead of pyruvate kinase (PK) (Reeves, 1968; Saavedra et al., 2005). PP_i-dependent glycolytic pathway is also found in other bacteria, such as *Propionibacterium shermanii* (O'Brien et al., 1975) and *Pseudomonas marina* (Sawyer et al., 1977), and the anaerobic *G. lamblia* (Li and Phillips, 1995).

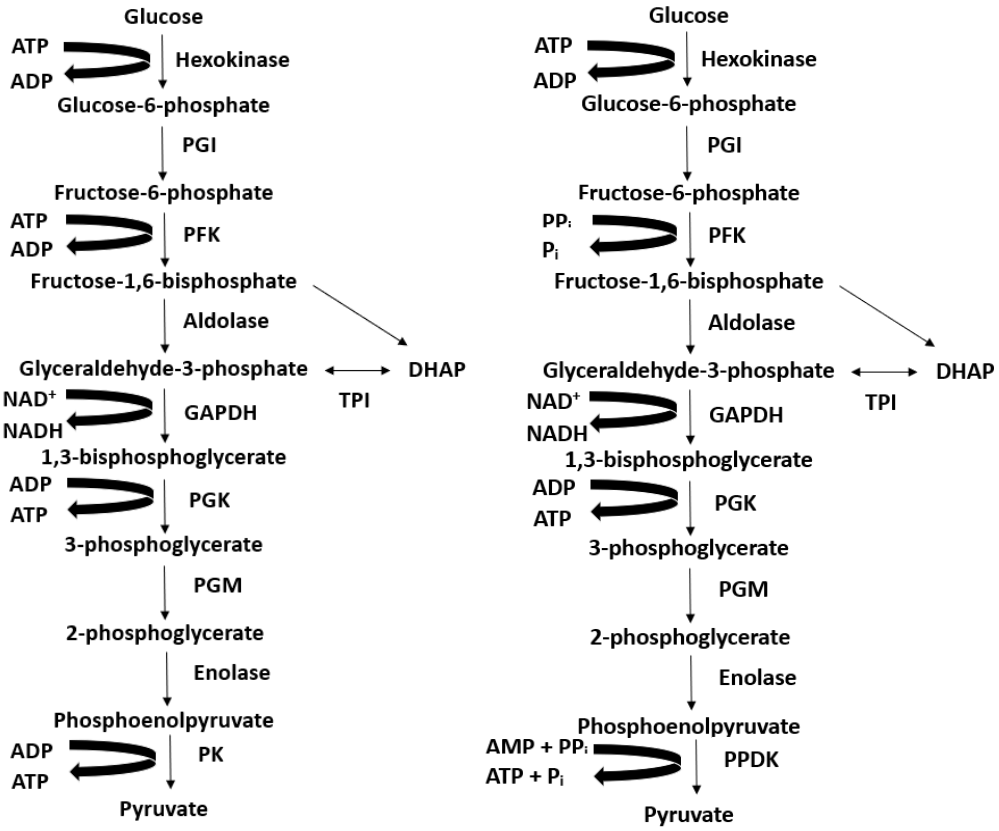

Figure 1.4. Glycolytic pathway comparison. The pathway on the left is the typical eukaryotic glycolytic pathway, while the pathway on the right is that of *E. histolytica*. Abbreviations: PGI (Phosphoglucose isomerase), PFK (Phosphofructokinase), GAPDH (Glyceraldehyde 3-phosphate dehydrogenase), PGK (Phosphoglycerate kinase), PGM (Phosphoglyceratemutase), PK (Pyruvate kinase), PP_i-PFK (PP_i-dependent Phosphofructokinase), PPDK (PP_i-dependent pyruvate phosphate dikinase).

In typical eukaryotes, pyruvate produced by glycolysis in the cytosol enters mitochondria and is converted to acetyl-CoA by pyruvate dehydrogenase complex (PDC). In contrast, PDC is replaced by pyruvate: ferredoxin oxidoreductase (PFOR) in

the extended glycolytic pathway of *E. histolytica* and the conversion of pyruvate to acetyl-CoA occurs in cytosol as mitochondria is absent (Lo and Reeves, 1978). Acetate and ethanol are the two major products from the extended pathway from acetyl-CoA (Figure 1.5) (Pineda et al., 2013). Acetate is generated from acetyl-CoA by ADP-forming acetyl-CoA synthetase (ACD), while ethanol is generated from the bifunctional aldehyde-alcohol dehydrogenase (ADHE) (Reeves et al., 1977). Under aerobic conditions, it has been shown that acetate is the major product. In contrast, ethanol is the major product under anaerobic conditions (Pineda et al., 2013).

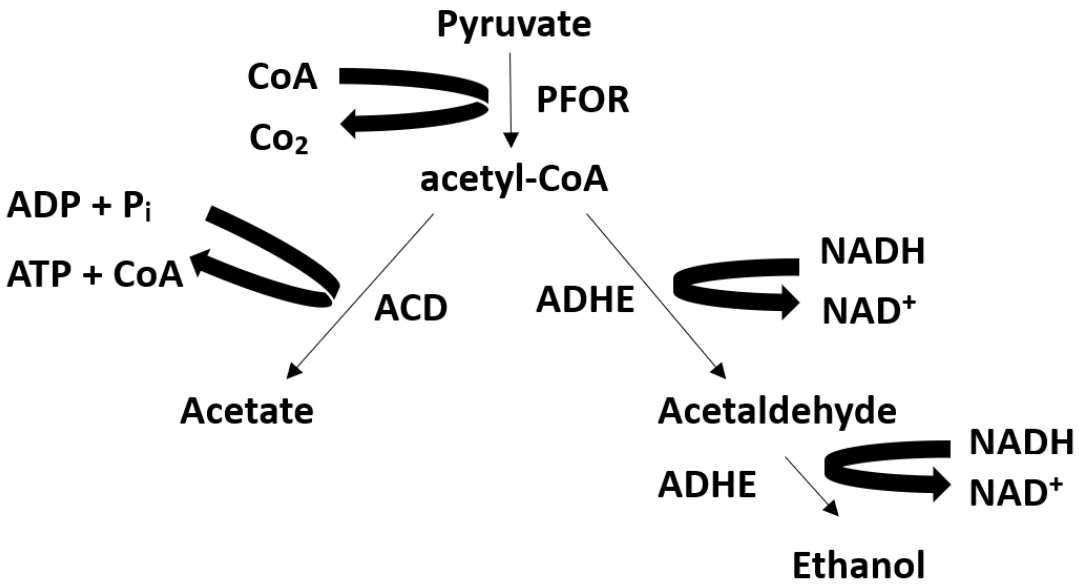

Figure 1.5. The extended glycolytic pathway of *E. histolytica*. Abbreviations: PFOR (Pyruvate: ferredoxin oxidoreductase), ACD (ADP-forming acetyl-CoA synthetase), ADHE (bifunctional alcohol/ aldehyde dehydrogenase)

Phosphofructokinase

PFK, the subject of this dissertation, is part of the phosphofructokinase B (PFKB) family of sugar kinases and catalyzes the phosphorylation of fructose 6-phosphate (F6P) to fructose 1,6-bisphosphate [Eq.1] (Park and Gupta, 2008; Wegener and Krause, 2002). Canonical PFK is highly regulated as conversion of F6P to fructose 1,6-bisphosphate is the first committed step of glycolysis. PFK is activated by AMP, ADP, and fructose 2,6-bisphosphate and is inhibited by citrate and ATP.

[Eq.1] PFK F6P + ATP ⇌ Fructose 1,6-bisphosphate + ADP $+H^+$

In *E. histolytica*, there are four putative *PFK* genes but only two have been characterized. EhPFK3 (EHI_103590) has been shown to be ATP-dependent, while EhPFK4 (EHI_000730) has been shown to be PP_i-dependent (Chi et al., 2001). EhPFK1 (EHI_187040) and EhPFK2 (EHI_163630) have not been characterized; however, both have high sequence identity with EhPFK3, suggesting they are ATP-dependent. A structure has not been determined for any EhPFK.

Previously, the 48 kDa EhPFK3 was reported as PP_i-dependent, however another group was unable to detect any PP_i-PFK activity with this enzyme (Bruchhaus et al., 1996; Chi et al., 2001). Chi *et al*. (Chi et al., 2001) found that recombinant EhPFK3 enzyme only bound to N-6-aminohexylcarboxymethyl-ATP-Sepharose and Blue Sepharose, which are commonly used to purify various ATP-dependent PFKs (Kotlarz and Buc, 1981). Since the recombinant protein failed to bind to phosphocellulose, which is commonly used to purify PP_i-PFKs, it was concluded that EhPFK3 uses ATP as the phosphoryl donor (Chi et al., 2001; Deng et al., 1998). Kinetic studies showed that

EhPFK3 requires a pre-incubation step with ATP as part of activation process. Without prior activation, Chi *et al*. (Chi et al., 2001) failed to detect any enzymatic activity in the assay. Size exclusion chromatography revealed that EhPFK3 exists as a dimer pre-activation and forms a tetramer after activation (Chi et al., 2001). EhPFK3 showed cooperative kinetics with respect to F6P and it could not phosphorylate other sugars, such as glucose or mannose. Interestingly, EhPFK3 could utilize other nucleoside triphosphates (NTPs) as phosphoryl donors. No regulators other than phosphoenolpyruvate (PEP) were found, which inhibited PFK3 activity (Chi et al., 2001).

The 60 kDa PP_i-dependent EhPFK4 is a dimer and is the only known PP_i-dependent PFK in *E. histolytica* (Chi et al., 2001). Unlike EhPFK3, EhPFK4 is unable to utilize NTPs as phosphoryl donors. The mRNA levels for EhPFK4 are 10-fold higher than for EhPFK3 in trophozoite extract (Chi et al., 2001). If *E. histolytica* is presumed to rely on modified PP_i-dependent glycolytic pathway to generate energy, then the source of PP_i must be considered. Anabolic processes involving synthesis of glycogen, protein, and nucleic acids may provide adequate PP_i for PFK (Reeves et al., 1976). Other possible sources could be from conversion of PEP to oxalacetate catalyzed by PEP carboxykinase (PEPCK) [Eq.2] or by PP_i-dependent acetate kinase (PP_i-ACK) [Eq. 3] (Reeves et al., 1976).

[Eq.2] PEPCK $PEP + P_i + CO_2 \rightleftharpoons oxaloacetate + PP_i$

[Eq.3] PP_i-ACK $Acetyl\ Phosphate + P_i \rightleftharpoons Acetate + PP_i$

EhPP_i-ACK has been characterized shown to favor acetate/ PP_i production (Fowler et al., 2012). However, a recent study has shown that ACK's primary role may

be in maintaining the balance of NAD^+/NADH during growth on glucose (Dang et al., 2022). Interestingly, a site-directed mutagenesis study showed that making one amino acid substitution in the catalytic site changes EhPFK4's preference from PP_i to ATP. When the study was repeated using *E. coli* ATP-dependent PFK, a switch in substrate preference was not observed, although activity with ATP was lost (Chi and Kemp, 2000).

ATP-Dependent PFKs in Prokaryotes

Several bacterial ATP-dependent PFKs have been studied previously and one of the most studied PFK is from *E. coli*. A structure of *E. coli* PFK has been resolved using molecular replacement of the solved structure of *Bacillus stearothermophilus* PFK. The resulting structure is a homotetramer that is complexed with fructose 1,6-bisphosphate and ADP, which are its reaction products (Shirakihara and Evans, 1988). Each subunit of the enzyme is made up of two domains and three layers, in which a central β-sheet layer is sandwiched between two α-helices (Shirakihara and Evans, 1988). Kinetic analysis showed that it displays cooperative kinetics with respect to the F6P substrate, as shown by the sigmoidal curve. In contrast, kinetics analysis with respect to ATP revealed a hyperbolic curve that is indicative of Michaelis-Menten kinetics (Blangy et al., 1968). Unlike EhPFK3, *E.coli* PFK was unable to utilize other NTPs as phosphoryl donors, which was shown by higher K_m values compared to ATP (Blangy et al., 1968). Residues important for NTP binding were identified and substitution of Arg at position 82 with either Ala or Glu led to decreased preference for ATP and increased preference for other NTPs (Wang and Kemp, 1999). *E. coli* PFK is activated by ADP and inhibited by PEP.

Both effectors bind at the same effector site and they both decreased the Hill coefficient by 3-fold, which showed that they also influenced the cooperativity of the enzyme in respect to F6P (Blangy et al., 1968; Shirakihara and Evans, 1988).

PFKs from several Gram-positive bacteria have been characterized. *B. stearothermophilus* is a thermophile that causes flat sour spoilage in food and is used as a thermostable DNA polymerase and as a biological indicator for sterilization (Huesca-Espitia et al., 2016; Ito, 1981; Kotzekidou, 2014). Two structures of *B. stearothermophilus* PFK in an inactive T-state complexed with PEP and in an active R-state complexed with F6P are available (Evans et al., 1997; Evans and Hudson, 1979). *B. stearothermophilus* PFK is a homotetramer and each subunit contains three binding sites. Two of these are binding sites for the F6P and ATP substrates and the third one is an allosteric effector binding site (Evans and Hudson, 1979). The kinetic characteristics of the *B. stearothermophilus* PFK are similar to those of *E. coli* PFK in that it also displays cooperative kinetics in respect to F6P but not to ATP, and is also regulated by ADP and PEP (Evans and Hudson, 1979).

Lactobacillus acidophilus is an anaerobic microbe that has been shown to promote probiotic effect. Mice supplemented with *L. acidophilus* showed increased levels of other probiotic bacteria and another study has shown that *L. acidophilus* inhibits growth of *Salmonella typhi*, which causes typhoid fever (Abdel-Daim et al., 2013; Vemuri et al., 2022). *Lactobacillus plantarum* has also been shown to have a probiotic effect as well play a role in maintaining intestinal permeability and antioxidant activity (Ahrne and Hagslatt, 2011; Li et al., 2012). PFK from both bacteria are homotetramers,

however they showed significant differences in their kinetic and biochemical properties (Simon and Hofer, 1977). *L. acidophilus* PFK displayed cooperative kinetics with respect to F6P, just like the PFKs from *E. coli* and *B. stearothermophilus*. However, the *L. planetarium* PFK displayed Michaelis-Menten kinetics (Simon and Hofer, 1977). The enzymes also showed differences in the regulation of enzymatic activity. Although both enzymes were activated by NH_4^+ ions, *L. acidophilus* PFK was activated by fructose 1,6-bisphosphate, while *L. plantarum* PFK was not. Fructose 1,6-bisphosphate decreased the Hill coefficient by 3-fold, which was also observed for *E. coli* PFK (Blangy et al., 1968; Simon and Hofer, 1977). Both enzymes were inhibited by ADP, although *L. plantarum* PFK required a higher concentration of ADP for inhibition (Simon and Hofer, 1977). That PFKs from two very closely related organisms with similar energy metabolism, fermentation of glucose to lactate, have such notable differences in their kinetic properties suggest that important evolutionary events may have shaped these changes (Simon and Hofer, 1977).

ATP-Dependent PFKs in Eukaryotes

Many eukaryotic ATP-dependent PFKs from eukaryotes have also been characterized, the most notable of which is the PFK from *Trypanosoma brucei*, the causative agent of African sleeping sickness that is fatal if left untreated (Stich et al., 2002). A structure of *T. brucei* PFK with ATP bound has been solved (Figure 1.6) (McNae et al., 2009). There is an embracing arm that is part of Domain A, which plays a role in linkage with other subunits. Residues involved in ATP binding are located in

Domain B and a large inserted loop is located in Domain C, which makes up part of the active site. Compared to structures of other known ATP-dependent PFKs, the large inserted loop as well as the C-terminal extension seems to be unique to *T. brucei* (McNae et al., 2009).

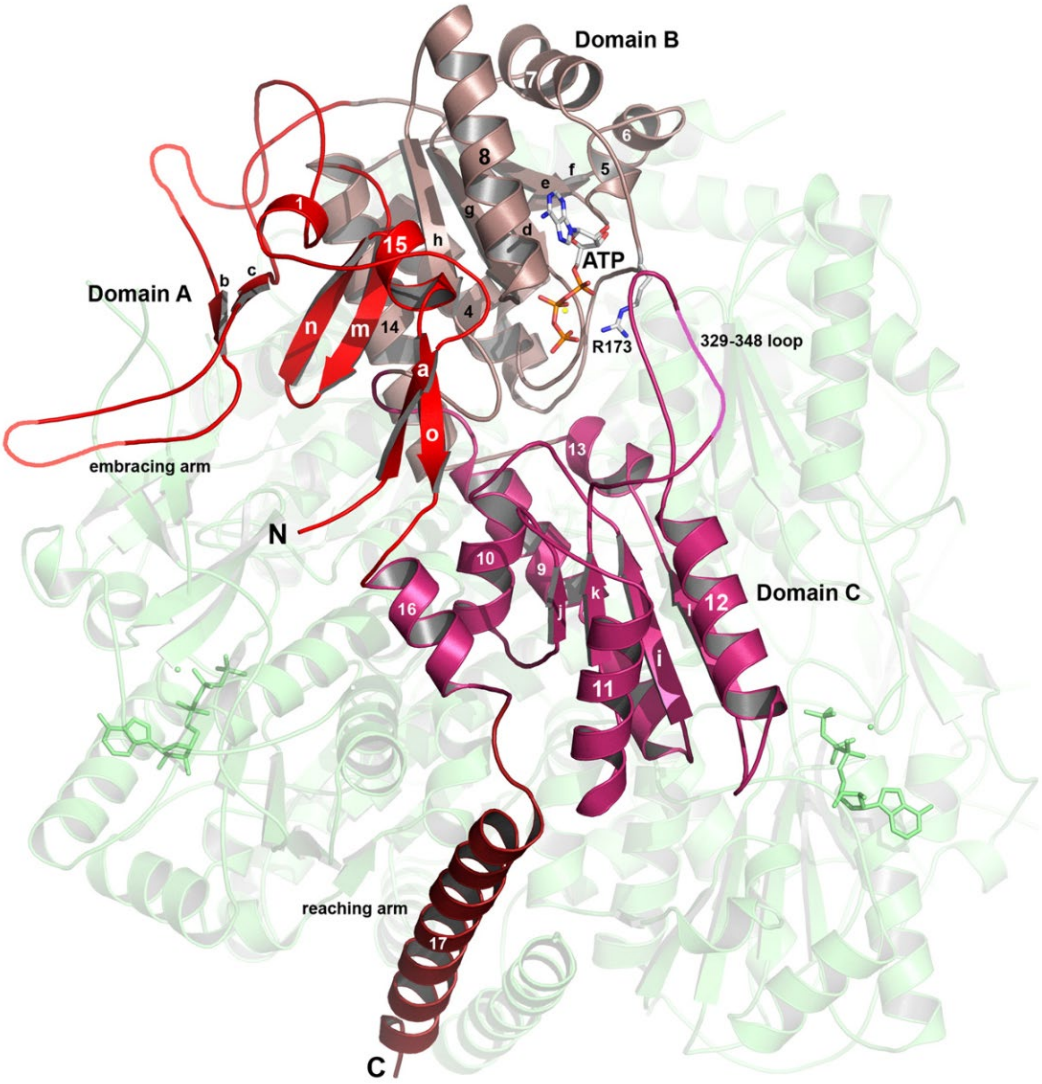

Figure 1.6. Structure of *T. brucei* PFK with Mg-ATP complex. Single subunit of the tetramer is shown in a cartoon representation. Different domains (Domain A, B, and C) are color coded differently. Figure obtained from McNae et al., 2009. DOI: 10.1016/j.jmb.2008.11.047. Permission granted from Elsevier and Copyright Clearance Center's RightsLink service.

Kinetic characterization showed that the enzyme displays cooperative kinetics with respect to both substrates, F6P and ATP (Fernandes et al., 2020). Interestingly, an earlier study showed that AMP and ADP are activators and PEP is an inhibitor of *T. brucei* PFK, while a more recent study identified AMP as the sole regulator (Cronin and Tipton, 1985; Fernandes et al., 2020). Although *T. brucei* PFK can utilize GTP as a phosphoryl donor, the physiological significance is probably low as total cellular concentration of GTP is much lower than ATP (Graven et al., 2014). That *T. brucei* PFK uses ATP instead of PP_i as a phosphoryl donor despite sequence comparison showing closer relationship to the PP_i-dependent family suggests an evolutionary change in phosphoryl donor specificity (McNae et al., 2009; Michels et al., 1997). Kinetic characterization of PFK from *Trypanosoma cruzi*, a parasite that causes Chagas disease, revealed several similarities and differences with *T. brucei* PFK. *T. cruzi* PFK is also a tetramer that can be activated by AMP and can utilize GTP as a phosphoryl donor. However, it only displayed cooperative kinetics in respect to F6P, unlike the *T. brucei* PFK for which cooperative kinetics was observed with both substrates (Fernandes et al., 2020, 2016).

Kinetic characterization of the PFK from *Setaria cervi*, a bovine filarial parasite, has also been performed. *S. cervi* PFK showed a Michaelis-Menten type hyperbolic curve in respect to both F6P and ATP; however, the curve shifted to a sigmoidal shape in respect to F6P at the inhibitory concentration of ATP (Sharma, 2011). Testing activity with different divalent cations showed that this enzyme displays highest activity with

Mg^{2+} and lower activity with Ca^{2+} and Mn^{2+} (Sharma, 2011). PEP inhibits the enzymatic activity, and no activators has been identified (Sharma, 2011).

PFK from the budding yeast *Saccharomyces cerevisiae* has an unusual structure of a hetero-octamer that is made up of four α-subunits and four β-subunits, unlike the homotetramer structures discussed previously for the other PFKs (Kricke et al., 1999). A kinetics study has shown that this PFK only displays cooperative kinetics in respect to F6P. It is activated by AMP, ADP, and fructose 2,6-bisphosphate, while inhibited by ATP and citrate (Kessler et al., 1982; McNae et al., 2009).

PP_i-Dependent PFKs

There are bacteria with PP_i-dependent PFK, such as the Gram-negative *Porphyromonas gingivalis*. *P. gingivalis* is associated with oral inflammatory infections as it is found in oral cavity (How et al., 2016). This enzyme displayed Michaelis-Menten kinetics with respect to both substrates and no effectors were reported (Arimoto et al., 2002). As this bacterium does not utilize sugars as an energy source, not much known is about its glucose metabolism or the role of PP_i-dependent PFK (Arimoto et al., 2002). One possible role for this enzyme is in gluconeogenesis by acting as a fructose 1,6-bisphosphatase, which has been proposed for PP_i-dependent PFK enzyme in another bacteria *Amycolatopsis methanolica* (Alves et al., 1994).

Plants have both ATP-dependent and PP_i-dependent PFKs and PP_i is thought to act as an alternate source for phosphorylation when ATP level is low (Mustroph et al., 2013). Other proposed roles of PP_i-dependent PFK are in maintaining equilibrium of

hexose and triose phosphates (Carlisle et al., 1990). The PP_i-dependent PFK from *Solanum tuberosum* (potato) is a heterotetrameric protein composed of two α- and two β-subunits (Carlisle et al., 1990). The α-subunits are thought to be involved in regulation by fructose 2,6-bisphosphate, while the β-subunits are thought to be involved in the active site (Cheng and Tao, 1990; Yan and Tao, 1984). Kinetic characterization showed that *S. tuberosum* PFK displays cooperative kinetics with respect to F6P, but Michaelis-Menten kinetics with respect to PP_i. Fructose 2,6-bisphosphate activated the enzyme and the sigmoidal curve with respect to F6P became hyperbolic in the presence of activators (Van Schaftingen et al., 1982).

G. lamblia is a flagellated protozoan parasite that causes diarrheal disease giardiasis (Hooshyar et al., 2019). *G. lamblia* PFK displayed Michaelis-Menten kinetics in respect to both substrates F6P and PP_i and HPLC gel filtration showed that this enzyme is a monomer (Li and Phillips, 1995). Known effectors of PFK activity identified in other organisms, such as fructose 2,6-bisphosphate and AMP, were found not to influence *G. lamblia* PFK activity. In addition, NTPS, including ATP, could not replace PP_i as a phosphoryl donor (Li and Phillips, 1995). PP_i-dependent PFK from *Naegleria fowleri*, commonly known as brain eating amoeba, has also been characterized biochemically (Mertens et al., 1993). Enzymatic characterization revealed a hyperbolic curve for both substrates and no other effectors were identified except AMP as a potent activator (Mertens et al., 1993). Size exclusion chromatography showed that this enzyme has an inactive monomer form as well as an active tetramer form. The role of PP_i-PFK in *N. fowleri* is uncertain as this amoeba mainly obtains nutrients through ingestion of

bacteria and it has been shown that there is little utilization of glucose (Mertens et al., 1993; Weik and John, 1977). What is known about the characterized PFKs is summarized in Table 1.1.

Characterized PFKs in Prokaryotes and Eukaryotes			
Organism	**Phosphoryl Donor**	**Activator**	**Inhibitor**
E. coli	ATP	ADP	PEP
B. stearothermophilus	ATP	ADP	PEP
L. acidophilus	ATP	ND	Fructose 1,6-bisphosphate
L. plantarum	ATP	ND	ND
T. brucei	ATP	AMP	ND
T. cruzi	ATP	AMP	ND
S. cervi	ATP	ND	PEP
S. cerevisiae	ATP	AMP, ADP, Fructose 2,6-bisphosphate	ATP, citrate
P. gingivalis	PP_i	ND	ND
S. tuberosum	PP_i	Fructose 2,6-bisphosphate	ND
G. lamblia	PP_i	ND	ND
N. fowleri	PP_i	ND	ND

Table 1.1. **Characterized PFKs from various organisms with phosphoryl donor and effectors shown.** ND = not detected.

References

Abdel-Daim, A., Hassouna, N., Hafez, M., Ashor, M.S.A., Aboulwafa, M.M., 2013. Antagonistic Activity of Lactobacillus Isolates against Salmonella typhi In Vitro. Biomed Res Int 2013, 680605. https://doi.org/10.1155/2013/680605

Ahrne, S., Hagslatt, M.-L.J., 2011. Effect of Lactobacilli on Paracellular Permeability in the Gut. Nutrients 3, 104–117. https://doi.org/10.3390/nu3010104

Alves, A.M., Euverink, G.J., Hektor, H.J., Hessels, G.I., van der Vlag, J., Vrijbloed, J.W., Hondmann, D., Visser, J., Dijkhuizen, L., 1994. Enzymes of glucose and methanol metabolism in the actinomycete Amycolatopsis methanolica. Journal of Bacteriology 176, 6827–6835. https://doi.org/10.1128/jb.176.22.6827-6835.1994

Arimoto, T., Ansai, T., Yu, W., Turner, A.J., Takehara, T., 2002. Kinetic analysis of PPi-dependent phosphofructokinase from Porphyromonas gingivalis. FEMS Microbiology Letters 207, 35–38. https://doi.org/10.1111/j.1574-6968.2002.tb11024.x

Bansal, D., Sehgal, R., Chawla, Y., Mahajan, R.C., Malla, N., 2004. In vitro activity of antiamoebic drugs against clinical isolates of Entamoeba histolytica and Entamoeba dispar. Ann Clin Microbiol Antimicrob 3, 27. https://doi.org/10.1186/1476-0711-3-27

Baxt, L.A., Singh, U., 2008. New insights into Entamoeba histolytica pathogenesis. Curr Opin Infect Dis 21, 489–494. https://doi.org/10.1097/QCO.0b013e32830ce75f

Blangy, D., Buc, H., Monod, J., 1968. Kinetics of the allosteric interactions of phosphofructokinase from Escherichia coli. Journal of Molecular Biology 31, 13–35. https://doi.org/10.1016/0022-2836(68)90051-X

Bruchhaus, I., Jacobs, T., Denart, M., Tannich, E., 1996. Pyrophosphate-dependent phosphofructokinase of Entamoeba histolytica: molecular cloning, recombinant expression and inhibition by pyrophosphate analogues. Biochem J 316, 57–63.

Burchard, G.D., Mirelman, D., 1988. Entamoeba histolytica: virulence potential and sensitivity to metronidazole and emetine of four isolates possessing nonpathogenic zymodemes. Exp Parasitol 66, 231–242. https://doi.org/10.1016/0014-4894(88)90095-1

Burgess, S.L., Gilchrist, C.A., Lynn, T.C., Petri, W.A., 2017. Parasitic Protozoa and Interactions with the Host Intestinal Microbiota. Infection and Immunity 85, 10.1128/iai.00101-17. https://doi.org/10.1128/iai.00101-17

Carlisle, S.M., Blakeley, S.D., Hemmingsen, S.M., Trevanion, S.J., Hiyoshi, T., Kruger, N.J., Dennis, D.T., 1990. Pyrophosphate-dependent phosphofructokinase. Conservation of protein sequence between the alpha- and beta-subunits and with the ATP-dependent phosphofructokinase. Journal of Biological Chemistry 265, 18366–18371. https://doi.org/10.1016/S0021-9258(17)44761-2

Carrero, J.C., Reyes-López, M., Serrano-Luna, J., Shibayama, M., Unzueta, J., León-Sicairos, N., de la Garza, M., 2020. Intestinal amoebiasis: 160 years of its first detection and still remains as a health problem in developing countries. International Journal of Medical Microbiology 310, 151358. https://doi.org/10.1016/j.ijmm.2019.151358

CDC - DPDx - Amebiasis [WWW Document], 2019. URL https://www.cdc.gov/dpdx/amebiasis/index.html (accessed 7.25.23).

Cheng, H.F., Tao, M., 1990. Differential proteolysis of the subunits of pyrophosphate-dependent 6-phosphofructo-1-phosphotransferase. Journal of Biological Chemistry 265, 2173–2177. https://doi.org/10.1016/S0021-9258(19)39957-0

Chi, A., Kemp, R.G., 2000. The Primordial High Energy Compound: ATP or Inorganic Pyrophosphate?*. Journal of Biological Chemistry 275, 35677–35679. https://doi.org/10.1074/jbc.C000581200

Chi, A.S., Deng, Z., Albach, R.A., Kemp, R.G., 2001. The Two Phosphofructokinase Gene Products of Entamoeba histolytica*. Journal of Biological Chemistry 276, 19974–19981. https://doi.org/10.1074/jbc.M011584200

Chou, A., Austin, R.L., 2023. Entamoeba histolytica Infection, in: StatPearls. StatPearls Publishing, Treasure Island (FL).

Clark, C.G., Alsmark, U.C.M., Tazreiter, M., Saito-Nakano, Y., Ali, V., Marion, S., Weber, C., Mukherjee, C., Bruchhaus, I., Tannich, E., Leippe, M., Sicheritz-Ponten, T., Foster, P.G., Samuelson, J., Noël, C.J., Hirt, R.P., Embley, T.M., Gilchrist, C.A., Mann, B.J., Singh, U., Ackers, J.P., Bhattacharya, S., Bhattacharya, A., Lohia, A., Guillén, N., Duchêne, M., Nozaki, T., Hall, N., 2007. Structure and Content of the Entamoeba histolytica Genome, in: Advances in Parasitology. Academic Press, pp. 51–190. https://doi.org/10.1016/S0065-308X(07)65002-7

Coombs, B.C.L., G.H., 1991. Amino acids catabolism in anaerobic protists, in: Biochemical Protozoology As A Basis For Drug Design. CRC Press.

Cornick, S., Moreau, F., Gaisano, H.Y., Chadee, K., 2017. Entamoeba histolytica-Induced Mucin Exocytosis Is Mediated by VAMP8 and Is Critical in Mucosal Innate Host Defense. mBio 8, e01323-17. https://doi.org/10.1128/mBio.01323-17

Cronin, C.N., Tipton, K.F., 1985. Purification and regulatory properties of phosphofructokinase from Trypanosoma (Trypanozoon) brucei brucei. Biochem J 227, 113–124.

Dang, T., Angel, M., Cho, J., Nguyen, D., Ingram-Smith, C., 2022. The Role of Acetate Kinase in the Human Parasite Entamoeba histolytica. Parasitologia 2, 147–159. https://doi.org/10.3390/parasitologia2020014

Deng, Z., Huang, M., Singh, K., Albach, R.A., Latshaw, S.P., Chang, K.P., Kemp, R.G., 1998. Cloning and expression of the gene for the active PPi-dependent phosphofructokinase of Entamoeba histolytica. Biochem J 329, 659–664.

Dingsdag, S.A., Hunter, N., 2018. Metronidazole: an update on metabolism, structure–cytotoxicity and resistance mechanisms. Journal of Antimicrobial Chemotherapy 73, 265–279. https://doi.org/10.1093/jac/dkx351

Evans, P.R., Farrants, G.W., Hudson, P.J., Britton, H.G., Phillips, D.C., Blake, C.C.F., Watson, H.C., 1997. Phosphofructokinase: structure and control. Philosophical Transactions of the Royal Society of London. B, Biological Sciences 293, 53–62. https://doi.org/10.1098/rstb.1981.0059

Evans, P.R., Hudson, P.J., 1979. Structure and control of phosphofructokinase from Bacillus stearothermophilus. Nature 279, 500–504. https://doi.org/10.1038/279500a0

Fernandes, P.M., Kinkead, J., McNae, I., Michels, P., Walkinshaw, M., 2016. Biochemical and biophysical studies of Trypanosoma cruzi phosphofructokinase as a target against Chagas disease. The Lancet 387, S43. https://doi.org/10.1016/S0140-6736(16)00430-X

Fernandes, P.M., Kinkead, J., McNae, I.W., Vásquez-Valdivieso, M., Wear, M.A., Michels, P.A.M., Walkinshaw, M.D., 2020. Kinetic and structural studies of Trypanosoma and Leishmania phosphofructokinases show evolutionary divergence and identify AMP as a switch regulating glycolysis versus gluconeogenesis. FEBS J 287, 2847–2861. https://doi.org/10.1111/febs.15177

Fowler, M.L., Ingram-Smith, C., Smith, K.S., 2012. Novel Pyrophosphate-Forming Acetate Kinase from the Protist Entamoeba histolytica. Eukaryot Cell 11, 1249–1256. https://doi.org/10.1128/EC.00169-12

Gonzales, M.L.M., Dans, L.F., Sio-Aguilar, J., 2019. Antiamoebic drugs for treating amoebic colitis. Cochrane Database Syst Rev 2019, CD006085. https://doi.org/10.1002/14651858.CD006085.pub3

Graven, P., Tambalo, M., Scapozza, L., Perozzo, R., 2014. Purine metabolite and energy charge analysis of Trypanosoma brucei cells in different growth phases using an optimized ion-pair RP-HPLC/UV for the quantification of adenine and guanine pools. Experimental Parasitology 141, 28–38. https://doi.org/10.1016/j.exppara.2014.03.006

Hamzah, Z., Petmitr, S., Mungthin, M., Leelayoova, S., Chavalitshewinkoon-Petmitr, P., 2006. Differential Detection of Entamoeba histolytica, Entamoeba dispar, and Entamoeba moshkovskii by a Single-Round PCR Assay. J Clin Microbiol 44, 3196–3200. https://doi.org/10.1128/JCM.00778-06

Haque, R., 2007. Human Intestinal Parasites. J Health Popul Nutr 25, 387–391.

Haque, R., Ali, I.M., Sack, R.B., Farr, B.M., Ramakrishnan, G., Petri, W.A., Jr, 2001. Amebiasis and Mucosal IgA Antibody against the Entamoeba histolytica Adherence Lectin in Bangladeshi Children. The Journal of Infectious Diseases 183, 1787–1793. https://doi.org/10.1086/320740

He, C., Nora, G.P., Schneider, E.L., Kerr, I.D., Hansell, E., Hirata, K., Gonzalez, D., Sajid, M., Boyd, S.E., Hruz, P., Cobo, E.R., Le, C., Liu, W., Eckmann, L., Dorrestein, P.C., Houpt, E.R., Brinen, L.S., Craik, C.S., Roush, W.R., McKerrow, J., Reed, S.L., 2010. A Novel Entamoeba histolytica Cysteine Proteinase, EhCP4, Is Key for Invasive Amebiasis and a Therapeutic Target. J Biol Chem 285, 18516–18527. https://doi.org/10.1074/jbc.M109.086181

Hemphill, A., Müller, N., Müller, J., 2019. Comparative Pathobiology of the Intestinal Protozoan Parasites Giardia lamblia, Entamoeba histolytica, and Cryptosporidium parvum. Pathogens 8, 116. https://doi.org/10.3390/pathogens8030116

Hooshyar, H., Rostamkhani, P., Arbabi, M., Delavari, M., 2019. Giardia lamblia infection: review of current diagnostic strategies. Gastroenterol Hepatol Bed Bench 12, 3–12.

How, K.Y., Song, K.P., Chan, K.G., 2016. Porphyromonas gingivalis: An Overview of Periodontopathic Pathogen below the Gum Line. Front Microbiol 7, 53. https://doi.org/10.3389/fmicb.2016.00053

Huesca-Espitia, L.C., Suvira, M., Rosenbeck, K., Korza, G., Setlow, B., Li, W., Wang, S., Li, Y. -q., Setlow, P., 2016. Effects of steam autoclave treatment on Geobacillus stearothermophilus spores. Journal of Applied Microbiology 121, 1300–1311. https://doi.org/10.1111/jam.13257

Huston, C.D., Haque, R., Petri, W.A., 1999. Molecular-based diagnosis of Entamoeba histolytica infection. Expert Reviews in Molecular Medicine 1, 1–11. https://doi.org/10.1017/S1462399499000599

Ito, K.A., 1981. Thermophilic Organisms in Food Spoilage: Flat-Sour Aerobes. Journal of Food Protection 44, 157–163. https://doi.org/10.4315/0362-028X-44.2.157

Iyer, L.R., Verma, A.K., Paul, J., Bhattacharya, A., 2019. Phagocytosis of Gut Bacteria by Entamoeba histolytica. Frontiers in Cellular and Infection Microbiology 9.

Jacobsen, K.H., Ribeiro, P.S., Quist, B.K., Rydbeck, B.V., 2007. Prevalence of Intestinal Parasites in Young Quichua Children in the Highlands of Rural Ecuador. J Health Popul Nutr 25, 399–405.

Keene, W.E., Petitt, M.G., Allen, S., McKerrow, J.H., 1986. The major neutral proteinase of Entamoeba histolytica. J Exp Med 163, 536–549. https://doi.org/10.1084/jem.163.3.536

Kessler, R., Nissler, K., Schellenberger, W., Hofmann, E., 1982. Fructose-2,6-bisphosphate increases the binding affinity of yeast phosphofructokinase to AMP. Biochemical and Biophysical Research Communications 107, 506–510. https://doi.org/10.1016/0006-291X(82)91520-0

Kissoon-Singh, V., Moreau, F., Trusevych, E., Chadee, K., 2013. Entamoeba histolytica Exacerbates Epithelial Tight Junction Permeability and Proinflammatory Responses in Muc2 Mice. The American Journal of Pathology 182, 852–865. https://doi.org/10.1016/j.ajpath.2012.11.035

Knodler, L.A., Schofield, P.J., Edwards, M.R., 1995. L-Arginine transport and metabolism in Giardia intestinalis support its position as a transition between the prokaryotic and eukaryotic kingdoms. Microbiology 141, 2063–2070. https://doi.org/10.1099/13500872-141-9-2063

Kotlarz, D., Buc, H., 1981. Regulatory properties of phosphofructokinase 2 from Escherichia coli. Eur J Biochem 117, 569–574. https://doi.org/10.1111/j.1432-1033.1981.tb06375.x

Kotzekidou, P., 2014. BACILLUS | Geobacillus stearothermophilus (Formerly Bacillus stearothermophilus), in: Batt, C.A., Tortorello, M.L. (Eds.), Encyclopedia of Food Microbiology (Second Edition). Academic Press, Oxford, pp. 129–134. https://doi.org/10.1016/B978-0-12-384730-0.00020-3

Kricke, J., Mayer, F., Kopperschläger, G., Kriegel, T., 1999. Phosphofructokinase-1 from Saccharomyces cerevisiae: analysis of molecular structure and function by electron microscopy and self-catalysed affinity labelling. International Journal of Biological Macromolecules 24, 27–35. https://doi.org/10.1016/S0141-8130(98)00063-4

Kucik, C.J., Martin, G.L., Sortor, B.V., 2004. Common Intestinal Parasites. afp 69, 1161–1169.

Li, S., Zhao, Y., Zhang, L., Zhang, X., Huang, L., Li, D., Niu, C., Yang, Z., Wang, Q., 2012. Antioxidant activity of Lactobacillus plantarum strains isolated from traditional Chinese fermented foods. Food Chemistry 135, 1914–1919. https://doi.org/10.1016/j.foodchem.2012.06.048

Li, Z.J., Phillips, N.F.B., 1995. Pyrophosphate-Dependent Phosphofructokinase from Giardia lamblia: Purification and Characterization. Protein Expression and Purification 6, 319–328. https://doi.org/10.1006/prep.1995.1042

Lidell, M.E., Moncada, D.M., Chadee, K., Hansson, G.C., 2006. Entamoeba histolytica cysteine proteases cleave the MUC2 mucin in its C-terminal domain and dissolve the protective colonic mucus gel. Proc Natl Acad Sci U S A 103, 9298–9303. https://doi.org/10.1073/pnas.0600623103

Lo, H.S., Reeves, R.E., 1978. Pyruvate-to-ethanol pathway in Entamoeba histolytica. Biochem J 171, 225–230.

Loftus, B., Anderson, I., Davies, R., Alsmark, U.C.M., Samuelson, J., Amedeo, P., Roncaglia, P., Berriman, M., Hirt, R.P., Mann, B.J., Nozaki, T., Suh, B., Pop, M., Duchene, M., Ackers, J., Tannich, E., Leippe, M., Hofer, M., Bruchhaus, I., Willhoeft, U., Bhattacharya, A., Chillingworth, T., Churcher, C., Hance, Z., Harris, B., Harris, D., Jagels, K., Moule, S., Mungall, K., Ormond, D., Squares, R., Whitehead, S., Quail, M.A., Rabbinowitsch, E., Norbertczak, H., Price, C., Wang, Z., Guillén, N., Gilchrist, C., Stroup, S.E., Bhattacharya, S., Lohia, A., Foster, P.G., Sicheritz-Ponten, T., Weber, C., Singh, U., Mukherjee, C., El-Sayed, N.M., Petri, W.A., Clark, C.G., Embley, T.M., Barrell, B., Fraser, C.M., Hall, N., 2005. The genome of the protist parasite Entamoeba histolytica. Nature 433, 865–868. https://doi.org/10.1038/nature03291

Lohia, A., 2003. The cell cycle of Entamoeba histolytica. Mol Cell Biochem 253, 217-222. https://doi.org/10.1026055631421

Lorenzi, H.A., Puiu, D., Miller, J.R., Brinkac, L.M., Amedeo, P., Hall, N., Caler, E.V., 2010. New Assembly, Reannotation and Analysis of the Entamoeba histolytica Genome Reveal New Genomic Features and Protein Content Information. PLOS Neglected Tropical Diseases 4, e716. https://doi.org/10.1371/journal.pntd.0000716

Marie, C., Petri, W.A., 2014. Regulation of Virulence of Entamoeba histolytica. Annu Rev Microbiol 68, 493–520. https://doi.org/10.1146/annurev-micro-091313-103550

McNae, I.W., Martinez-Oyanedel, J., Keillor, J.W., Michels, P.A.M., Fothergill-Gilmore, L.A., Walkinshaw, M.D., 2009. The Crystal Structure of ATP-bound

Phosphofructokinase from Trypanosoma brucei Reveals Conformational Transitions Different from those of Other Phosphofructokinases. Journal of Molecular Biology 385, 1519–1533. https://doi.org/10.1016/j.jmb.2008.11.047

Mertens, E., De Jonckheere, J., Van Schaftingen, E., 1993. Pyrophosphate-dependent phosphofructokinase from the amoeba Naegleria fowleri, an AMP-sensitive enzyme. Biochem J 292, 797–803.

Metronidazole, 2012., in: LiverTox: Clinical and Research Information on Drug-Induced Liver Injury. National Institute of Diabetes and Digestive and Kidney Diseases, Bethesda (MD).

Meza, I., Clarke, M., 2004. Dynamics of endocytic traffic of Entamoeba histolytica revealed by confocal microscopy and flow cytometry. Cell Motility 59, 215–226. https://doi.org/10.1002/cm.20038

Michels, P.A.M., Chevalier, N., Opperdoes, F.R., Rider, M.H., Rigden, D.J., 1997. The Glycosomal ATP-Dependent Phosphofructokinase of Trypanosoma Brucei must have Evolved from an Ancestral Pyrophosphate-Dependent Enzyme. European Journal of Biochemistry 250, 698–704. https://doi.org/10.1111/j.1432-1033.1997.00698.x

Mustroph, A., Stock, J., Hess, N., Aldous, S., Dreilich, A., Grimm, B., 2013. Characterization of the Phosphofructokinase Gene Family in Rice and Its Expression Under Oxygen Deficiency Stress. Front Plant Sci 4, 125. https://doi.org/10.3389/fpls.2013.00125

Nasrallah, J., Akhoundi, M., Haouchine, D., Marteau, A., Mantelet, S., Wind, P., Benamouzig, R., Bouchaud, O., Dhote, R., Izri, A., 2022. Updates on the worldwide burden of amoebiasis: A case series and literature review. Journal of Infection and Public Health 10, 1134-1141. https://doi.org/10.1016/j.jiph.2022.08.013

O'Brien, W., Bowien, S., Wood, H., 1975. Isolation and characterization of a pyrophosphate-dependent phosphofructokinase from Propionibacterium shermanii. Journal of Biological Chemistry 250, 8690–8695. https://doi.org/10.1016/S0021-9258(19)40727-8

Oliveira, A., Araújo, A., Rodrigues, L.C., Silva, C.S., Reis, R.L., Neves, N.M., Leão, P., Martins, A., 2022. Metronidazole Delivery Nanosystem Able To Reduce the Pathogenicity of Bacteria in Colorectal Infection. Biomacromolecules 23, 2415–2427. https://doi.org/10.1021/acs.biomac.2c00186

Park, J., Gupta, R.S., 2008. Adenosine kinase and ribokinase – the RK family of proteins. Cell. Mol. Life Sci. 65, 2875–2896. https://doi.org/10.1007/s00018-008-8123-1

Petri, W.A., 2003. Therapy of intestinal protozoa. Trends in Parasitology 19, 523–526. https://doi.org/10.1016/j.pt.2003.09.003

Petri, W.A., Haque, R., Mann, B.J., 2002. The bittersweet interface of parasite and host: lectin-carbohydrate interactions during human invasion by the parasite Entamoeba histolytica. Annu Rev Microbiol 56, 39–64. https://doi.org/10.1146/annurev.micro.56.012302.160959

Petri, W.A., Ravdin, J.I., 1991. Protection of gerbils from amebic liver abscess by immunization with the galactose-specific adherence lectin of Entamoeba histolytica. Infect Immun 59, 97–101.

Phillips, B.P., Gorstein, F., 1966. Effects of Different Species of Bacteria on the Pathology of Enteric Amebiasis in Monocontaminated Guinea Pigs. The American Journal of Tropical Medicine and Hygiene 15, 863–868. https://doi.org/10.4269/ajtmh.1966.15.863

Pineda, E., Encalada, R., Olivos-García, A., Néquiz, M., Moreno-Sánchez, R., Saavedra, E., 2013. The bifunctional aldehyde–alcohol dehydrogenase controls ethanol and acetate production in Entamoeba histolytica under aerobic conditions. FEBS Letters 587, 178–184. https://doi.org/10.1016/j.febslet.2012.11.020

Pritt, B.S., Clark, C.G., 2008. Amebiasis. Mayo Clinic Proceedings 83, 1154–1160. https://doi.org/10.4065/83.10.1154

Quach, J., St-Pierre, J., Chadee, K., 2014. The future for vaccine development against Entamoeba histolytica. Hum Vaccin Immunother 10, 1514–1521. https://doi.org/10.4161/hv.27796

Que, X., Reed, S.L., 2000. Cysteine Proteinases and the Pathogenesis of Amebiasis. Clin Microbiol Rev 13, 196–206.

Reed, S.L., Ember, J.A., Herdman, D.S., DiScipio, R.G., Hugli, T.E., Gigli, I., 1995. The extracellular neutral cysteine proteinase of Entamoeba histolytica degrades anaphylatoxins C3a and C5a. The Journal of Immunology 155, 266–274. https://doi.org/10.4049/jimmunol.155.1.266

Reeves, R.E., 1976. How useful is the energy in inorganic pyrophosphate? Trends in Biochemical Sciences 1, 53–55. https://doi.org/10.1016/S0968-0004(76)80189-2

Reeves, R.E., 1968. A New Enzyme with the Glycolytic Function of Pyruvate Kinase. Journal of Biological Chemistry 243, 3202–3204. https://doi.org/10.1016/S0021-9258(18)93395-8

Reeves, R.E., Serrano, R., South, D.J., 1976. 6-phosphofructokinase (pyrophosphate). Properties of the enzyme from Entamoeba histolytica and its reaction mechanism. Journal of Biological Chemistry 251, 2958–2962. https://doi.org/10.1016/S0021-9258(17)33484-1

Reeves, R.E., Warren, L.G., Susskind, B., Lo, H.S., 1977. An energy-conserving pyruvate-to-acetate pathway in Entamoeba histolytica. Pyruvate synthase and a new acetate thiokinase. Journal of Biological Chemistry 252, 726–731. https://doi.org/10.1016/S0021-9258(17)32778-3

Rosenbaum, R.M., Wittner, M., 1970. Ultrastructure of Bacterized and Axenic Trophozoites of Entamoeba Histolytica With Particular Reference to Helical Bodies. J Cell Biol 45, 367–382.

Saavedra, E., Encalada, R., Pineda, E., Jasso-Chávez, R., Moreno-Sánchez, R., 2005. Glycolysis in Entamoeba histolytica. The FEBS Journal 272, 1767–1783. https://doi.org/10.1111/j.1742-4658.2005.04610.x

Samanta, S.K., Ghosh, S.K., 2012. The chitin biosynthesis pathway in Entamoeba and the role of glucosamine-6-P isomerase by RNA interference. Molecular and Biochemical Parasitology 186, 60–68. https://doi.org/10.1016/j.molbiopara.2012.09.011

Samarawickrema, N., 1997. Involvement of superoxide dismutase and pyruvate:ferredoxin oxidoreductase in mechanisms of metronidazole resistance in Entamoeba histolytica. Journal of Antimicrobial Chemotherapy 40, 833–840. https://doi.org/10.1093/jac/40.6.833

Samuelson, J., Robbins, P., 2011. A simple fibril and lectin model for cyst walls of Entamoeba and perhaps Giardia. Trends Parasitol 27, 17–22. https://doi.org/10.1016/j.pt.2010.09.002

Sawyer, M.H., Baumann, P., Baumann, L., 1977. Pathways of D-fructose and D-glucose catabolism in marine species of Alcaligenes, Pseudomonas marina, and Alteromonas communis. Arch Microbiol 112, 169–172. https://doi.org/10.1007/BF00429331

Serrano-Luna, J., Piña-Vázquez, C., Reyes-López, M., Ortiz-Estrada, G., de la Garza, M., 2013. Proteases from Entamoeba spp. and Pathogenic Free-Living Amoebae as Virulence Factors. J Trop Med 2013, 890603. https://doi.org/10.1155/2013/890603

Sharma, B., 2011. Kinetic Characterisation of Phosphofructokinase Purified from Setaria cervi: A Bovine Filarial Parasite. Enzyme Res 2011, 939472. https://doi.org/10.4061/2011/939472

Shirakihara, Y., Evans, P.R., 1988. Crystal structure of the complex of phosphofructokinase from Escherichia coli with its reaction products. Journal of Molecular Biology 204, 973–994. https://doi.org/10.1016/0022-2836(88)90056-3

Shirley, D.-A.T., Farr, L., Watanabe, K., Moonah, S., 2018. A Review of the Global Burden, New Diagnostics, and Current Therapeutics for Amebiasis. Open Forum Infect Dis 5, ofy161. https://doi.org/10.1093/ofid/ofy161

Simon, W.A., Hofer, H.W., 1977. Allosteric and non-allosteric phosphofructokinases from Lactobacilli purification and properties of phosphofructokinases from L. Plantarum and L. Acidophilus. Biochimica et Biophysica Acta (BBA) - Enzymology 481, 450–462. https://doi.org/10.1016/0005-2744(77)90278-9

Somlata, Bhattacharya, A., 2015. Phagocytosis in Entamoeba histolytica, in: Nozaki, T., Bhattacharya, A. (Eds.), Amebiasis: Biology and Pathogenesis of Entamoeba. Springer Japan, Tokyo, pp. 189–206. https://doi.org/10.1007/978-4-431-55200-0_12

Stanley, S.L., 2003. Amoebiasis. The Lancet 361, 1025–1034. https://doi.org/10.1016/S0140-6736(03)12830-9

Stich, A., Abel, P.M., Krishna, S., 2002. Human African trypanosomiasis. BMJ 325, 203–206.

Tanyuksel, M., Petri, W.A., 2003. Laboratory Diagnosis of Amebiasis. Clin Microbiol Rev 16, 713–729. https://doi.org/10.1128/CMR.16.4.713-729.2003

Tovy, A., Hertz, R., Siman-Tov, R., Syan, S., Faust, D., Guillen, N., Ankri, S., 2011. Glucose Starvation Boosts Entamoeba histolytica Virulence. PLoS Negl Trop Dis 5, e1247. https://doi.org/10.1371/journal.pntd.0001247

Tsutsumi, V., Shibayama, M., 2006. Experimental Amebiasis: A Selected Review of Some In Vivo Models. Archives of Medical Research, Amebiasis 37, 210–220. https://doi.org/10.1016/j.arcmed.2005.09.011

Van Schaftingen, E., Lederer, B., Bartrons, R., Hers, H.-G., 1982. A Kinetic Study of Pyrophosphate: Fructose-6-Phosphate Phosphotransferase from Potato Tubers. European Journal of Biochemistry 129, 191–195. https://doi.org/10.1111/j.1432-1033.1982.tb07039.x

Vemuri, R., Martoni, C.J., Kavanagh, K., Eri, R., 2022. Lactobacillus acidophilus DDS-1 Modulates the Gut Microbial Co-Occurrence Networks in Aging Mice. Nutrients 14, 977. https://doi.org/10.3390/nu14050977

Verma, K., Datta, S., 2017. Heavy subunit of cell surface Gal/GalNAc lectin (Hgl) undergoes degradation via endo-lysosomal compartments in Entamoeba histolytica. Small GTPases 10, 456–465. https://doi.org/10.1080/21541248.2017.1340106

Wang, X., Kemp, R.G., 1999. Identification of Residues of Escherichia coli Phosphofructokinase That Contribute to Nucleotide Binding and Specificity. Biochemistry 38, 4313–4318. https://doi.org/10.1021/bi982940q

Wegener, G., Krause, U., 2002. Different modes of activating phosphofructokinase, a key regulatory enzyme of glycolysis, in working vertebrate muscle. Biochem Soc Trans 30, 264–270.

Weik, R.R., John, D.T., 1977. Agitated Mass Cultivation of Naegleria fowleri. The Journal of Parasitology 63, 868–871. https://doi.org/10.2307/3279896

Wesel, J., Ingram-Smith, C., 2023. Glycogen Metabolism and Its Role in Growth and Encystation in Entamoeba histolytica. Life 13, 1529. https://doi.org/10.3390/life13071529

Wesel, J., Shuman, J., Bastuzel, I., Dickerson, J., Ingram-Smith, C., 2021. Encystation of Entamoeba histolytica in Axenic Culture. Microorganisms 9, 873. https://doi.org/10.3390/microorganisms9040873

World Health Organization, 2015. WHO estimates of the global burden of foodborne diseases: foodborne disease burden epidemiology reference group 2007-2015. World Health Organization, Geneva.

Yan, T.F., Tao, M., 1984. Multiple forms of pyrophosphate:D-fructose-6-phosphate 1-phosphotransferase from wheat seedlings. Regulation by fructose 2,6-bisphosphate. Journal of Biological Chemistry 259, 5087–5092. https://doi.org/10.1016/S0021-9258(17)42960-7

Yang, N., Matthew, M.A., Yao, C., 2023. Roles of Cysteine Proteases in Biology and Pathogenesis of Parasites. Microorganisms 11, 1397. https://doi.org/10.3390/microorganisms11061397

CHAPTER II

KINETIC CHARACTERIZATION OF THE PHOSPHOFRUCTOKINASE ENZYMES IN ENTAMOEBA HISTOLYTICA

Abstract

Entamoeba histolytica is the causative agent of amebiasis and liver abscess. This pathogenic protist lacks enzymes for many common metabolic pathways including the TCA cycle and oxidative phosphorylation. As a result, *E. histolytica* is thought to rely on its modified PP_i-dependent glycolytic pathway to generate ATP. Phosphofructokinase (PFK), which catalyzes the conversion of fructose 6-phosphate (F6P) to fructose 1,6-bisphosphate, is a central enzyme in this pathway. However, there are four putative *PFK* genes in the genome. One encodes a PP_i-dependent enzyme that is considered to be the major player during glycolysis. The other three PFKs are thought to encode ATP-dependent enzymes by sequence identity, and whose roles have not yet been defined. I purified and kinetically characterized two recombinant PFK enzymes, EhPFK2 and EhPFK3. Both enzymes were shown to be ATP-dependent and both displayed cooperative kinetics instead of Michaelis-Menten kinetics with respect to F6P and ATP. Kinetic analysis showed that EhPFK2 is more efficient enzyme than EhPFK3. The two enzymes displayed differences in their utilization of nucleoside triphosphates and divalent metal cofactors. My kinetic characterization of these two isozymes suggest that ATP-dependent PFKs may play different roles in energy metabolism compared to PP_i-dependent PFK.

Introduction

Entamoeba histolytica is a protozoan that causes amoebic dysentery and amoebic liver abscess. It infects over 100 million people worldwide and causes up to 100,000 deaths per year (World Health Organization, 2015). It is endemic in developing countries due to poor sanitary practices (Stanley, 2003). Although treatments, such as metronidazole and paromomycin, are available, there are side effects associated with these drugs (Carrero et al., 2020). To overcome poor efficacy as well as various side effects, new drugs and treatments need to be developed.

E. histolytica has two stage life cycle in which transmission begins when dormant cysts are shed into the environment from the host (Wesel et al., 2021). Cysts undergo excystation to infectious trophozoites in the small intestine upon ingestion of contaminated food or water. Then, trophozoites colonize the large intestine and undergo encystation to cysts (Stanley, 2003; Wesel et al., 2021). The life cycle continues as both cysts and trophozoites are shed into the environment (Huston et al., 1999).

This amitochondriate parasite is different from other typical eukaryotic organisms in that it lacks many common metabolic pathways. It also lacks pathways for purine and pyrimidine biosynthesis as well as for many amino acids (Loftus et al., 2005), and relies on obtaining many of these building blocks from its environment, often by phagocytosis of other cells (Somlata and Bhattacharya, 2015). It lacks enzymes for citric acid cycle and oxidative phosphorylation (Clark et al., 2007). As a result, *E. histolytica* is presumed to rely on a modified PP_i-dependent glycolytic pathway to generate ATP (Bruchhaus et al., 1996; Reeves et al., 1976). Use of a PP_i-dependent phosphofructokinase (PP_i-PFK)

instead of an ATP-dependent PFK (ATP-PFK) to convert fructose 6-phosphate (F6P) to fructose 1,6-bisphosphate (F1,6BP) leads to production of three ATP per pyruvate (Reeves, 1976).

The *E. histolytica* genome has multiple genes encoding several glycolytic enzymes, including hexokinase (HXK), PFK, glyceraldehyde 3-phosphate dehydrogenase (GAPDH), and pyruvate phosphate dikinase (PPDK). Of the four putative *PFK* genes, only two have been characterized previously. PFK3 (EHI_103590) has been shown to be an ATP-utilizing enzyme, while PFK4 (EHI_000730) has been shown to be PP_i-dependent (Chi et al., 2001). Although PFK1 (EHI_187040) and PFK2 (EHI_163630) have not been characterized, they are thought to be ATP-dependent as they share high identity with PFK3. The presence of multiple ATP-dependent PFKs, despite modified PP_i-PFK glycolytic pathway seen as the key energy pathway, raises the possibility that these ATP-dependent PFKs could have other functions. In addition, RNA-seq data from reptile parasite *Entamoeba invadens* showed upregulation of one of the two ATP-PFK during excystation, which suggests there could be a switching mechanism between different PFK enzymes (Ehrenkaufer et al., 2013).

I produced and characterized recombinant EhPFK2 and EhPFK3 to understand the differences between these isozymes. My results show that both EhPFK2 and EhPFK3 are ATP-dependent enzymes that cannot utilize PP_i as a phosphoryl donor. Both enzymes displayed positive cooperativity for both F6P and ATP, but differences in other kinetic parameters indicate that EhPFK2 is the more efficient enzyme. They also showed differences in the utilization of other phosphate donors as well as divalent cation

cofactors. The kinetic differences observed between EhPFK2 and EhPFK3 and that they are ATP-dependent enzymes suggest that they may be playing different roles in the metabolism from the PP_i-dependent PFK4, but their exact role is unknown and will require further investigation into their regulation and analyzing their structures.

Materials and Methods

Chemicals and reagents

Chemicals were purchased from Sigma-Aldrich, Fisher Scientific, and Gold Biotechnology. Coupling enzymes, aldolase (A8811) and α-Glycerophosphate dehydrogenase-Triosephosphate Isomerase (G1881), were purchased from Sigma-Aldrich. Codon optimized *E. histolytica PFK2* and *PFK3* were synthesized by GenScript and cloned into pET21b expression vector with 10-His tags on the C-terminal for nickel affinity column purification.

Protein production and purification

The recombinant plasmids pET21b-*PFK*2 and pET21b-*PFK*3 were transformed into *E. coli* RosettaBlue^{TM} (DE3) pLysS. Cells were grown in Luria-Bertani (LB) medium with 50 µg/mL of ampicillin and 34 µg/mL of chloramphenicol shaking at 200 rpm at 37°C until an absorbance at 600 nm of ~0.8. To induce protein expression, isopropyl β-D-1-thiogalactopyranoside (IPTG) was added to a final concentration of 1 mM. Cells were grown at 25°C for an additional 16-18 hours at 200 rpm. Cells were then harvested via centrifugation and stored at -80°C prior to protein purification.

Cell extract was prepared by resuspending the cells in buffer A (25 mM Tris-HCl, 150 mM NaCl, and 10% glycerol [pH 7.0]) and passing the suspension twice through a French pressure cell at approximately 1300 psi. Cell extracts were first clarified at 12,000 *x g* for 20 minutes at 4°C and then by ultracentrifugation at 140,000 *x g* for two hours at 4°C. Extracts were subjected to column chromatography using an AKTA fast protein

liquid chromatography apparatus (GE Healthcare). Cell extracts were applied to a 5 mL HisTrap HP column (GE Healthcare). After washing the column with five column volumes of buffer A, it was developed with a linear gradient from 20 mM to 500 mM imidazole in buffer A. Appropriate fractions determined to contain PFK2 and PFK3 were collected and dialyzed overnight in buffer containing 25 mM Tris-HCl and 10% glycerol. Aliquots of purified protein were stored at -80°C. SDS-PAGE was used to check the purity of the proteins. Concentrations were determined using the Bio-Rad protein assay based on the Bradford dye-binding method with bovine serum albumin as the standard.

Enzyme assay

PFK enzymatic activity was determined spectrophotometrically at 340 nm by using a four-step coupled assay (Eq.1). In the first step of the coupled assay, F6P is converted to F1,6BP by PFK. In the second step, aldolase converts F1,6BP to glyceraldehyde 3-phosphate (GAP) and dihydroxyacetone phosphate (DHAP). In the third step, GAP is converted to DHAP through triosephosphate isomerase (TPI). In the last step, NADH is oxidized to NAD^+, which can be measured at 340 nm. Reaction mixture contained 100 mM Tris-HCl [pH 7.0], 3 mM $MgCl_2$, 1 mM NADH, 2 units of auxiliary enzymes (aldolase, GDH, and TPI), and varying concentrations of the substrates (ATP and F6P). Reactions were pre-warmed to 37°C in a 96-well plate before reactions were initiated by addition of EhPFK2 or EhPFK3. The concentration of one substrate was varied, while the concentration of the other substrate was held constant at a saturating level. The saturating concentrations of F6P were 15 mM and 20 mM for EhPFK2 and

EhPFK3 respectively. The saturating concentrations of ATP were 1.5 mM and 2 mM for EhPFK2 and EhPFK3 respectively. Kinetic parameters were determined by fitting the data to the Michaelis-Menten equation ($V_0 = V[S]/K_m + [S]$) or the Hill equation ($V_0 = V + [S]^h/K_{0.5}^h + [S]^h$), in which V_0 is the initial velocity, [S] is the substrate concentration, V is maximum velocity, $K_{0.5}$ is the substrate concentration at the half-maximal velocity, and h is the Hill constant. Data were plotted using GraphPad Prism 5 software.

[Eq.1] Step 1: PFK F6P + ATP → F1,6BP + ADP + H^+

Step 2: Aldolase F1,6BP → GAP + DHAP

Step 3: TPI GAP → DHAP

Step 4: GDH 2 DHAP + 2 NADH + $2H^+$ → 2 glycerol 3-phosphate + 2 NAD^+

To test other nucleoside triphosphates (NTP) as possible phosphoryl donors, the same reaction mixture and conditions were used except ATP was substituted with other NTPs. To test other divalent cations as possible cofactors for EhPFK2 and EhPFK3, magnesium was substituted with other divalent cations and activity with magnesium was set as 100% activity.

Results

E. histolytica has four phosphofructokinase isozymes

In *E. histolytica*, four genes encoding putative PFKs have been identified (Table 2.1). Comparison of their deduced amino acid sequences revealed that EhPFK1 (EHI_187040) and EhPFK2 (EHI_163630) share 97% identity, differing only in 12 amino acids out of 439 amino acids total. EhPFK3 (EHI_103590) shares 75% identity with both EhPFK1 and EhPFK2. EhPFK4 (EHI_000730), the largest of the four isozymes and the only known PP_i-dependent PFK, shares less than 30% identity with the other three EhPFKs. EhPFK3 has been shown to be an ATP-dependent enzyme, but a full characterization has not been performed, and neither EhPFK1 nor EhPFK2 have been characterized (Chi et al., 2001). Based on the high sequence conservation among these three isozymes (Figure 2.1), I propose that all three are ATP-dependent. I have purified recombinant EhPFK2 and EhPFK3 and kinetically characterized both. Since EhPFK1 and EhPFK2 are nearly identical, I focused on characterizing EhPFK2 and EhPFK3 and comparing them as I did not expect to see much difference between EhPFK1 and EhPFK2.

Sequence Identity Between Phosphofructokinase Isozymes					
Enzyme	**Gene Locus**	**Size**	**PFK1**	**PFK2**	**PFK3**
PFK1	EHI_187040	439 aa (48 kDa)	-	97%	75%
PFK2	EHI_163630	439 aa (48 kDa)	97%	-	75%
PFK3	EHI_103590	439 aa (48 kDa)	75%	75%	-
PFK4	EHI_000730	546 aa (60 kDa)	< 30%		

Table 2.1. Comparison of *E. histolytica* PFK protein sequences.

```
EhPFK1      MTERRHVHQRNDLLIAKKPEEPLPSLEITSLGECKYENTYASPEPFVNGMKMSMSAIKID        60
EhPFK2      MSERRHVHQRNDLLIAKKPEEPLPSLKITSLGECKYENTYASPEPFVDGMTMSMSAIKID        60
EhPFK3      ----MSVKRRDHILIPKNPDAPLPSLKIEEVGECTIDNIYASPEPFVNGMTMKLSAVKNH        56
                 *::*:.:** *:*: *****:* .:***. :* ********:**.*.:**:* .

EhPFK1      GIPVNECEVDLAGPMEKIFFIPERTKVGIVTCGGLCPGLNNVIRGLVMNLQNRYGVKQIY        120
EhPFK2      GIPVNECEAELAGPMEKIFFIPERTKVGIVTCGGLCPGLNNVIRGLVMNLQNRYGVKQIY        120
EhPFK3      GIERDSGEVELAGPMEKIFYNPETTKVAIVTCGGLCPGLNNVIRGLVLNLYNRYHVNNIF        116
            **  :. *.:*********: ** ***.******************:** *** *::*:

EhPFK1      GLKYGYEGLVPELSEQMKLDTLTVSDIHQRGGTILGTSRGAQDPKIMAQFLIDNNFNILF        180
EhPFK2      GLKYGYEGLVPELSEQMKLDTSVVDDIHQRGGTILGTSRGAQDPKIMAQFLIDNNFNILF        180
EhPFK3      GLRWGYEGLVPELSEVQRLTPEIVSDIHQKGGSILGTSRGAQSPEVMAQFLIDNNFNILF        176
            **::***********  :*    *.****:**:*********.*::**************

EhPFK1      TLGGDGTLRGANAINKELRRRGSPIAVVGIPKTIDNDICYTDSTFGFDTAVELAQEAINS        240
EhPFK2      TLGGDGTLRGANAINKELRRRGSPIAVVGIPKTIDNDICYTDSTFGFDTAVELAQEAINS        240
EhPFK3      TLGGDGTLRGANAINKELRRRKVPITVVGIPKTIDNDICYTDSTFGFQTAVGLSQEAINA        236
            ********************  **:*********************:*** *:*****:

EhPFK1      VHYEAKSAKNGVGIVKLMGRDAGFIALYASVASGDVNLVLIPEVDTPIEEILRMTERRLM        300
EhPFK2      VHCEAKSAKNGVGIVKLMGRDAGFIALYASVASGDVNLVLIPEVDTPIEEILKMTERRLM        300
EhPFK3      VHSEAKSAKNGIGIVRLMGRDAGFIALYASLANGDANLVLIPEIDIPITQICEFVGKRIM        296
            ** ********:***:**************:*.**.*******:* ** :* .:. :*:*

EhPFK1      SKGHIVIVIAEGACQNLKPKGLDLGSDKSGNIVHWDAVTYIRQEIDKYLENKKI-EHTIK        359
EhPFK2      SKGHIVIVIAEGACQNLKPKGLDLGSDKSGNIVHWDAVTYIRQEIDKYLENKKI-EHTIK        359
EhPFK3      SKGHVVIVVAEGALQNQKPKDLDLGTDKSGNILHWDSINYLRDSITKYLKSIGIEEHTIK        356
            ****:***:**** ** ***.****:******:***::.*:*:.* ***:.  * *****

EhPFK1      FVDPSYMIRSAPCSAADAHFCLCLANAAVHVAMAGKTGLVICHHHNNFVSIPIERACYYL        419
EhPFK2      FVDPSYMIRSAPCSAADAHFCLCLANAAVHVAMAGKTGLVICHHHNNFVSIPIERACYYL        419
EhPFK3      FVDPSYMIRSAPCSAADAHFCMCLANAAVHVAMAGKTGLVICHHHNNFVSVPIDRTSYYI        416
            ********************:**************************:**:*:.**:

EhPFK1      KRVNPEGPMLSMMKSIEMVE        439
EhPFK2      KRVNPEGPMLSMMKSIESVE        439
EhPFK3      KRVNTDGPLYTMMTAIEKPK        436
            **** :**: :**.:**  :
```

Figure 2.1. Multiple sequence alignment of *E. histolytica* PFK isozymes. Amino acid sequences of PFKs from *E. histolytica* were aligned using Clustal Omega (https://www.ebi.ac.uk/Tools/msa/clustalo/) using the default parameters. Completely conserved residues are indicated by an asterisk (*), highly conserved residues are indicated by a colon (:), and less highly conserved residues are indicated by a period (.).

Kinetic analysis of recombinant *E. histolytica* PFK2 and PFK3

Recombinant EhPFK2 and EhPFK3 were produced in *E. coli* and purified by nickel affinity chromatography. SDS-PAGE analysis showed purified proteins with high purity with approximate size of 50 kDa, which corresponds well with calculated molecular masses of 48 kDa (Figure 2.2).

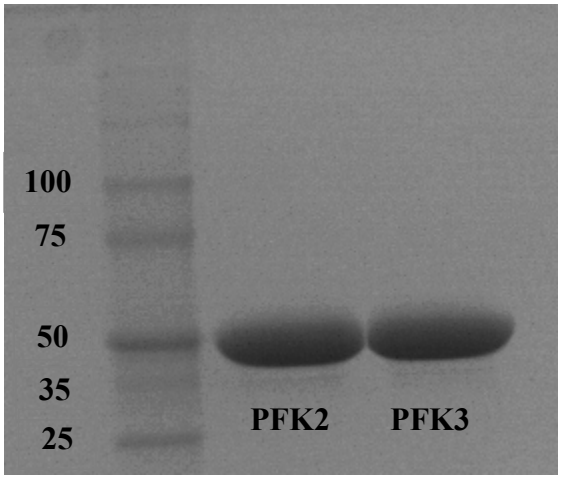

Figure 2.2. SDS-PAGE analysis of purified *E. histolytica* PFK2 and PFK3. Recombinant EhPFK2 and EhPFK3 were separated by SDS-PAGE. Protein molecular weight markers are shown on the left side of the image with sizes shown in kDa.

Kinetic parameters for EhPFK2 and EhPFK3 were determined by varying the concentration of one substrate (F6P or ATP), while the concentration of the other substrate was held at a constant saturating level. The curves for both EhPFK2 and EhPFK3 were sigmoidal, not hyperbolic as you would expect from Michaelis-Menten kinetics (Figure 2.3). Both enzymes displayed cooperative kinetics with respect to F6P and ATP as indicated by the Hill coefficient values (n_H) (Table 2.2). EhPFK2 showed a 4-fold lower $K_{0.5}$ with respect to F6P and a 2-fold lower $K_{0.5}$ with respect to ATP compared to EhPFK3. Lower $K_{0.5}$ indicates higher affinity for the substrates, so EhPFK2 has higher substrate affinities compared to EhPFK3. In terms of the turnover number (k_{cat}), EhPFK2 exhibited a 6-fold higher k_{cat} compared to EhPFK3. Furthermore, EhPFK2 displayed much higher catalytic efficiency ($k_{cat}/K_{0.5}$) with both substrates compared to EhPFK3, suggesting that EhPFK2 is more efficient enzyme.

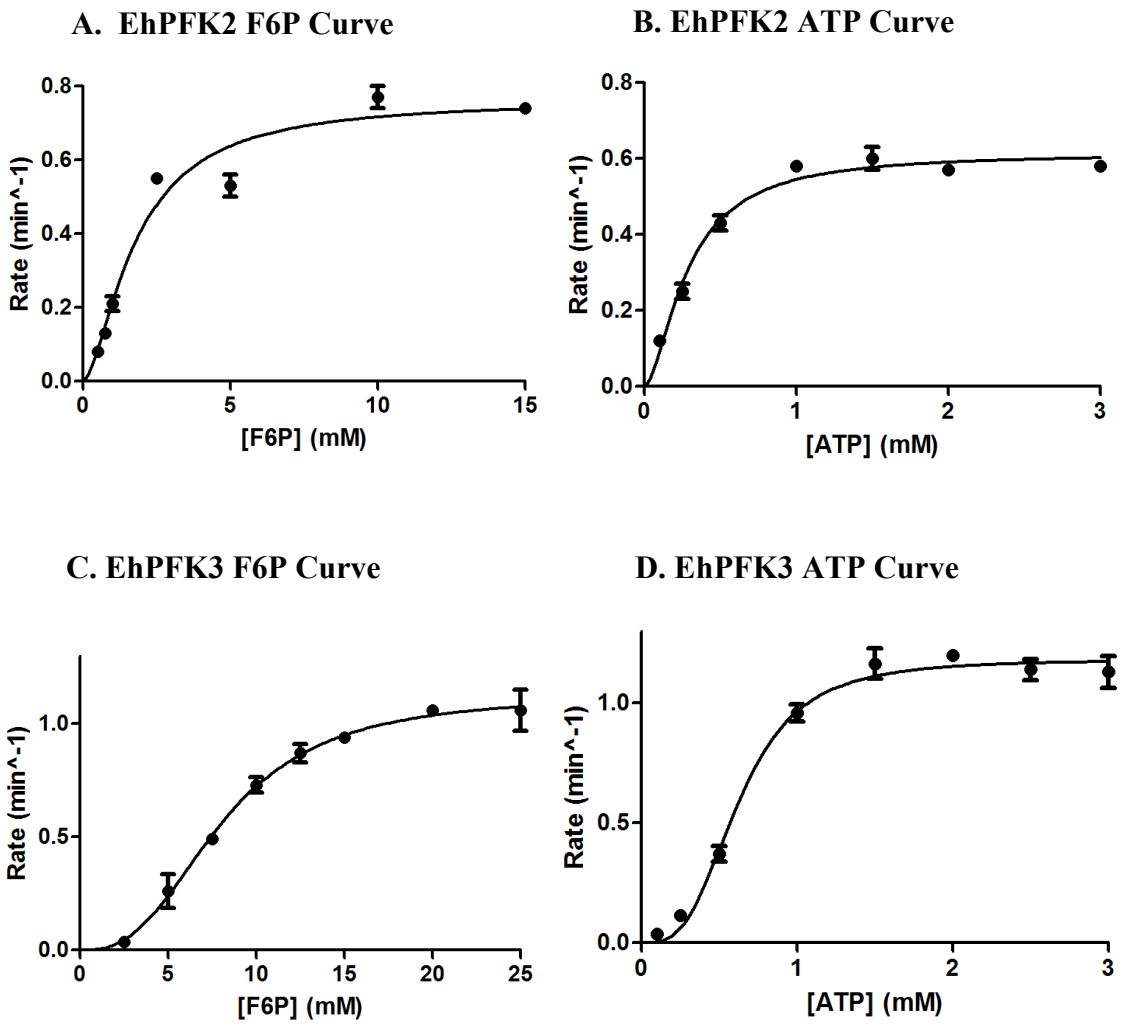

Figure 2.3. Sigmoidal curves of EhPFK2 and EhPFK3. **A:** EhPFK2 curve generated at varying concentration of F6P at 1.5 mM ATP **B:** EhPFK2 curve generated at varying concentration of ATP at 15 mM F6P. **C:** EhPFK3 curve generated at varying concentration of F6P at 2 mM ATP **D:** EhPFK3 curve generated at varying concentration of ATP at 20 mM F6P.

Kinetic Parameters with F6P and ATP as Substrates		
	PFK2	**PFK3**
F6P $K_{0.5}$ (mM)	1.8 ± 0.1	8.0 ± 0.4
ATP $K_{0.5}$ (mM)	0.28 ± 0.01	0.63 ± 0.01
F6P n_H	1.6 ± 0.1	2.7 ± 0.3
ATP n_H	1.6 ± 0.1	3.1 ± 0.7
F6P k_{cat} (s^{-1})	90.8 ± 1.3	14.3 ± 0.3
ATP k_{cat} (s^{-1})	70.3 ± 0.5	16.2 ± 0.3
F6P $k_{cat}/K_{0.5}$ ($mM^{-1}s^{-1}$)	50.5 ± 0.8	1.78 ± 0.03
ATP $k_{cat}/K_{0.5}$ ($mM^{-1}s^{-1}$)	251.0 ± 1.8	25.6 ± 0.4

Table 2.2. Kinetic parameters of *E. histolytica* PFK2 and PFK3. Enzymatic activity was measured by keeping one of the substrates at saturating level while varying the concentration of the other substrate from low to high concentrations. Kinetic parameters were calculated by fitting the data into GraphPad Prism 5 software.

E. histolytica PFK2 and PFK3 are ATP-dependent enzymes and they differ in utilization of other nucleoside triphosphates as phosphoryl donors

To determine whether both EhPFK2 and EhPFK3 were ATP-dependent and not PP_i-dependent enzymes, enzymatic activity was measured using PP_i as the phosphoryl donor. No activity was observed with PP_i concentrations up to 3 mM, suggesting that EhPFK2 and EhPFK3 are indeed ATP utilizing enzymes (Figure 2.4).

A. EhPFK2

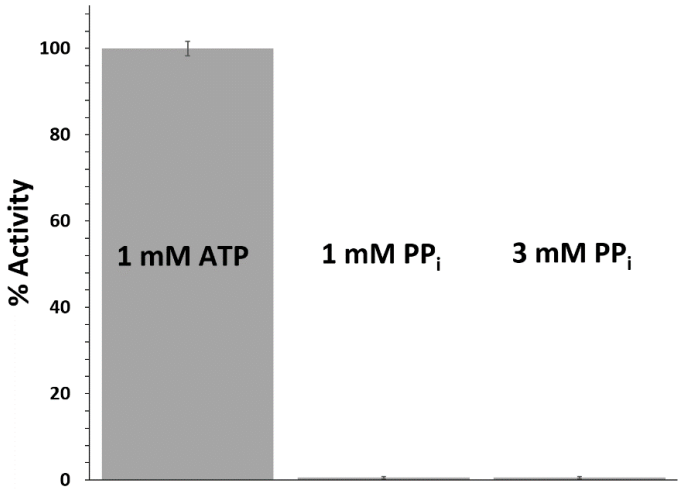

B. EhPFK3

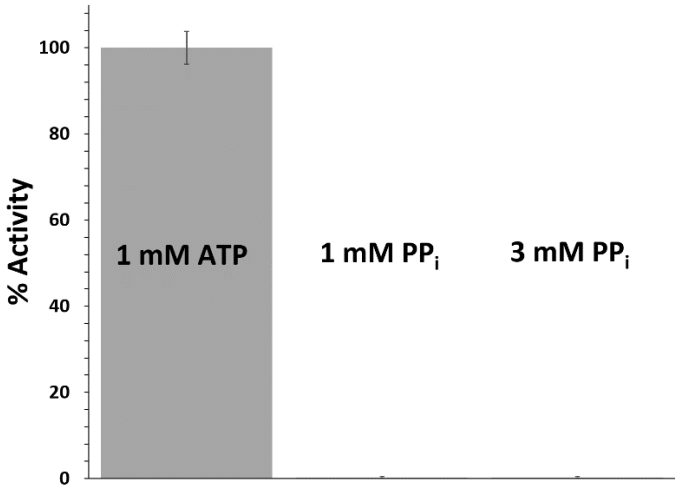

Figure 2.4. Utilization of PP_i as a phosphoryl donor by *E. histolytica* PFK2 and PFK3. **A:** EhPFK2 **B:** EhPFK3. 1 mM PP_i and 3 mM PP_i was tested as substrates and activity was determined. Activity was normalized to that observed with 1 mM ATP, which was set at 100%. All assays were performed in triplicate and error bars represent standard deviation.

To determine if EhPFK2 and EhPFK3 can use other NTPs as phosphoryl donors, kinetic parameters were determined with GTP, UTP, or CTP in place of ATP (Table 2.3). EhPFK2 was able to utilize all NTPs tested, while EhPFK3 could only use GTP as the phosphoryl donor in place of ATP. Interestingly, EhPFK2 appears to slightly prefer GTP over ATP as a substrate as indicated by lower $K_{0.5}$ and higher catalytic efficiency. GTP showed a 3-fold lower $K_{0.5}$ and 3-fold higher catalytic efficiency compared to ATP. CTP also showed lower $K_{0.5}$ and higher catalytic efficiency compared to ATP; however, the result was not as pronounced as GTP.

Kinetic Parameters for NTPs for EhPFK2 and EhPFK3				
Phosphoryl Donor	**$K_{0.5}$ (mM)**	**F6P $K_{0.5}$ (mM)**	**k_{cat} (s^{-1})**	**$k_{cat}/K_{0.5}$ ($mM^{-1}s^{-1}$)**
EhPFK2				
ATP	0.28 ± 0.01	1.8 ± 0.1	70.3 ± 0.5	251.0 ± 1.8
GTP	0.11 ± 0.01	0.97 ± 0.19	85 ± 4	776 ± 35
UTP	0.53 ± 0.02	4.8 ± 0.7	100 ± 2	188 ± 4
CTP	0.28 ± 0.02	3.2 ± 0.02	89 ± 3	319 ± 10
EhPFK3				
ATP	0.63 ± 0.01	8.0 ± 0.4	16.2 ± 0.3	25.6 ± 0.4
GTP	0.40 ± 0.06	9.7 ± 0.6	14 ± 1	35 ± 2
UTP	ND	ND	ND	ND
CTP	ND	ND	ND	ND

Table 2.3. Kinetic parameters of *E. histolytica* PFK2 and PFK3 with other NTPs as phosphoryl donor. Enzymatic activity was measured by keeping one of the substrates at saturating level, while varying the concentration of the other substrate from low to high concentrations. Kinetic parameters were calculated by fitting the data with GraphPad Prism 5 software. ND = not detected.

Utilization of other divalent cations as cofactors

The effects of other divalent cations on the activity of EhPFK2 and EhPFK3 were determined (Figure 2.5). For EhPFK2, the strongest activity was observed with Mg^{2+} and Mn^{2+} was the only other divalent cation that gave substantial activity, with ~30% that

observed with Mg^{2+}. Minimal activity was observed with Ca^{2+}, Co^{2+}, or Ni^{2+}. For EhPFK3, ~30% activity was observed with Mn2+ and ~15% with Ca^{2+}. Less than 10% activity was observed with Co^{2+} or Ni^{2+} (Figure 2.5).

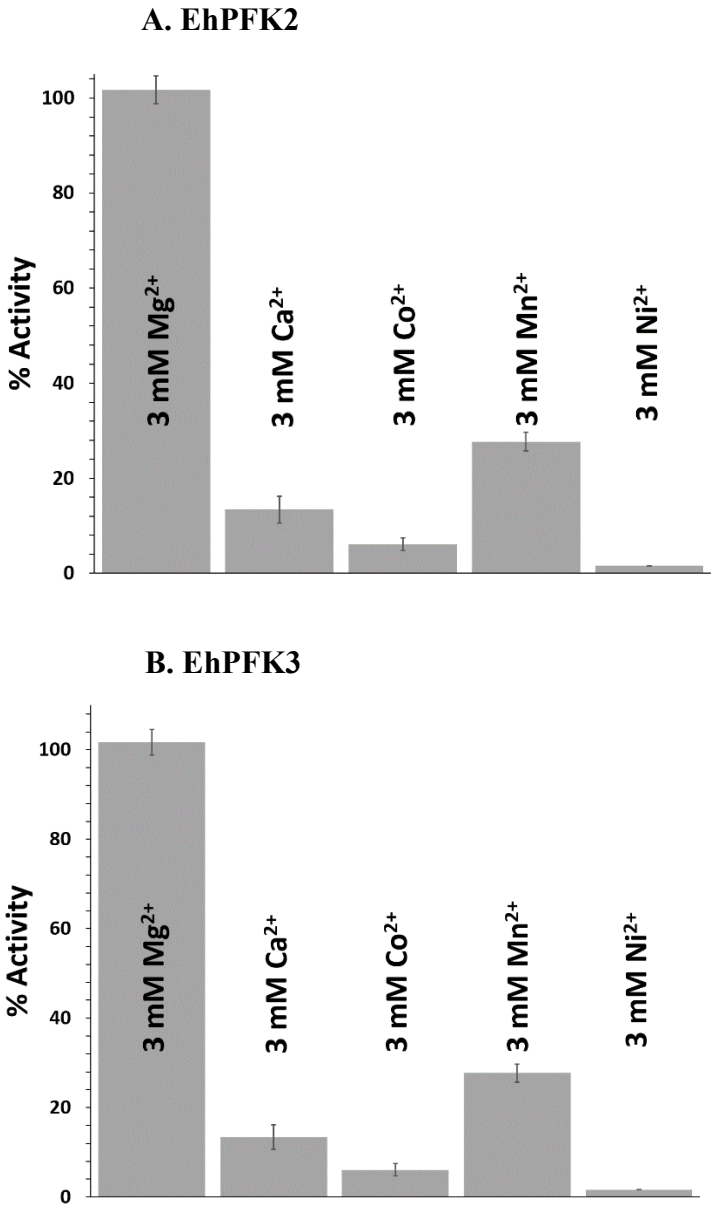

Figure 2.5. Utilization of divalent cations by *E. histolytica* PFK2 and PFK3. **A:** EhPFK2 **B:** EhPFK3. Magnesium was substituted with various divalent cations at 3 mM and activity was determined. Activity was normalized to that observed with magnesium, which was set at 100%. All assays were performed in triplicate and error bars represent standard deviation.

Discussion

Although PP_i-dependent EhPFK4 is thought to be the major player in energy metabolism as part of the PP_i-dependent glycolytic pathway, the presence of three genes encoding ATP-dependent PFK in the *E. histolytica* genome suggests ATP-dependent PFK plays an important role in *E. histolytica* metabolism. EhPFK1 and 2 are 99% identical and presumably have similar kinetic and substrate profiles. EhPFK3 is only 75% identical to PFK1 and PFK2, and distinct differences were observed between the kinetic characteristics of PFK2 and PFK3.

Kinetic characterization of recombinant EhPFK2 and EhPFK3 showed that both enzymes are ATP-dependent and display cooperative kinetics with respect to F6P and ATP. The Hill coefficient value describes cooperativity and values greater than 1 suggest positive cooperativity in which binding of one substrate to the enzyme increases the affinity for other substrates to bind. Hill coefficient values for EhPFK2 were 1.6 for both substrates. For EhPFK3, Hill coefficient values were 2.7 and 3.1 for F6P and ATP respectively. EhPFK3 had a 2-fold higher Hill coefficient values for both substrates compared to EhPFK2, which suggests that EhPFK3 display higher cooperativity for binding of the substrates. EhPFK2 showed lower $K_{0.5}$ for both substrates compared to EhPFK3, which suggests that EhPFK2 has higher affinity for both ATP and F6P. EhPFK2 also showed higher k_{cat} and catalytic efficiency compared to EhPFK3. Overall, kinetics data suggests that EhPFK2 is a more efficient enzyme compared to EhPFK3.

Comparing our results for EhPFK3 with those by Chi *et al.* reveals similarities and differences in kinetic parameters (Chi et al., 2001). Chi *et al*. found that PFK3

exhibited cooperativity for F6P with a Hill coefficient of 2.3, but it displayed Michaelis-Menten kinetics with ATP. They observed a $K_{0.5}$ for F6P of 3.8 mM, 2 times lower than observed in this study. Likewise, they observed a lower $K_{0.5}$ for ATP of 0.12 mM, which was 5 times lower than observed here. Interestingly, the results of Chi *et al*. for PFK3 are more comparable to our results for EhPFK2. One very interesting difference between this study and that of Chi *et al*. is that they had to preincubate the enzyme with ATP for 30 minutes before the assay. Without the activation step, they could not detect any activity with PFK3 enzyme even if ATP concentration was high in the reaction mixture (Chi et al., 2001). In contrast, our purified EhPFK3 did not require any activation step. These differences I observed could be attributed to variance in the purification steps and assay conditions. For example, Chi *et al*. used N-terminal His-tags and carried out enzyme assays in 30°C, while I used C-terminal His-tags and performed enzyme assays at 37°C (Chi et al., 2001).

EhPFK1, PFK2, and PFK3 share high sequence identity with ATP-dependent PFKs but low sequence identity with the PP_i-dependent EhPFK4, suggesting they are ATP-dependent enzymes. However, both ATP-dependent and PP_i-dependent activities were previously reported for PFK3 (Bruchhaus et al., 1996; Chi et al., 2001) and neither PFK1 nor PFK2 had been characterized, leaving unresolved whether these enzymes utilize ATP, PP_i, or both as the phosphoryl donor substrate. I demonstrated that both PFK2 and PFK3 utilize ATP but cannot use PP_i as a substrate.

As previous site-directed mutagenesis study on EhPFK4 showed that it was able to utilize other NTPS, I tested GTP, UTP, and CTP as phosphoryl donors for EhPFK2

and EhPFK3 (Chi and Kemp, 2000). Interestingly, I observed that both EhPFK2 and EhPFK3 can use other NTPs, but the substrate range differs. EhPFK2 uses GTP, UTP, and CTP, while EhPFK3 can only utilize GTP. ATP and GTP are purines with two rings, while UTP and CTP are pyrimidines with one ring. This suggests there are fundamental differences in the NTP binding pocket between the two enzymes.

The EhPFK2 NTP binding pocket has less specificity and is able to bind both purines and pyrimidines. In contrast, NTP binding in EhPFK3 is more specific such that only the larger purine structure is accommodated, suggesting that important interactions occur between the active site and both ring structures of purines whereas PFK2 may require more limited interactions. Interestingly, GTP appears to be the preferred substrate over ATP for EhPFK2 as shown by lower $K_{0.5}$ and higher catalytic efficiency. However, this may not be relevant physiologically where the intracellular concentration of GTP is about 1,000 lower than that of ATP (Zala et al., 2017). Divalent cation study showed differences in utilization of metal ion cofactors, although magnesium still showed highest activity with both enzymes.

The presence of three ATP-dependent PFKs and the differences between them raised the question of their roles in *E. histolytica* metabolism. *E. invadens*, the reptile parasite which has served as the model for studying *Entamoeba* stage conversion (Ehrenkaufer et al., 2013), has three putative PFKs, one PP_i-dependent PFK (EIN_344630) and two ATP-dependent PFKs (EIN_053990 and EIN_080900). One of the putative ATP-dependent PFKs shows high identity to EhPFK1 and EhPFK2 and the other shows high identity to EhPFK3. Transcriptomics data from *E. invadens* revealed

that transcript levels for one of the two ATP-dependent PFK genes, for which the encoded protein shows strongest identity to EhPFK1/2, increased 230-fold during excystation, while transcript levels for the PP_i-dependent PFK gene strongly decreased levels during encystation (Ehrenkaufer et al., 2013). This suggests that the isozymes play different physiological roles and that there may be a switching mechanism between different PFKs in *E. histolytica* depending on the life cycle stage and the environment that the parasite encounters.

Conclusions

Our results demonstrate that PFK2 and PFK3 from *E. histolytica* are indeed ATP-dependent enzymes. Kinetics data suggest that EhPFK2 is the stronger enzyme, with both higher affinity for both substrates and turnover rate. Although they are 75% identical at the amino acid level, they show differences in their kinetic parameters as well as utilization of other NTPs and divalent cations. The presence of multiple genes encoding ATP-dependent PFKs in the *E. histolytica* genome and different kinetic characteristics between the enzymes suggest that they may play other roles in energy metabolism or be required under different conditions. As for *E. invadens*, expression of the different ATP-dependent PFK genes may change depending on the environment or the life stage. Further investigation into the kinetic characteristic of these enzymes, including regulation by allosteric effectors as well as structural modeling, will provide insight into the function of these enzymes and potential roles in metabolic regulation.

References

Bruchhaus, I., Jacobs, T., Denart, M., Tannich, E., 1996. Pyrophosphate-dependent phosphofructokinase of Entamoeba histolytica: molecular cloning, recombinant expression and inhibition by pyrophosphate analogues. Biochem J 316, 57–63.

Carrero, J.C., Reyes-López, M., Serrano-Luna, J., Shibayama, M., Unzueta, J., León-Sicairos, N., de la Garza, M., 2020. Intestinal amoebiasis: 160 years of its first detection and still remains as a health problem in developing countries. International Journal of Medical Microbiology 310, 151358. https://doi.org/10.1016/j.ijmm.2019.151358

Chi, A., Kemp, R.G., 2000. The Primordial High Energy Compound: ATP or Inorganic Pyrophosphate?*. Journal of Biological Chemistry 275, 35677–35679. https://doi.org/10.1074/jbc.C000581200

Chi, A.S., Deng, Z., Albach, R.A., Kemp, R.G., 2001. The Two Phosphofructokinase Gene Products of Entamoeba histolytica*. Journal of Biological Chemistry 276, 19974–19981. https://doi.org/10.1074/jbc.M011584200

Clark, C.G., Alsmark, U.C.M., Tazreiter, M., Saito-Nakano, Y., Ali, V., Marion, S., Weber, C., Mukherjee, C., Bruchhaus, I., Tannich, E., Leippe, M., Sicheritz-Ponten, T., Foster, P.G., Samuelson, J., Noël, C.J., Hirt, R.P., Embley, T.M., Gilchrist, C.A., Mann, B.J., Singh, U., Ackers, J.P., Bhattacharya, S., Bhattacharya, A., Lohia, A., Guillén, N., Duchêne, M., Nozaki, T., Hall, N., 2007. Structure and Content of the Entamoeba histolytica Genome, in: Advances in Parasitology. Academic Press, pp. 51–190. https://doi.org/10.1016/S0065-308X(07)65002-7

Ehrenkaufer, G.M., Weedall, G.D., Williams, D., Lorenzi, H.A., Caler, E., Hall, N., Singh, U., 2013. The genome and transcriptome of the enteric parasite Entamoeba invadens, a model for encystation. Genome Biol 14, R77. https://doi.org/10.1186/gb-2013-14-7-r77

Huston, C.D., Haque, R., Petri, W.A., 1999. Molecular-based diagnosis of Entamoeba histolytica infection. Expert Reviews in Molecular Medicine 1, 1–11. https://doi.org/10.1017/S1462399499000599

Loftus, B., Anderson, I., Davies, R., Alsmark, U.C.M., Samuelson, J., Amedeo, P., Roncaglia, P., Berriman, M., Hirt, R.P., Mann, B.J., Nozaki, T., Suh, B., Pop, M., Duchene, M., Ackers, J., Tannich, E., Leippe, M., Hofer, M., Bruchhaus, I., Willhoeft, U., Bhattacharya, A., Chillingworth, T., Churcher, C., Hance, Z., Harris, B., Harris, D., Jagels, K., Moule, S., Mungall, K., Ormond, D., Squares, R., Whitehead, S., Quail, M.A., Rabbinowitsch, E., Norbertczak, H., Price, C., Wang, Z., Guillén, N., Gilchrist, C., Stroup, S.E., Bhattacharya, S., Lohia, A., Foster, P.G., Sicheritz-Ponten, T., Weber, C.,

Singh, U., Mukherjee, C., El-Sayed, N.M., Petri, W.A., Clark, C.G., Embley, T.M., Barrell, B., Fraser, C.M., Hall, N., 2005. The genome of the protist parasite Entamoeba histolytica. Nature 433, 865–868. https://doi.org/10.1038/nature03291

Reeves, R.E., 1976. How useful is the energy in inorganic pyrophosphate? Trends in Biochemical Sciences 1, 53–55. https://doi.org/10.1016/S0968-0004(76)80189-2

Reeves, R.E., Serrano, R., South, D.J., 1976. 6-phosphofructokinase (pyrophosphate). Properties of the enzyme from Entamoeba histolytica and its reaction mechanism. Journal of Biological Chemistry 251, 2958–2962. https://doi.org/10.1016/S0021-9258(17)33484-1

Somlata, Bhattacharya, A., 2015. Phagocytosis in Entamoeba histolytica, in: Nozaki, T., Bhattacharya, A. (Eds.), Amebiasis: Biology and Pathogenesis of Entamoeba. Springer Japan, Tokyo, pp. 189–206. https://doi.org/10.1007/978-4-431-55200-0_12

Stanley, S.L., 2003. Amoebiasis. The Lancet 361, 1025–1034. https://doi.org/10.1016/S0140-6736(03)12830-9

Wesel, J., Shuman, J., Bastuzel, I., Dickerson, J., Ingram-Smith, C., 2021. Encystation of Entamoeba histolytica in Axenic Culture. Microorganisms 9, 873. https://doi.org/10.3390/microorganisms9040873

World Health Organization, 2015. WHO estimates of the global burden of foodborne diseases: foodborne disease burden epidemiology reference group 2007-2015. World Health Organization, Geneva.

Zala, D., Schlattner, U., Desvignes, T., Bobe, J., Roux, A., Chavrier, P., Boissan, M., 2017. The advantage of channeling nucleotides for very processive functions. F1000Res 6, 724. https://doi.org/10.12688/f1000research.11561.2

CHAPTER III

REGULATION AND MODELING OF THE PHOSPHOFRUCTOKINASE ENZYMES IN ENTAMOEBA HISTOLYTICA

Abstract

Entamoeba histolytica is a water- and food-borne intestinal parasite that causes amoebiasis and liver abscess and causes symptomatic disease in 100 million people each year leading to ~100,000 deaths. This amitochondriate parasite lacks many metabolic pathways including the tricarboxylic acid cycle and oxidative phosphorylation, and cannot synthesize purines, pyrimidines, or most amino acids. As a result, *E. histolytica* is presumed to rely on its modified pyrophosphate (PP_i)-dependent glycolytic pathway for ATP production during growth on glucose. However, the *E. histolytica* genome encodes four putative phosphofructokinases (PFK), one of which is PP_i-dependent and the other three of which are ATP-dependent. I have produced and purified two recombinant ATP-PFKs (designated as PFK2 and 3) to analyze how they are regulated. Various ligands such as AMP that have been shown to regulate PFKs in other organisms have been tested to analyze their effects on *E. histolytica* PFK activities. Specifically, I have identified AMP, ADP, and CoA as activators and phosphoenolpyruvate (PEP), PP_i, and citrate as inhibitors, with CoA being the most potent activator and PEP being the most potent inhibitor. I have shown experimentally and through structural model predictions that PEP, PP_i, and citrate all bind at different allosteric sites. In addition, these inhibitors had different effects with respect to ATP and fructose 6-phosphate (F6P) substrate binding.

The differences in their regulation as well as enzymatic activity from the previous study (Chapter 2) suggest that the four PFKs play different metabolic roles.

Introduction

Entamoeba histolytica is an intestinal parasite that is water- and food- borne and causes up to 100,000 deaths per year (Stanley, 2003; World Health Organization, 2015). *E. histolytica* has several unique characteristics in respect to its metabolism. This amitochondriate lacks a functional citric acid cycle, oxidative phosphorylation, and the biosynthetic pathways of most amino acids, purines, and pyrimidines (Clark et al., 2007; Loftus et al., 2005). Therefore, this amitochondriate parasite is thought to rely on a PP_i-dependent glycolytic pathway to generate energy (Reeves et al., 1976).

Phosphofructokinase (PFK), which catalyzes the conversion of fructose 6-phosphate (F6P) to fructose 1,6-bisphosphate (F1,6BP), is a key regulated glycolytic enzyme in many other organisms (Park and Gupta, 2008; Wegener and Krause, 2002). PFK is activated by ADP and inhibited by phosphoenolpyruvate (PEP) in bacteria *Escherichia coli* and *Bacillus stearothermophilus* (Blangy et al., 1968; Evans and Hudson, 1979). PFK from the eukaryotic *Trypanosoma brucei* and *Trypanosoma cruzi* is activated by AMP (Fernandes et al., 2020). A previous study on ATP-dependent PFK3 from *E. histolytica* showed that PEP was the only regulator of the enzyme and other effectors tested did not have any effect on the activity of the enzyme (Chi et al., 2001).

To gain insight into regulation and structure of ATP-dependent PFKs in *E. histolytica*, I tested various ligands to determine their effects on the enzymatic activity of PFK2 (EHI_163630) and PFK3 (EHI_103590). Our results show that AMP, ADP, and CoA are activators, while PEP, citrate, and PP_i are inhibitors. Each of these inhibitors affect binding of substrates differently for EhPFK2 and EhPFK3. In addition, results from

inhibition experiments with multiple effectors as well as structural modeling and docking showed that these effectors all bind at different allosteric sites. These regulatory differences suggest that ATP-dependent PFKs might play different metabolic roles despite their similar sequences.

Materials and Methods

Chemicals and reagents

Chemicals were purchased from Sigma-Aldrich, Fisher Scientific, and Gold Biotechnology. Coupling enzymes, aldolase (A8811) and α-Glycerophosphate dehydrogenase-Triosephosphate Isomerase (G1881), were purchased from Sigma-Aldrich. Codon optimized *E. histolytica PFK2* and *PFK3* were synthesized by GenScript and cloned into pET21b expression vector with 10-His tags on the C-terminal for nickel affinity column purification.

Protein production and purification / enzyme assay

Protein purification and enzyme assay were performed as described in Chapter 2 of this dissertation.

Analysis of PFK effectors

Enzyme assays were performed in the absence and presence of various ligands at $K_{0.5}$ concentration of both substrates. Enzyme activity in the absence of effectors was set as 100 percent activity. Once inhibitors have been identified, their effects on binding of substrates were determined by generating progress curves in the absence and presence of various inhibitors. The highest concentration of F6P and ATP in the assay were increased to 30 mM and 3 mM respectively, to observe any restoration of activity due to higher substrate concentrations. For the IC_{50} experiment, $K_{0.5}$ concentration of both substrates were used to observe the effect of inhibitors on the activity of *E. histolytica* PFK

enzymes. First, the IC_{50} concentration of individual inhibitors was determined by fitting the data into log (inhibitor) vs. response curve in GraphPad Prism 5 software. Then, IC_{50} of one inhibitor was determined again in the presence of a second inhibitor that was held at constant at its IC_{50} concentration. Reactions were performed in triplicate. BioTek Eon Microplate Spectrophotometer was used to follow the progress of the reactions (BioTek, Winooski, VT). Data were plotted using GraphPad Prism 5 software (GraphPad Software, San Diego, CA).

Effector competition experiment

For competition experiments, enzyme assays were performed in the absence and presence of the strongest activator and inhibitor at $K_{0.5}$ concentration of both substrates. For the activator, AC_{50}, the half-maximal activation concentration, and AC_{max}, the effector concentration for maximum activation, were used. For the inhibitor, IC_{50}, the half-maximal inhibitory concentration, and IC_{max}, the effector concentration for maximum inhibition, were used. Enzyme activity in the absence of any effector was set as 100 percent activity. For the first part of the assay, both ligands were included in the reaction mixture before adding the enzyme to initiate the reaction. For the second part of the assay, the activator and the enzyme were incubated together in the reaction mixture that was missing one of the substrates for 5 minutes. After incubating the reaction mixture at 37°C for 5 minutes, the inhibitor was added and the substrate was added to initiate the reaction. Reactions were performed in triplicates. BioTek Eon Microplate Spectrophotometer was used to measure the absorbance (BioTek, Winooski, VT).

In silico modeling of *E. histolytica* PFK structures

The amino acid sequences for EhPFK2 and EhPFK3 were used to generate predicted models with Swiss-Model (Waterhouse et al., 2018; https://swissmodel.expasy.org/) and AlphaFold (Jumper et al., 2021; Varadi et al., 2022; https://alphafold.ebi.ac.uk/). For the homology based Swiss-Model, PFK from *Trypanosoma brucei* was used as a template (McNae et al., 2009; PDB ID:3F5M). The template was selected based on sequence identity, coverage, and Global Model Quality Estimate (GMQE) scores. For determination of allosteric binding sites for AMP and PEP, models of EhPFK2 and EhPFK3 were superimposed on the crystal structures of *T. brucei* PFK and *B. stearothermophilus* PFK with ligands bound. Model images were visualized in PyMOL (The PyMOL Molecular Graphics System, Version 2.0 Schrödinger, LLC; https://pymol.org/2/#page-top). For the protein-ligand docking simulation, SwissDock (Grosdidier et al., 2011a, 2011b; http://www.swissdock.ch/) was used. To choose the best protein-ligand model, model with lowest -ΔG was chosen.

Results

AMP, ADP, and CoA activate both EhPFK2 and EhPFK3

Ligands, such as AMP and PEP, that were shown to modulate PFK activity from other organisms were tested on EhPFK2 and EhPFK3 (Figure 3.1 and 3.2). AMP, ADP, and CoA were found to increase activity of both EhPFK2 and EhPFK3. CoA was the strongest activator for both enzymes, with over 40% increased activity in the presence versus absence of CoA. The concentration of CoA required to achieve this increase in activity was 6-fold higher for EhPFK3 than EhPFK2. Both AMP and ADP showed ~20% increase in activity in the presence versus absence of these ligands for EhPFK2 at 1 mM. For EhPFK3, AMP showed a greater increase in activity compared to ADP. AMP increased the activity of EhPFK3 by ~30%, while ADP only increased by ~20%.

PEP, PPi, and citrate inhibit both EhPFK2 and EhPFK3

Citrate, PEP, and PP_i were found to be inhibitors of both enzymes (Figure 3.1 and 3.2). PEP showed the most pronounced effect for both enzymes, where it resulted in about 80% reduction in activity at 7 mM PEP. For EhPFK2, reduction in activity by citrate was only observed for concentrations higher than 5 mM, while 5 mM citrate decreased the activity over 20% for EhPFK3. Both EhPFK2 and EhPFK3 showed about 60% reduction in activity at 10 mM citrate. PP_i showed more pronounced effects of inhibition on EhPFK3 than EhPFK2. EhPFK2 activity was reduced by ~20%, while EhPFK3 activity was reduced by ~60% at 0.2 mM PP_i. ~60% reduction in activity was observed for EhPFK2 at 0.8 mM PP_i, while EhPFK3 showed ~80% reduction.

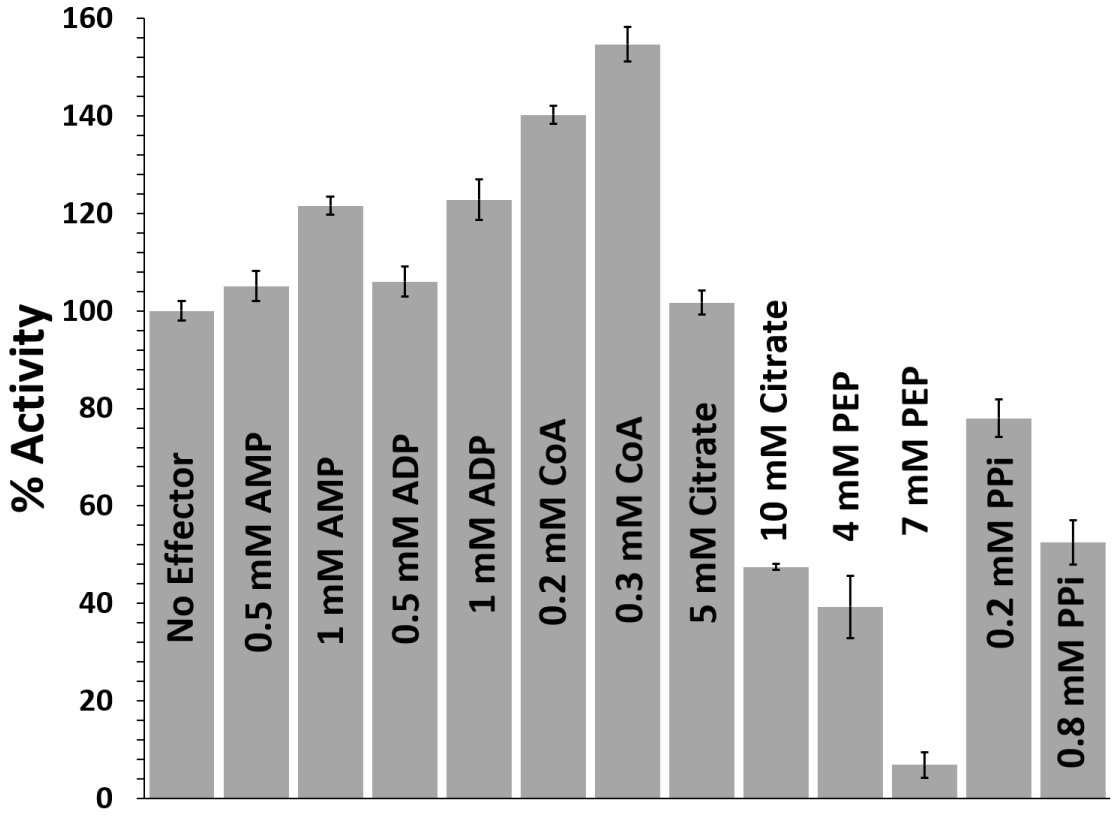

Figure 3.1. Effect of various ligands on activity of EhPFK2. Various small molecules were examined to see if they regulate EhPFK2 activity. Concentration of each of the substrates were at $K_{0.5}$. Absence of effector was set as 100% activity. Results shown are the mean ± standard deviation of triplicate reactions.

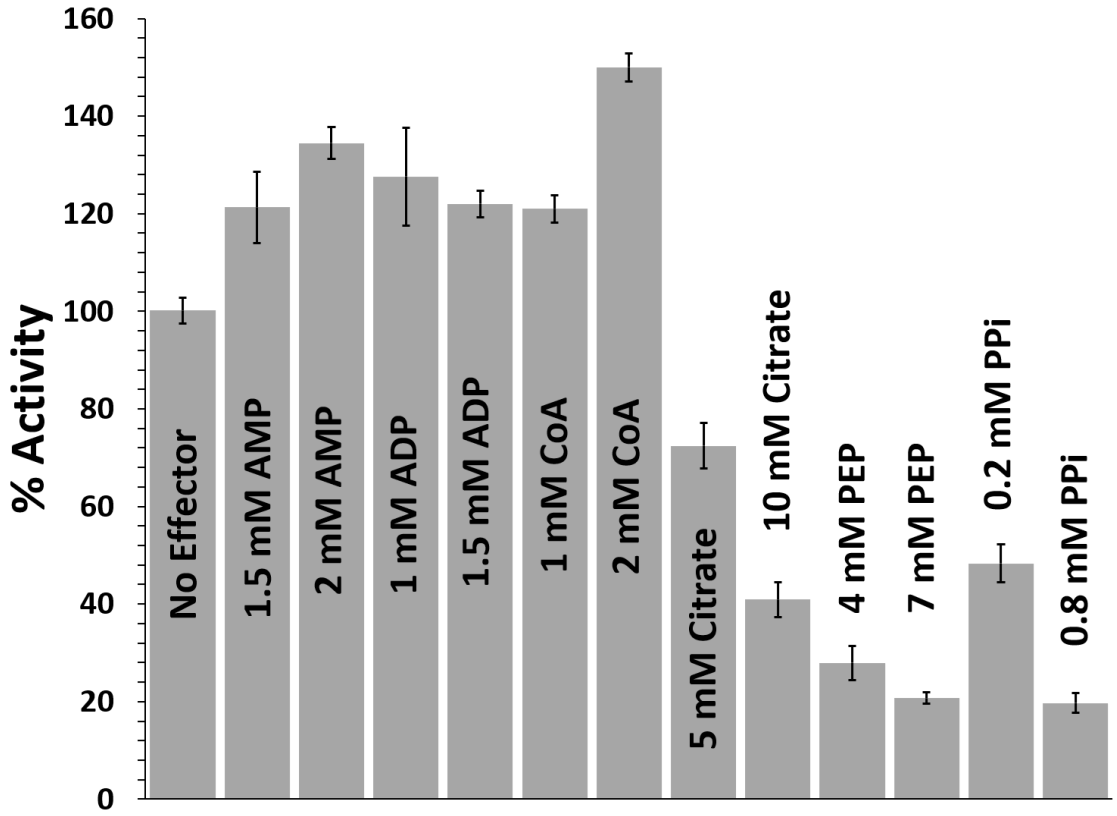

Figure 3.2. Effect of various ligands on activity of EhPFK3. Various ligands were examined to see if they regulate EhPFK3 activity. Concentration of each of the substrates were at $K_{0.5}$. Absence of effector was set as 100% activity. Results shown are the mean ± standard deviation of triplicate reactions.

PFK inhibitors have different effects on EhPFK2 and EhPFK3

Progress curves in the presence of increasing concentration of inhibitors were generated to determine whether each inhibitor exerts its effect on ATP or F6P binding. PEP was found to affect the $K_{0.5}$ of EhPFK2, leading to a 5-fold increase in the presence of 9 mM PEP. For EhPFK3, V_{max} decreased in the presence of PEP, but $K_{0.5}$ was not significantly affected (Figure 3.3). Neither PP_i nor citrate had a substantial effect on the $K_{0.5}$ for F6P for either EhPFK2 and EhPFK3 but did decrease V_{max} for both enzymes (Figure 3.4 and 3.5).

When examining the effect of inhibitors on binding of ATP, PEP was found to affect V_{max}, but not $K_{0.5}$ for both EhPFK2 and EhPFK3 (Figure 3.6). PP_i affected the $K_{0.5}$ for ATP for EhPFK2, increasing it by 3-fold at 3 mM PP_i, but did not substantially alter the $K_{0.5}$ for ATP for EhPFK3 (Figure 3.7). Citrate did not have much effect on $K_{0.5}$ of ATP for either EhPFK2 or EhPFK3, but decreased V_{max} for both (Figure 3.8).

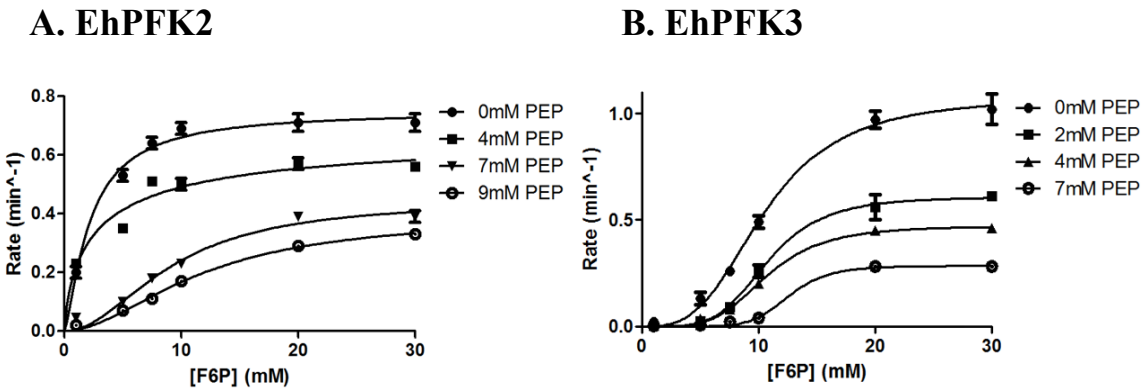

Figure 3.3. Effect of PEP on binding of F6P for EhPFK2 and EhPFK3. A: Substrate progress curve of EhPFK2 in the presence of PEP. **B:** Substrate progress curve of

EhPFK3 in the presence of PEP. ATP was held constant at the saturating level. Results shown are the mean ± standard deviation of triplicate reactions.

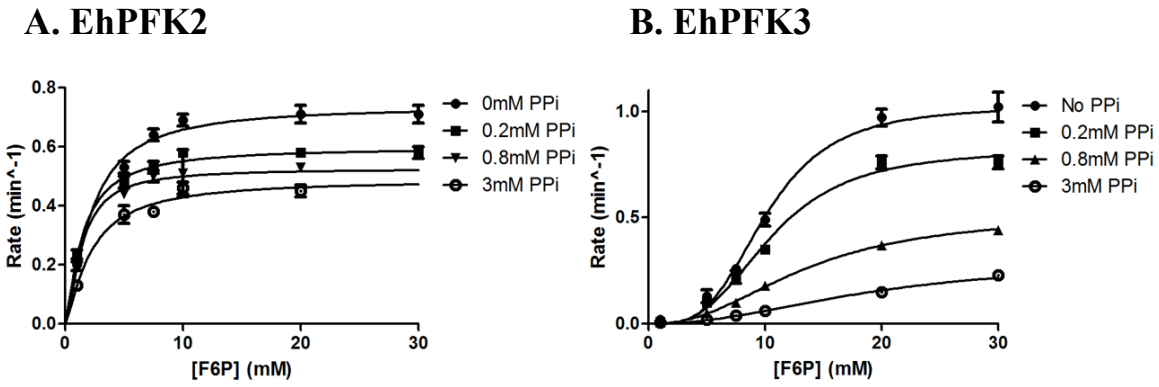

Figure 3.4. Effect of PP_i on binding of F6P for EhPFK2 and EhPFK3. A: Substrate progress curve of EhPFK2 in the presence of PP_i. **B:** Substrate progress curve of EhPFK3 in the presence of PP_i. ATP was held constant at the saturating level. Results shown are the mean ± standard deviation of triplicate reactions.

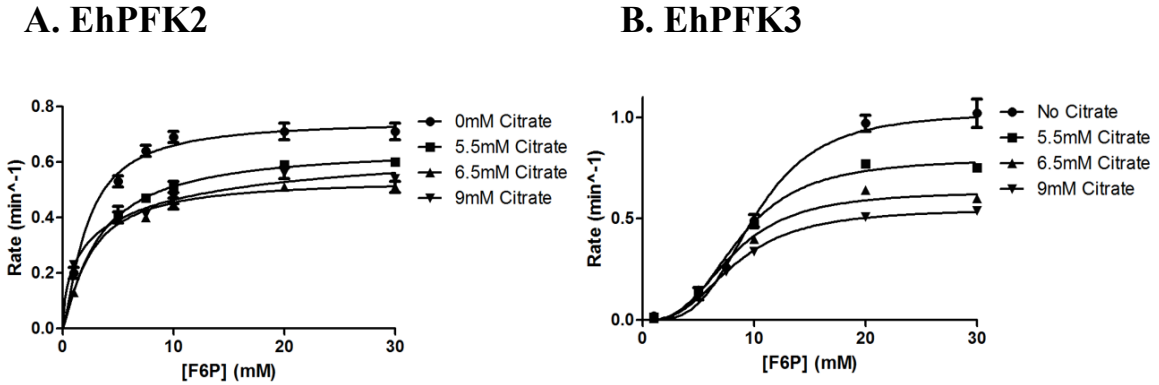

Figure 3.5. Effect of citrate on binding of F6P for EhPFK2 and EhPFK3. A: Substrate progress curve of EhPFK2 in the presence of citrate. **B:** Substrate progress

curve of EhPFK3 in the presence of citrate. ATP was held constant at the saturating level. Results shown are the mean ± standard deviation of triplicate reactions.

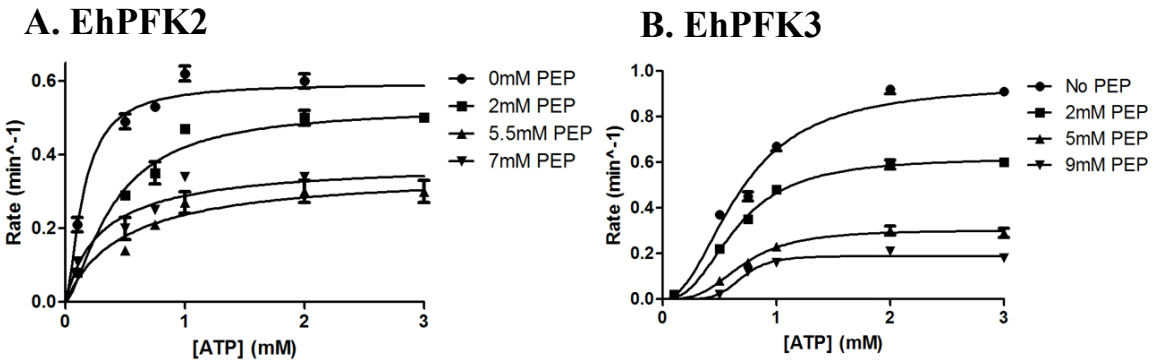

Figure 3.6. Effect of PEP on binding of ATP for EhPFK2 and EhPFK3. A: Substrate progress curve of EhPFK2 in the presence of PEP. **B:** Substrate progress curve of EhPFK3 in the presence of PEP. F6P was held constant at the saturating level. Results shown are the mean ± standard deviation of triplicate reactions.

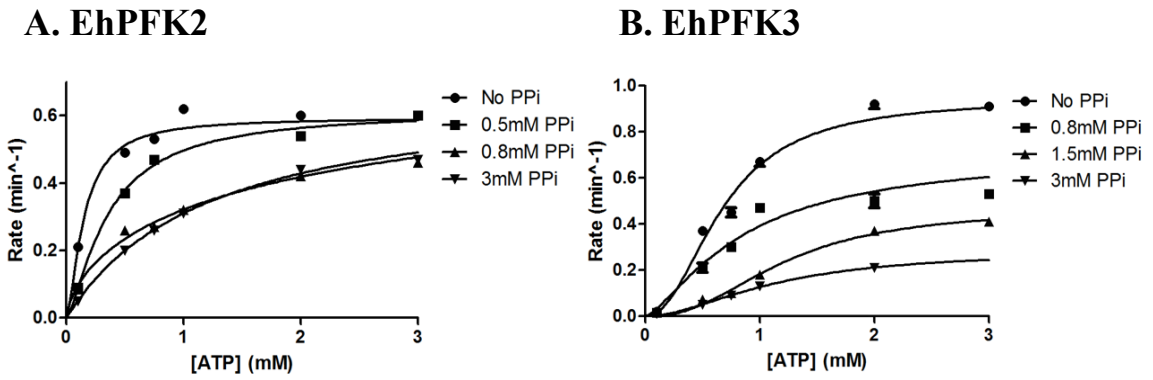

Figure 3.7. Effect of PP_i on binding of ATP for EhPFK2 and EhPFK3. A: Substrate progress curve of EhPFK2 in the presence of PP_i. **B:** Substrate progress curve of EhPFK3

in the presence of PP_i. F6P was held constant at the saturating level. Results shown are the mean ± standard deviation of triplicate reactions.

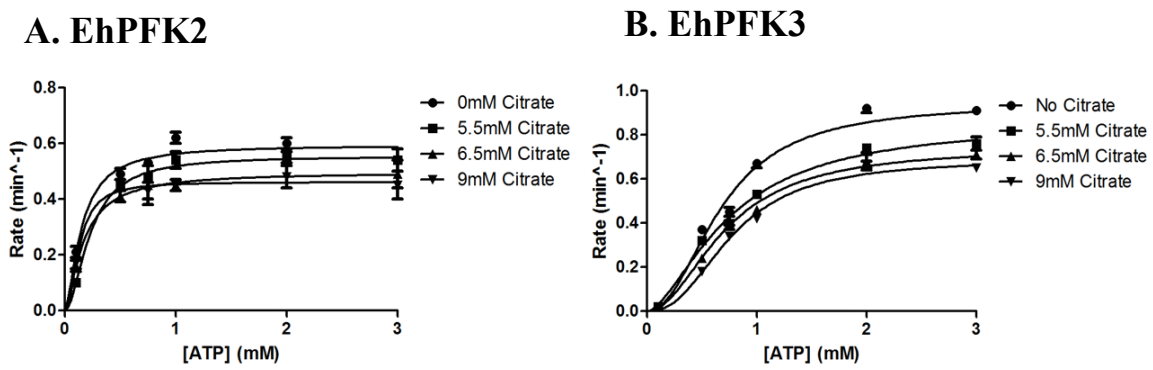

Figure 3.8. Effect of citrate on binding of ATP for EhPFK2 and EhPFK3. A: Substrate progress curve of EhPFK2 in the presence of citrate. **B:** Substrate progress curve of EhPFK3 in the presence of citrate. F6P was held constant at the saturating level. Results shown are the mean ± standard deviation of triplicate reactions.

Inhibitors do not share overlapping binding sites

To determine if any of the inhibitors bind at the same or overlapping sites, IC_{50} values were determined for each inhibitor in the presence or absence of another inhibitor with the rationale that if the inhibitors share an allosteric site or occupy overlapping binding sites (such that occupation of one occludes occupation of the other) then the IC_{50} of the second inhibitor will be affected.

For EhPFK2, the IC_{50} values for PEP, citrate, and PP_i were determined to be 4.0 mM, 6.5 mM, and 0.78 mM respectively (Table 3.1). In the presence of PEP at its IC_{50}

concentration, the IC_{50} values for citrate and PP_i were essentially unchanged (Table 3.1). Likewise, the presence of citrate at its IC_{50} concentration did not alter the IC_{50} value for PP_i (Table 3.1). For EhPFK3, the IC_{50} values for PEP, citrate, and PP_i were similar to those observed for PFK2 (Table 3.2). The inhibitors had no effect on the IC_{50} for any other inhibitor for EhPFK3, suggesting that the three inhibitors bind at independent sites.

EhPFK2 IC_{50} Experiment		
Inhibitor		
Varied	**Constant**	**IC_{50} (mM)**
Citrate		6.5 ± 0.2
Citrate	PEP	6.3 ± 0.1
PP_i		0.78 ± 0.08
PP_i	PEP	0.83 ± 0.14
PP_i	Citrate	0.76 ± 0.06
PEP		4.0 ± 0.5

Table 3.1. IC_{50} for EhPFK2 in the presence of various inhibitors. IC_{50} was measured in the absence and presence of multiple inhibitors for EhPFK2. One inhibitor was held constant at its IC_{50} concentration, while the concentration of the other inhibitor was varied to measure the new IC_{50}. Results shown are the mean ± standard deviation of triplicate reactions.

EhPFK3 IC_{50} Experiment		
Inhibitor		
Varied	**Constant**	**IC_{50} (mM)**
Citrate		7.6 ± 0.2
Citrate	PEP	7.2 ± 0.1
PP_i		0.58 ± 0.09
PP_i	PEP	0.51 ± 0.08
PP_i	Citrate	0.54 ± 0.10
PEP		1.8 ± 0.2

Table 3.2. IC_{50} for EhPFK3 in the presence of various inhibitors. IC_{50} was measured in the absence and presence of multiple inhibitors for EhPFK3. One inhibitor was held at constant IC_{50}, while the concentration of the other inhibitor was varied to measure the new IC_{50}. Results shown are the mean ± standard deviation of triplicate reactions.

Phosphoenolpyruvate is a strong inhibitor of EhPFK2

A competition experiment was performed to determine whether the presence of activator can overcome the effect of the presence of inhibitor, and vice versa. CoA and PEP were used since they showed the most pronounced activation and inhibitory effects, respectively. When EhPFK2 was preincubated in the presence of both CoA and PEP at the AC_{50} and IC_{50} concentrations, activity was reduced to ~40% that determined for the enzyme in the absence of either effector (Figure 3.9). When the concentrations of CoA and PEP were increased to their maximum effective concentrations (AC_{max} = 0.4 mM for CoA and IC_{max} = 7 mM for PEP), EhPFK2 activity decreased ~20% more. When EhPFK2 was preincubated with CoA at its AC_{50} concentration for 5 minutes before addition of PEP to its IC_{50} concentration, inhibition was slightly reduced with ~60% activity observed. However, when EhPFK2 was preincubated with CoA at its AC_{max} concentration and PEP was then added at its IC_{max} concentration, activity was strongly inhibited to just 5% that observed for EhPFK2 in the absence of any effector.

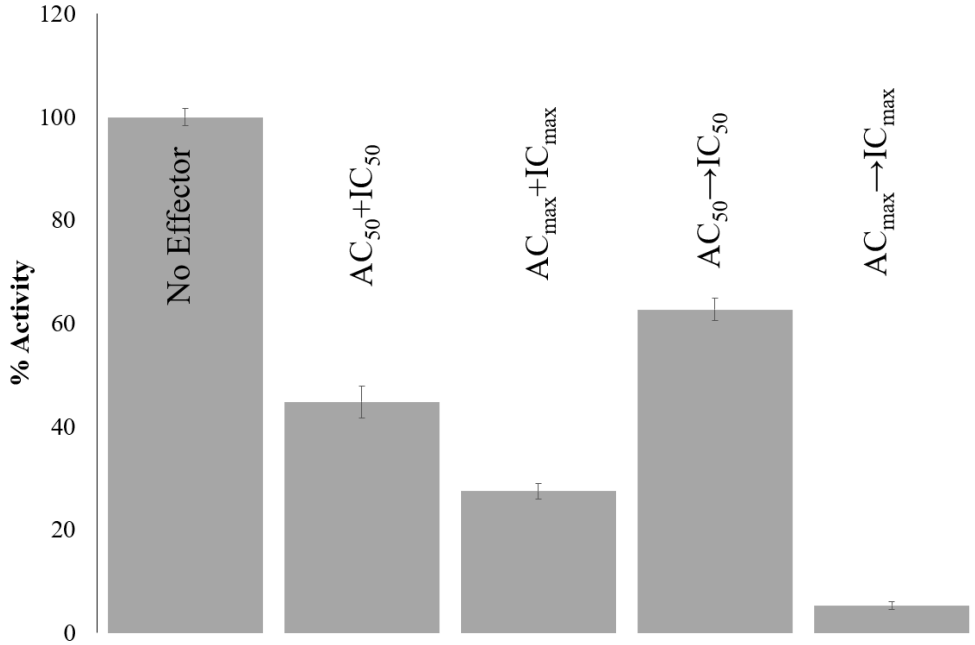

Figure 3.9. Competition experiment between CoA and PEP for EhPFK2. Percent activity was measured in the presence of both activator and inhibitor. Percent activity with no effector present was set as 100% activity.

The modeled structures of EhPFK2 and EhPFK3 are similar

Since crystal structures of EhPFK2 and EhPFK3 have not yet been solved, structural models were generated by homology-based modeling with Swiss-Model (Waterhouse et al., 2018; https://swissmodel.expasy.org/) and Alpha Fold (Jumper et al., 2021; Varadi et al., 2022; https://alphafold.ebi.ac.uk/) using the crystal structure of ATP-dependent *T. brucei* PFK (PDB ID:3F5M as the template (McNae et al., 2009). *T. brucei* PFK shared 43.45% identity with EhPFK2 and 40.78% identity with EhPFK3. PyMOL was used to visualize the structures (The PyMOL Molecular Graphics System, Version 2.0 Schrödinger, LLC; https://pymol.org/2/#page-top)

Although the two programs produced slightly different models, visual comparison of the models shows EhPFK2 and EhPFK3 are structurally similar (Figure 3.10). Domain A (in red) is composed of four small α-helices and three pairs of anti-parallel β- strands. Domain B (in cyan) is made up of four-stranded parallel β-sheet flanked by α-helices. Domain C (in orange) is composed of five-stranded parallel β-sheet flanked by α-helices.

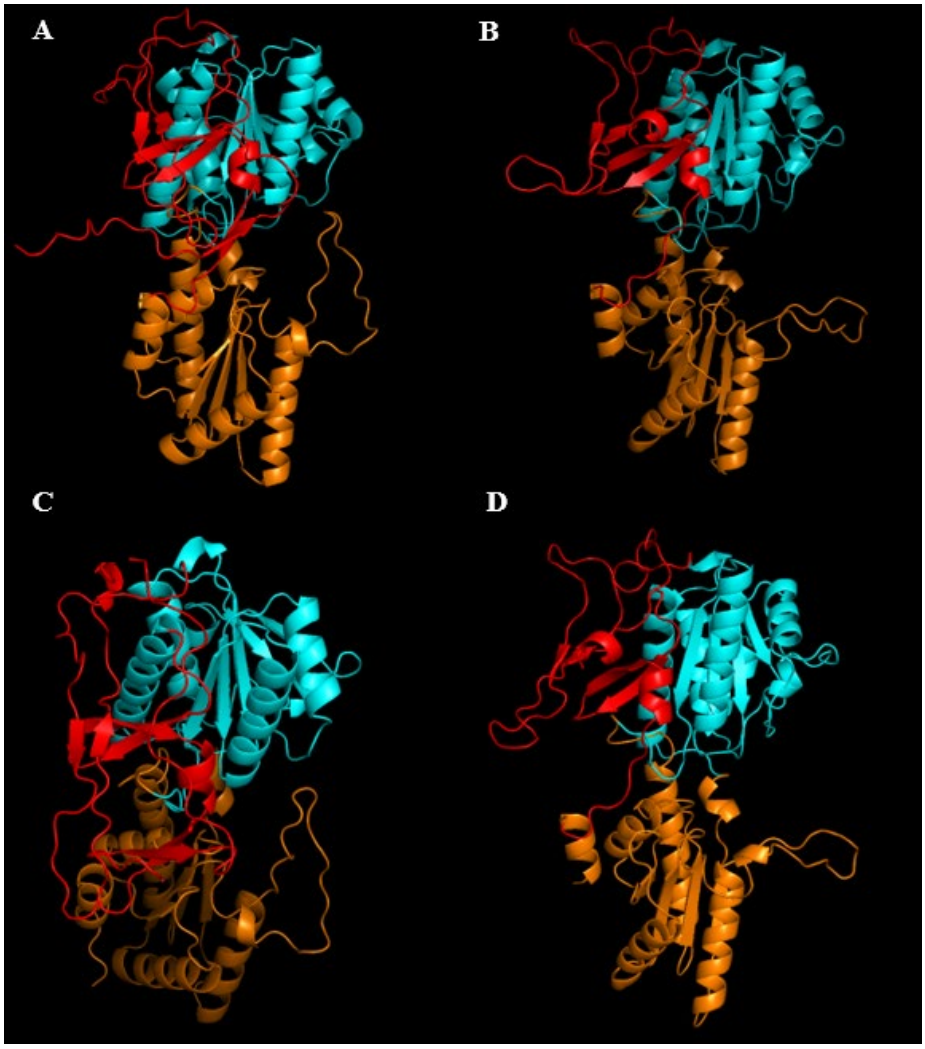

Figure 3.10. Structural models of EhPFK. A: Structural model of EhPFK2 from homology-based approach in Swiss-Mode using *T. brucei* PFK (43.45% identity with

EhPFK2). **B:** Structural model of EhPFK3 from AlphaFold prediction. **C:** Structural model of EhPFK3 from homology-based approach in Swiss-Model using *T. brucei* PFK (40.78% identity with EhPFK3). **D:** Structural model of EhPFK3 from AlphaFold prediction. **Red:** Domain A. **Cyan:** Domain B. **Orange:** Domain C.

AMP binding site in EhPFK2 and EhPFK3 compared to *T. brucei* PFK

Since a solved structure for *T. brucei* PFK with AMP bound (Fernandes et al., 2020; PDB ID: 6SY7) is available, I wanted to compare our predicted structures with it to determine the location of the AMP allosteric site. A previous study on *T. brucei* PFK identified important residues involved in AMP binding: Ala-288, Gln-289, Ala-290, Asn-291, Arg-312, Ser-316, Gln-446, Glu-449, and Ile-450 (Fernandes et al., 2020). By superimposing the crystal structure of *T. brucei* PFK with the modeled EhPFK2 and EhPFK3 structures, I was able to identify putative AMP binding residues: Gly-274, Asp-275, Asn-277, Arg-298, Lys-302, Met-431, Ser-434, and Ile-435 for EhPFK2 (Figure 3.11); and Gly-270, Asp-271, Asn-273, Arg-294, Lys-298, Met-427, Ala-430, and Ile-431 for EhPFK3 (Figure 3.12).

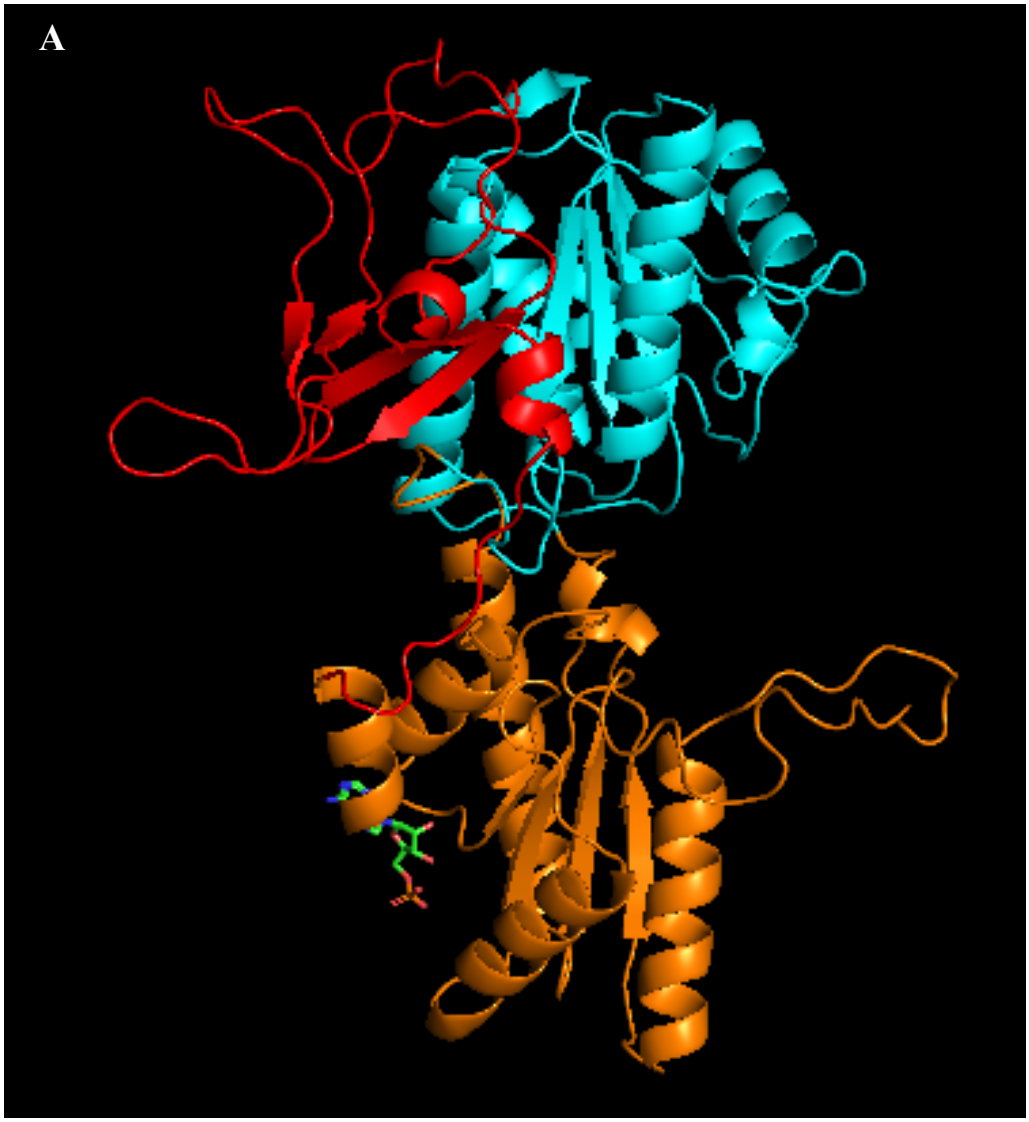
A

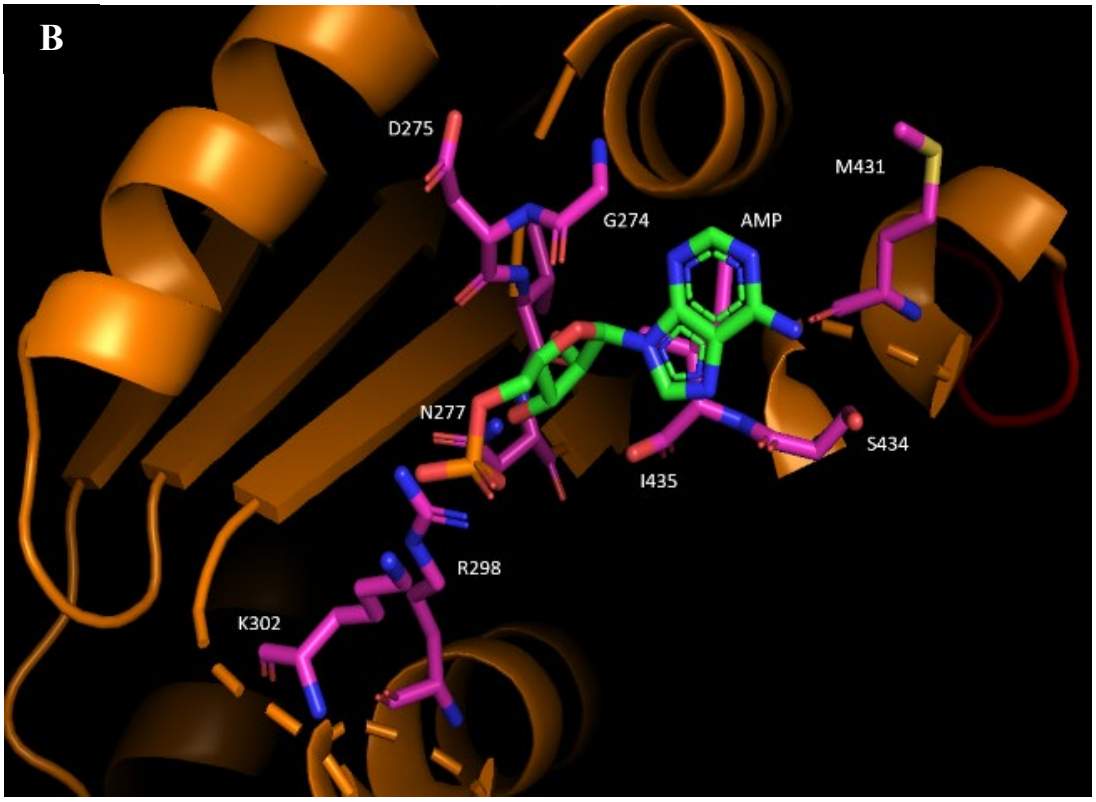

Figure 3.11. Structural model of EhPFK2 with AMP bound. A: Model of EhPFK2 with AMP bound. **B:** Residues that form the AMP binding site. AMP and residues involved in AMP allosteric site are shown in stick model. PyMOL was used to visualize the structure.

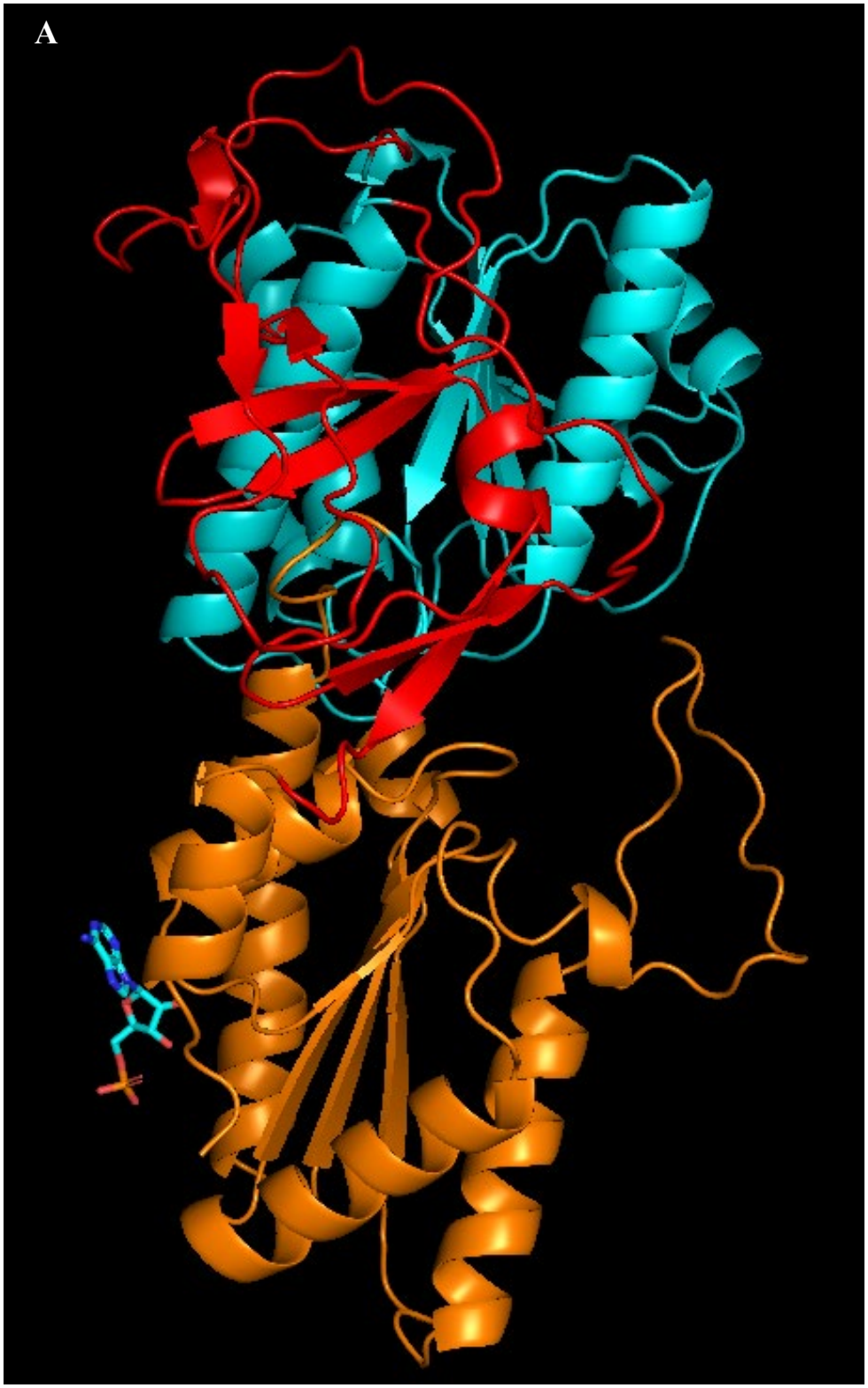
A

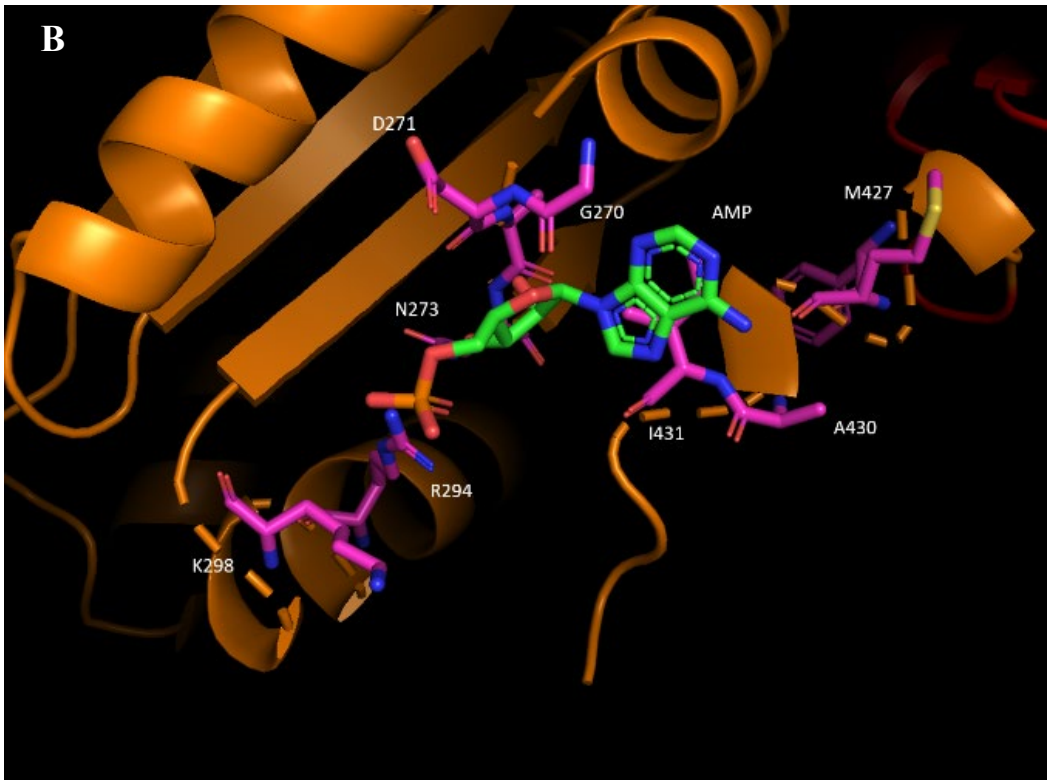

Figure 3.12. Structural model of EhPFK3 with AMP bound. A: Model of EhPFK3 with AMP bound. **B:** Residues that form the AMP binding site. AMP and residues involved in AMP allosteric site are shown in stick model. PyMOL was used to visualize the structure.

PEP binding site in EhPFK2 and EhPFK3 compared to *B. stearothermophilus* PFK

EHPFK2 and EhPFK3 were also modeled on the crystal structure of *B. stearothermophilus* PFK with PEP bound (Mosser et al., 2012; PDB ID:4I4I) to identify the putative PEP allosteric site. A previous study on *B. stearothermophilus* PFK identified Arg-21, Arg-25, and Asp-59 as residues important for PEP binding (Mosser et al., 2012). Superimposing the crystal structure of *B. stearothermophilus* PFK on the

EhPFK2 and EhPFK3 models revealed Arg-104, Met-108, and Asp-146 in EhPFK2 (Figure 3.13) and Arg-100, Leu-104, and Asp-142 in EhPFK3 (Figure 3.14) as part of the putative PEP binding site.

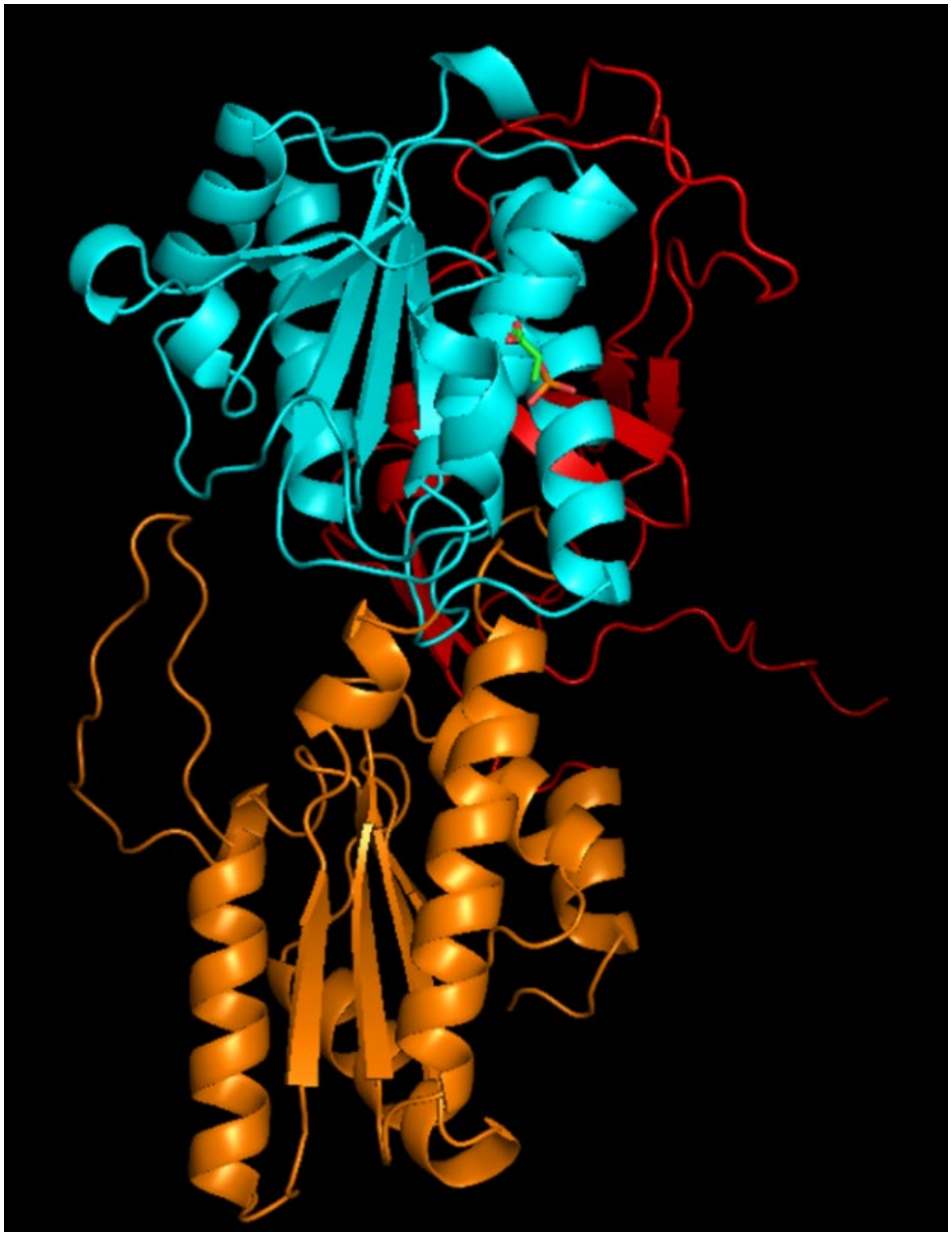

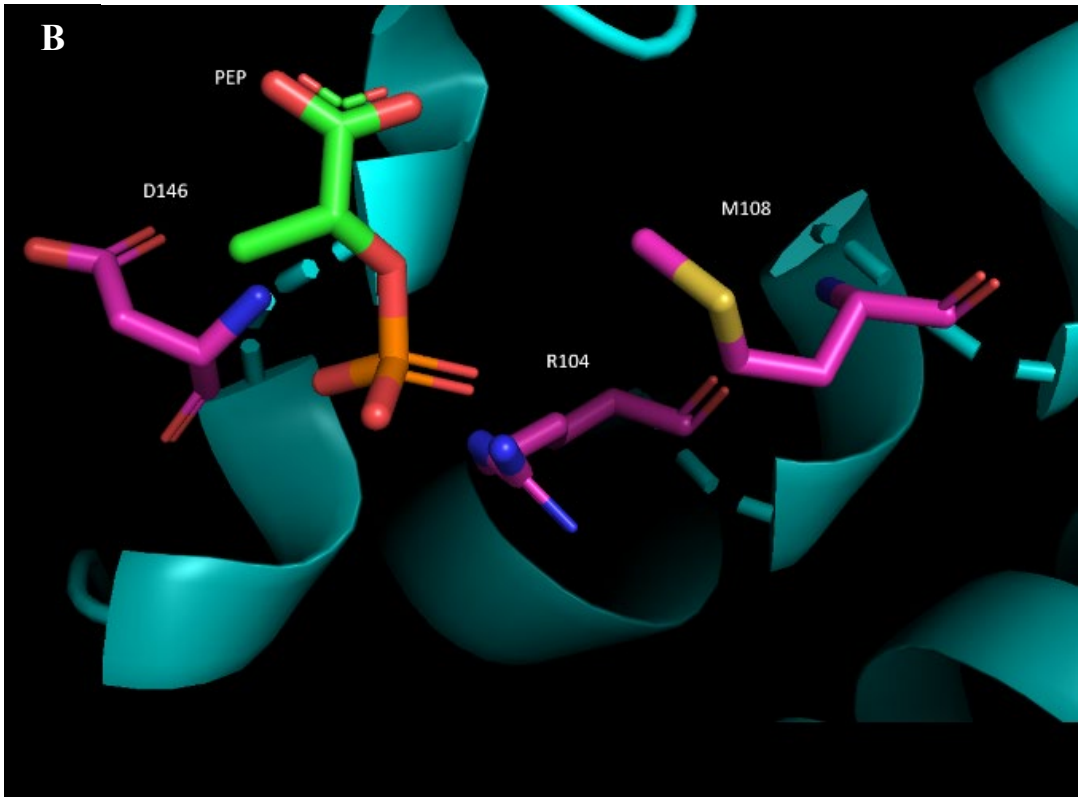

Figure 3.13. Structural model of EhPFK2 with PEP bound. A: Model of EhPFK2 with PEP bound. **B:** Residues that form the PEP binding site. PEP and residues involved in PEP allosteric site are shown in stick model. PyMOL was used to visualize the structure.

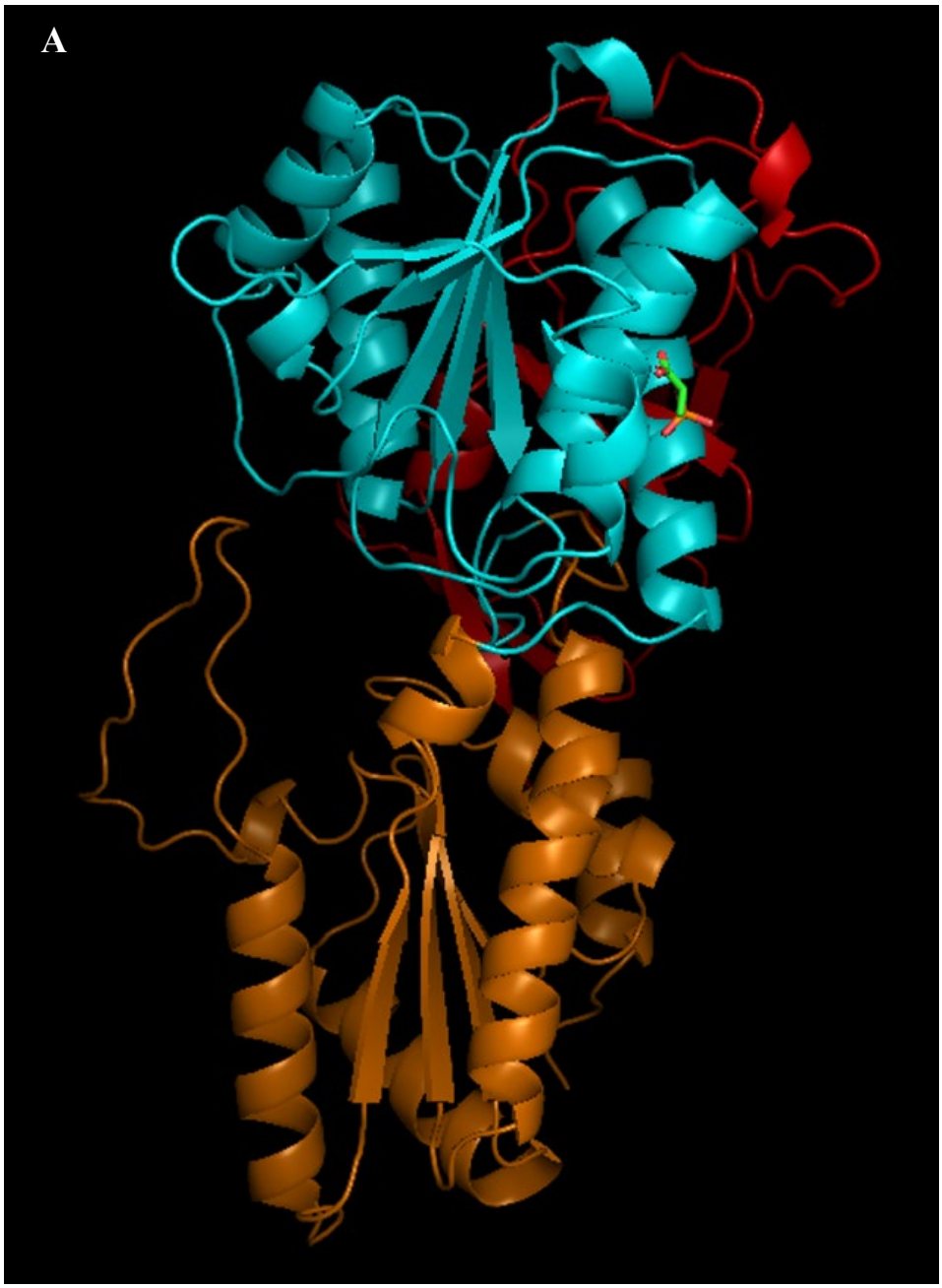
A

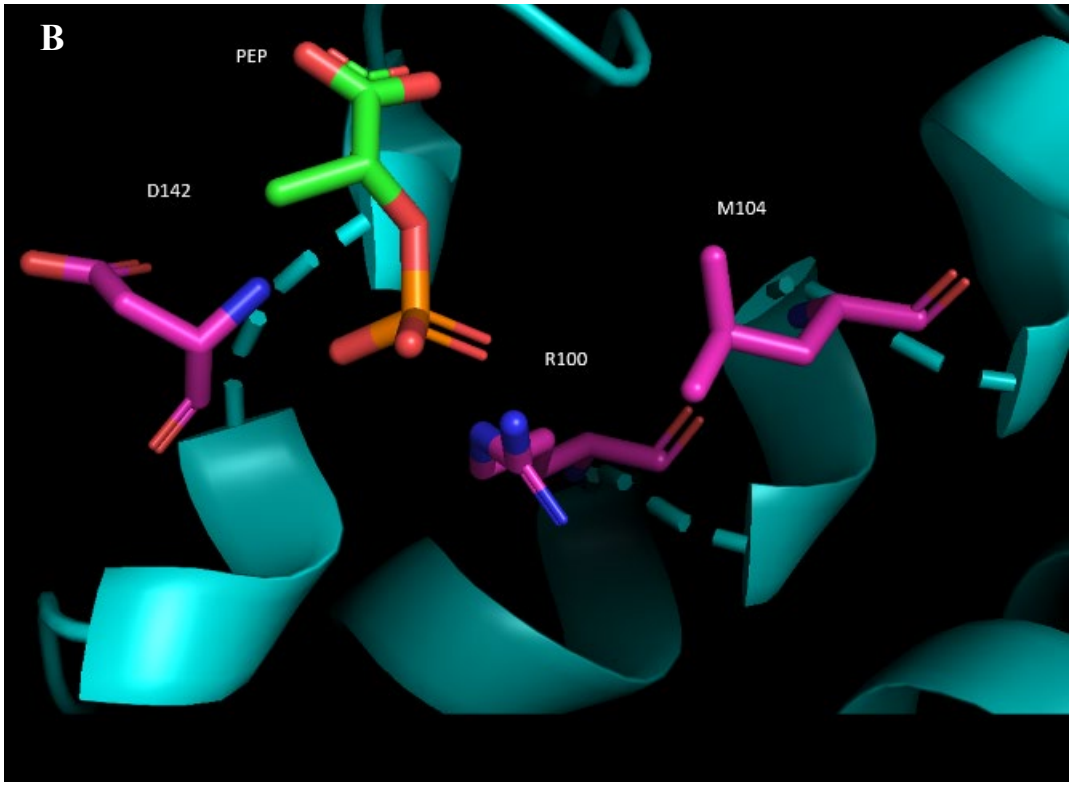

Figure 3.14. Structural model of EhPFK3 with PEP bound. A: Model of EhPFK3 with PEP bound. **B:** Residues that form the PEP binding site. PEP and residues involved in PEP allosteric site are shown in stick model. PyMOL was used to visualize the structure.

A sequence alignment of PFKs from *B. stearothermophilus*, *T. brucei*, and *E. histolytica* show conservation of some amino acid residues involved in AMP and PEP allosteric binding sites (Figure 3.15). For PEP binding site, Arg-21 is conserved across all four PFKs and Asp-59 is conserved between *B. stearothermophilus* and *E. histolytica*. For AMP binding site, Asn-291 and Arg-312 is conserved between *T. brucei* and *E. histolytica*, while Ile-431 is conserved across all four PFKs.

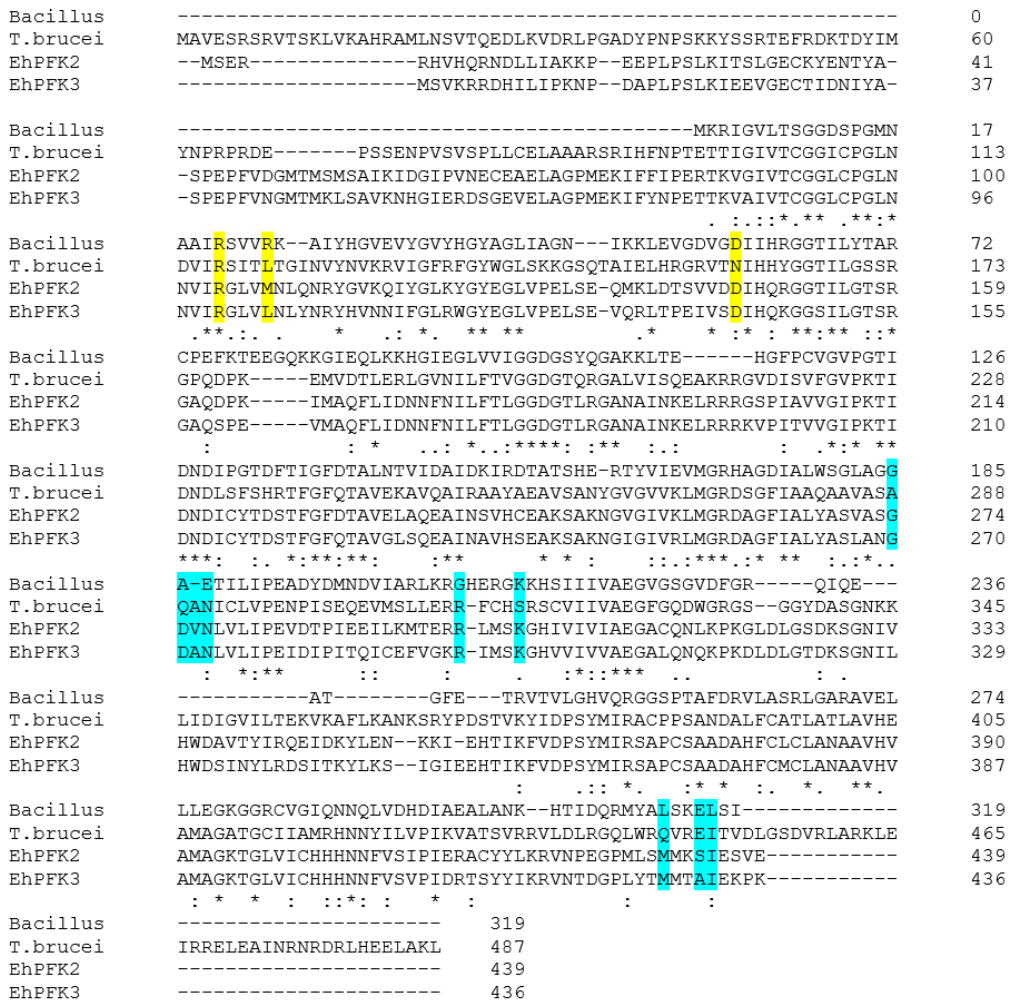

Figure 3.15. Multiple sequence alignment of PFKs in *B. stearothermophilus*, *T. brucei*, and *E. histolytica*. Amino acid sequences of PFKs from *B. stearothermophilus*, *T.brucei*, and *E. histolytica* were aligned using Clustal Omega (https://www.ebi.ac.uk/Tools/msa/clustalo/) using the default parameters. Residues highlighted in yellow are residues involved in PEP binding site. Residues highlighted in cyan are residues involved in AMP binding site. Completely conserved residues are indicated by an asterisk (*), highly conserved residues are indicated by a colon (:), and less highly conserved residues are indicated by a period (.).

Docking experiment show that citrate binds at different allosteric sites in EhPFK2 and EhPFK3

SwissDock (Grosdidier et al., 2011a, 2011b; http://www.swissdock.ch/) was used to predict the binding of citrate to EhPFK2 and EhPFK3 (Figure 3.16). The predicted model was chosen based on lowest -ΔG values, -9.18 kcal/mol for EhPFK2 and -11.13 kcal/mol for EhPFK3. This docking suggests the putative citrate binding site resides between domain A and B for EhPFK2 but within domain B for EhPFK3.

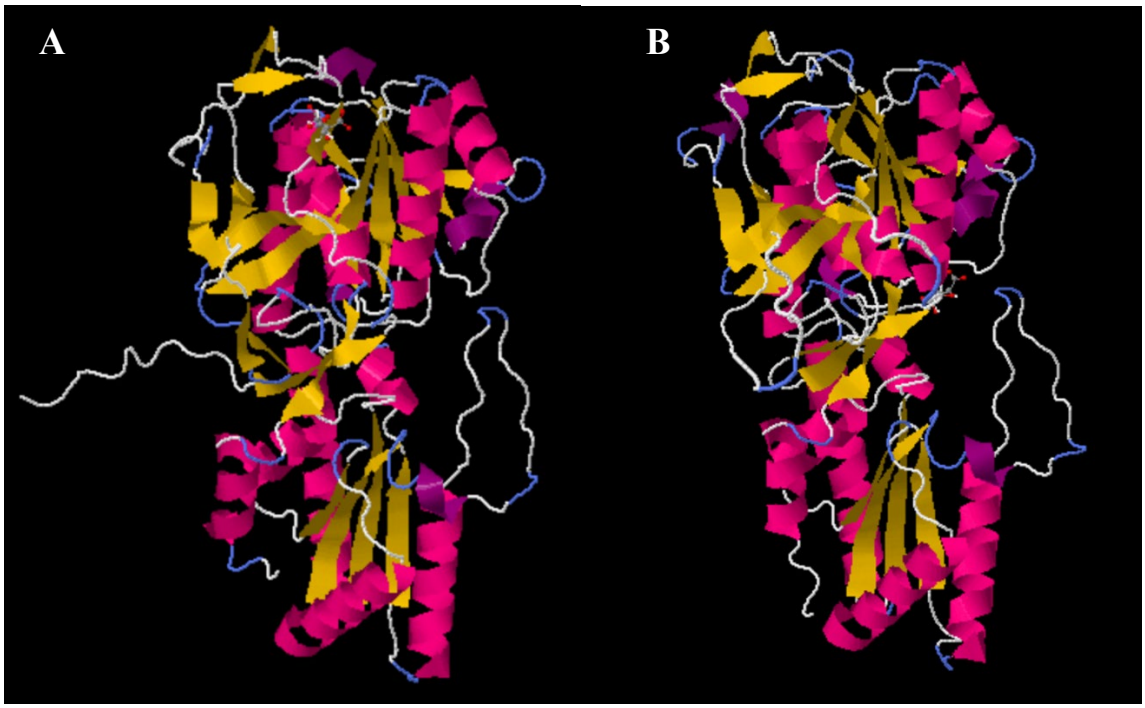

Figure 3.16. Model of EhPFK2 and EhPFK3 with citrate in docking prediction. A: EhPFK2 with citrate. **B:** EhPFK3 with citrate. SwissDock was used to predict docking of protein-ligand complex.

Discussion

PFK is typically a highly regulated enzyme in the glycolytic pathway. Here, I examined the regulation of the ATP-dependent PFKs of *E. histolytica*. I have identified effectors that regulate the activity of EhPFK2 and EhPFK3. AMP, ADP, and CoA activate both enzymes, whereas PEP, citrate, and PP_i inhibit enzymatic activity. The strongest activator was CoA and the strongest inhibitor was PEP. PP_i was also a strong inhibitor for EhPFK3 but inhibited EhPFK2 to a lesser extent. In chapter 2, I demonstrated that EhPFK2 and EhPFK3 are ATP-dependent enzymes that cannot utilize PP_i as a phosphoryl donor. The results here suggest that PP_i plays a role in regulating the activity of EhPFK2 and EhPFK3 instead. It was surprising to see that citrate affected activity of both EhPFK2 and EhPFK3, since *E. histolytica* lacks functional citric acid cycle (Clark et al., 2007). It may be that citrate is still able to bind to *E. histolytica* PFKs due to conservation of residues in the citrate allosteric site even if citrate does not play an important regulatory role in vivo.

To determine the effects of inhibitors on substrate binding, substrate progress curves were generated in the absence and presence of inhibitors and the effects on $K_{0.5}$ and V_{max} were observed. Our results show that inhibitors affect substrate binding in EhPFK2 and EhPFK3 differently. PEP increased the $K_{0.5}$ for F6P for EhPFK2 but exerted its effect on V_{max} for EhPFK3. Likewise, with EhPFK2 PP_i increased the $K_{0.5}$ for ATP but affect V_{max} for EhPFK3.

I examined whether any of the inhibitors share the same binding site by determining if one inhibitor affected the IC_{50} of another inhibitor. If two inhibitors share

the same binding site, then approximately half of the sites should be occupied by the inhibitor that was held constant, so the amount of the varied inhibitor required to reduce the activity by additional 50% should decrease. My results showed that the IC_{50} values for individual inhibitors did not change significantly in the presence of the second inhibitor. This suggests that citrate, PEP, and PP_i do not share any overlapping allosteric binding sites.

Competition experiments were performed to see if an activator could alleviate the effect of an inhibitor. For EhPFK2, CoA and PEP were chosen as they showed the most pronounced effects. When EhPFK2 was exposed simultaneously to CoA and PEP at their EC_{50} concentrations enzymatic activity was reduced by 60% but when both effectors were present at their EC_{max} concentrations, there was an even greater reduction in activity. When the enzyme was preincubated with CoA at its AC_{50} concentration and then PEP was added at its IC_{50} concentration, lower inhibition of activity was observed; however, when this same experiment was performed at EC_{max} concentration for both effectors, an even stronger reduction in activity was observed than when both effectors were present at EC_{50} concentrations without preincubation. What could have happened was that when CoA at half maximal concentration was incubated with EhPFK2 first, it caused a conformational change that prevented some PEP molecules from binding to the allosteric site. But when a greater amount of PEP was present, conformation change induced by CoA was not enough to counteract inhibition by PEP.

Structural models of EhPFK2 and EhPFK3 generated from homology-based Swiss-Model and AlphaFold were very similar to each other. Both models showed three

distinct domains and an inserted loop in domain C that has been shown to be involved in interaction with the active site in *T. brucei* (McNae et al., 2009). By overlapping the predicted structures of EhPFK2 and EhPFK3 with the crystal structure of *T. brucei* PFK with AMP bound, I determined that the putative AMP allosteric binding site is located in domain C, which is where the F6P binding site is located. Likewise, I identified the putative PEP allosteric binding site by overlapping the predicted models with the crystal structure of *B. stearothermophilus* PFK. The PEP allosteric site resides in domain B, which is where the ATP binding site is located.

Since crystal structure of PFK with citrate bound was not available in the protein database, I did docking simulation with SwissDock to identify a putative citrate binding site between domain A and B for EhPFK2 and within domain B for EhPFK3. Although different citrate allosteric binding sites were identified for the two enzymes, the predicted binding sites did not overlap with any of the allosteric binding sites for other effectors that I saw from Swiss-Model and AlphaFold, which supports our finding that inhibitors do not share any overlapping binding sites.

Canonical PFK1 (EC 2.7.1.11) is activated by AMP, ADP, and fructose 2,6-bisphosphate and inhibited by ATP and citrate. EhPFK2 and EhPFK3 were also activated by AMP and ADP. Interconversion of adenosine phosphates is catalyzed by adenylate kinase (Eq.1) (Dzeja and Terzic, 2009). High levels of AMP indicate that cell is starved for energy, so glycolysis must speed up to replenish ATP. Likewise, high levels of ADP indicate that there is high ATP usage, so glycolysis must speed up to convert ADP back to ATP.

[Eq.1] Adenylate kinase ADP + ADP ↔ AMP + ATP

Activation of EhPFK2 and EhPFK3 by CoA was surprising as it is not a typical activator for PFK. CoA is involved in oxidation of pyruvate to acetyl-CoA by Pyruvate: ferredoxin oxidoreductase (PFOR) in the extended glycolytic pathway (Eq.2). High levels of CoA could be a signal that there is accumulation of pyruvate in the cell, so glycolysis must speed up to drive the production of acetate and ethanol. Production of acetate and ethanol would not be possible without conversion of pyruvate to Acetyl-CoA as *E. histolytica* lacks enzymes for fatty acid β-oxidation (Saavedra et al., 2019).

[Eq.2] PFOR Pyruvate + CoA → Acetyl-CoA + CO_2

Fructose 2,6-bisphosphate is a potent activator of canonical PFK as it increases the affinity for F6P and alleviates the inhibition caused by ATP (Yalcin et al., 2009). Production of fructose 2,6-bisphosphate from F6P is catalyzed PFK2 (EC 2.7.1.105), which is different from PFK1. Testing of fructose 2,6-bisphosphate as a regulator of EhPFK2 and EhPFK3 was not done as four putative *PFK* genes from *E. histolytica* all encode PFK that produce fructose 1,6-bisphosphate, not fructose 2,6-bisphosphate.

EhPFK2 and EhPFK3 were both inhibited by citrate, which is also a known inhibitor of canonical PFK1. For other organisms with functional citric acid cycle, glycolysis would slow down under high levels of citrate as it signals that citric acid cycle is backed up. For *E. histolytica*, citrate probably does not play any important role in regulation of these enzymes *in vivo* as it lacks functional citric acid cycle (Clark et al., 2007). Inhibition of EhPFK2 and EhPFK3 by PP_i suggest that PP_i act as a potent inhibitor of these enzymes, instead of as a phosphoryl donor. Inhibition of PFK by PP_i was also

observed in a site-directed mutagenesis study when Chi *et al.* mutated Asp-175 to Gly-175 for EhPFK4. This single mutation switched PP_i-dependent EhPFK4's substrate specificity from PP_i to ATP. This newly created ATP-PFK was inhibited by PP_i (Chi and Kemp, 2000).

Conclusion

I have identified both positive and negative regulators of the ATP-dependent PFKs from *E. histolytica*. Although both EhPFK2 and EhPFK3 are both inhibited by PEP, citrate, and PP_i, the mode of regulation with respect to the substrates differs between the two enzymes. Further investigation is needed to fully understand the physiological role of the ATP-dependent PFKs in *E. histolytica* and their complex regulation.

References

Blangy, D., Buc, H., Monod, J., 1968. Kinetics of the allosteric interactions of phosphofructokinase from Escherichia coli. Journal of Molecular Biology 31, 13–35. https://doi.org/10.1016/0022-2836(68)90051-X

Chi, A., Kemp, R.G., 2000. The Primordial High Energy Compound: ATP or Inorganic Pyrophosphate?*. Journal of Biological Chemistry 275, 35677–35679. https://doi.org/10.1074/jbc.C000581200

Chi, A.S., Deng, Z., Albach, R.A., Kemp, R.G., 2001. The Two Phosphofructokinase Gene Products of Entamoeba histolytica*. Journal of Biological Chemistry 276, 19974–19981. https://doi.org/10.1074/jbc.M011584200

Clark, C.G., Alsmark, U.C.M., Tazreiter, M., Saito-Nakano, Y., Ali, V., Marion, S., Weber, C., Mukherjee, C., Bruchhaus, I., Tannich, E., Leippe, M., Sicheritz-Ponten, T., Foster, P.G., Samuelson, J., Noël, C.J., Hirt, R.P., Embley, T.M., Gilchrist, C.A., Mann, B.J., Singh, U., Ackers, J.P., Bhattacharya, S., Bhattacharya, A., Lohia, A., Guillén, N., Duchêne, M., Nozaki, T., Hall, N., 2007. Structure and Content of the Entamoeba histolytica Genome, in: Advances in Parasitology. Academic Press, pp. 51–190. https://doi.org/10.1016/S0065-308X(07)65002-7

Dzeja, P., Terzic, A., 2009. Adenylate Kinase and AMP Signaling Networks: Metabolic Monitoring, Signal Communication and Body Energy Sensing. Int J Mol Sci 10, 1729–1772. https://doi.org/10.3390/ijms10041729

Evans, P.R., Hudson, P.J., 1979. Structure and control of phosphofructokinase from Bacillus stearothermophilus. Nature 279, 500–504. https://doi.org/10.1038/279500a0

Fernandes, P.M., Kinkead, J., McNae, I.W., Vásquez-Valdivieso, M., Wear, M.A., Michels, P.A.M., Walkinshaw, M.D., 2020. Kinetic and structural studies of Trypanosoma and Leishmania phosphofructokinases show evolutionary divergence and identify AMP as a switch regulating glycolysis versus gluconeogenesis. FEBS J 287, 2847–2861. https://doi.org/10.1111/febs.15177

Grosdidier, A., Zoete, V., Michielin, O., 2011a. SwissDock, a protein-small molecule docking web service based on EADock DSS. Nucleic Acids Res 39, W270–W277. https://doi.org/10.1093/nar/gkr366

Grosdidier, A., Zoete, V., Michielin, O., 2011b. Fast docking using the CHARMM force field with EADock DSS. J Comput Chem 32, 2149–2159. https://doi.org/10.1002/jcc.21797

Jumper, J., Evans, R., Pritzel, A., Green, T., Figurnov, M., Ronneberger, O., Tunyasuvunakool, K., Bates, R., Žídek, A., Potapenko, A., Bridgland, A., Meyer, C., Kohl, S.A.A., Ballard, A.J., Cowie, A., Romera-Paredes, B., Nikolov, S., Jain, R., Adler, J., Back, T., Petersen, S., Reiman, D., Clancy, E., Zielinski, M., Steinegger, M., Pacholska, M., Berghammer, T., Bodenstein, S., Silver, D., Vinyals, O., Senior, A.W., Kavukcuoglu, K., Kohli, P., Hassabis, D., 2021. Highly accurate protein structure prediction with AlphaFold. Nature 596, 583–589. https://doi.org/10.1038/s41586-021-03819-2

Loftus, B., Anderson, I., Davies, R., Alsmark, U.C.M., Samuelson, J., Amedeo, P., Roncaglia, P., Berriman, M., Hirt, R.P., Mann, B.J., Nozaki, T., Suh, B., Pop, M., Duchene, M., Ackers, J., Tannich, E., Leippe, M., Hofer, M., Bruchhaus, I., Willhoeft, U., Bhattacharya, A., Chillingworth, T., Churcher, C., Hance, Z., Harris, B., Harris, D., Jagels, K., Moule, S., Mungall, K., Ormond, D., Squares, R., Whitehead, S., Quail, M.A., Rabbinowitsch, E., Norbertczak, H., Price, C., Wang, Z., Guillén, N., Gilchrist, C., Stroup, S.E., Bhattacharya, S., Lohia, A., Foster, P.G., Sicheritz-Ponten, T., Weber, C., Singh, U., Mukherjee, C., El-Sayed, N.M., Petri, W.A., Clark, C.G., Embley, T.M., Barrell, B., Fraser, C.M., Hall, N., 2005. The genome of the protist parasite Entamoeba histolytica. Nature 433, 865–868. https://doi.org/10.1038/nature03291

McNae, I.W., Martinez-Oyanedel, J., Keillor, J.W., Michels, P.A.M., Fothergill-Gilmore, L.A., Walkinshaw, M.D., 2009. The Crystal Structure of ATP-bound Phosphofructokinase from Trypanosoma brucei Reveals Conformational Transitions Different from those of Other Phosphofructokinases. Journal of Molecular Biology 385, 1519–1533. https://doi.org/10.1016/j.jmb.2008.11.047

Mosser, R., Reddy, M.C.M., Bruning, J.B., Sacchettini, J.C., Reinhart, G.D., 2012. Structure of the Apo Form of Bacillus stearothermophilus Phosphofructokinase. Biochemistry 51, 769–775. https://doi.org/10.1021/bi201548p

Park, J., Gupta, R.S., 2008. Adenosine kinase and ribokinase – the RK family of proteins. Cell. Mol. Life Sci. 65, 2875–2896. https://doi.org/10.1007/s00018-008-8123-1

Reeves, R.E., Serrano, R., South, D.J., 1976. 6-phosphofructokinase (pyrophosphate). Properties of the enzyme from Entamoeba histolytica and its reaction mechanism. Journal of Biological Chemistry 251, 2958–2962. https://doi.org/10.1016/S0021-9258(17)33484-1

Saavedra, E., Encalada, R., Vázquez, C., Olivos-García, A., Michels, P.A.M., Moreno-Sánchez, R., 2019. Control and regulation of the pyrophosphate-dependent glucose metabolism in Entamoeba histolytica. Molecular and Biochemical Parasitology 229, 75–87. https://doi.org/10.1016/j.molbiopara.2019.02.002

Stanley, S.L., 2003. Amoebiasis. The Lancet 361, 1025–1034. https://doi.org/10.1016/S0140-6736(03)12830-9

Varadi, M., Anyango, S., Deshpande, M., Nair, S., Natassia, C., Yordanova, G., Yuan, D., Stroe, O., Wood, G., Laydon, A., Žídek, A., Green, T., Tunyasuvunakool, K., Petersen, S., Jumper, J., Clancy, E., Green, R., Vora, A., Lutfi, M., Figurnov, M., Cowie, A., Hobbs, N., Kohli, P., Kleywegt, G., Birney, E., Hassabis, D., Velankar, S., 2022. AlphaFold Protein Structure Database: massively expanding the structural coverage of protein-sequence space with high-accuracy models. Nucleic Acids Research 50, D439–D444. https://doi.org/10.1093/nar/gkab1061

Waterhouse, A., Bertoni, M., Bienert, S., Studer, G., Tauriello, G., Gumienny, R., Heer, F.T., de Beer, T.A.P., Rempfer, C., Bordoli, L., Lepore, R., Schwede, T., 2018. SWISS-MODEL: homology modelling of protein structures and complexes. Nucleic Acids Res 46, W296–W303. https://doi.org/10.1093/nar/gky427

Wegener, G., Krause, U., 2002. Different modes of activating phosphofructokinase, a key regulatory enzyme of glycolysis, in working vertebrate muscle. Biochem Soc Trans 30, 264–270.

World Health Organization, 2015. WHO estimates of the global burden of foodborne diseases: foodborne disease burden epidemiology reference group 2007-2015. World Health Organization, Geneva.

Yalcin, A., Telang, S., Clem, B., Chesney, J., 2009. Regulation of glucose metabolism by 6-phosphofructo-2-kinase/fructose-2,6-bisphosphatases in cancer. Experimental and Molecular Pathology, Special Issue: Structural Biology 86, 174–179. https://doi.org/10.1016/j.yexmp.2009.01.003

CHAPTER IV

CONCLUSIONS AND FUTURE DIRECTIONS

Biochemical and kinetic characterization of phosphofructokinases from *E. histolytica*

This investigation into the roles of PFK in glycolysis began with the observation that there are four *PFK* genes, three of which were thought to encode for ATP-dependent enzymes, in the genome of *E. histolytica*. This was interesting as *E. histolytica* is thought to rely on a modified PP_i-dependent glycolysis as its primary energy pathway as it lacks many metabolic pathways, including the citric acid cycle and oxidative phosphorylation (Clark et al., 2007; Loftus et al., 2005). EhPFK2 has never been characterized before and although EhPFK3 has been partially characterized previously, I investigated both enzymes to allow a direct comparison of their kinetic characteristics including regulation by allosteric effectors. My results show that both EhPFK2 and EhPFK3 are ATP-dependent and PP_i acts as a potent inhibitor of the enzymes instead of as a phosphoryl donor. Although these enzymes share similar sequences, they displayed different kinetic and regulatory properties, such as difference in substrate affinities and the ways in which inhibitors affect binding of the substrates.

I hypothesize that PFK switching could be happening in *E. histolytica*, where different PFKs are utilized to fit the metabolic needs. Isozymes displaying different expression profiles as well as playing different roles have been demonstrated in other organisms. RNAseq study in *E. invadens* showed that the PP_i-*PFK* gene was

downregulated during encystation, while one of the ATP-*PFK* genes was upregulated during excystation (Ehrenkaufer et al., 2013).

A proteomics study in *Saccharomyces cerevisiae* revealed that isozymes of several metabolic enzymes, such as those involved in glycolysis and amino acid biosynthesis, were both up and down regulated under stress conditions (Zhang et al., 2018). They discovered that enolase1 played a role in promotion of gluconeogenesis under low glucose condition, while enolase2 did not (Zhang et al., 2018). A study on mammalian hexokinase showed that Type I isozyme functions in a catabolic role to generate energy, while Type II isozyme functions in an anabolic role to provide glucose 6-phosphate for glycogen synthesis and pentose phosphate pathway (Wilson, 2003).

In *E. histolytica*, PFK switching might occur in conditions that have a low level of PP_i. The only known sources of PP_i are from conversion of PEP to oxaloacetate and synthesis of glycogen, protein, and nucleic acids (Reeves et al., 1976). Acetate kinase from *E. histolytica* has also been proposed to be a contributor of PP_i, but a recent study has demonstrated that it functions to restore NADH imbalance in the extended glycolytic pathway (Dang et al., 2022; Reeves et al., 1976). If PP_i is not readily available, PP_i-PFK might be downregulated and ATP-PFK might be upregulated to continue the glycolytic pathway. EhPFK2 is likely to be the main player involved in such a PFK switching mechanism as it was shown to be a more efficient enzyme compared to EhPFK3, but it is possible that other ATP-PFKs are also involved. Our characterization of the enzymes provides a foundation for determining the functional differences between PFK enzymes.

Future Directions

In vivo study of these enzymes should be carried out to better understand their physiological roles. Generation of PFK RNAi strains and growing them under different conditions, such as normal glucose, low glucose, and high glucose media, would help in elucidating the physiological role of these enzymes and determining whether all isozymes are required for cell growth. Their role in encystation and excystation should also be investigated as transcriptomics study on *E. invadens* PFK suggest involvement of different PFKs in the life cycle (Ehrenkaufer et al., 2013)

Site-directed mutagenesis study on ATP-dependent PFKs might give useful insight on properties of these enzymes as well. A previous study on *E. histolytica* PP_i-dependent PFK showed that a single mutation changed its preference from PP_i to ATP for phosphoryl donor (Chi and Kemp, 2000). Furthermore, formation of a new binding site was demonstrated by the mutants being able to utilize other nucleoside triphosphate as phosphoryl donors (Chi and Kemp, 2000). It would be interesting to see if mutating Gly to Asp would change substrate preference from ATP to PP_i for EhPFK2 and EhPFK3. If these mutated enzymes are able to utilize PP_i as a substrate, then kinetic parameters and regulatory properties can be measured to compare it to EhPFK4 that is PP_i-dependent.

Resolving the structure of EhPFKs through various techniques, such as X-ray crystallography or cryo-electron microscopy, would be beneficial in understanding protein-ligand interactions. I predicted the structures of EhPFK2 and EhPFK3 through AlphaFold, however AlphaFold has several limitations, such as inability to predicts structures with ligands and cofactors (Bertoline et al., 2023). As a result, I had to rely on

superimposition of the resolved crystal structures of protein-ligand complex with the predicted models of EhPFK2 and EhPFK3 to deduce the location of allosteric binding sites. However, superimposition could not be done for all the effectors as not all protein-ligand complex were available in the protein database. Resolving the structure of EhPFK2 and EhPFK3 with ligands bound would allow for direct comparison with experimental data to see if effectors do bind at different allosteric sites and gain insight as to what fundamental differences exists between EhPFK2 and EhPFK3 active site that allows for both one ring and two ring structures for EhPFK2, but only two ring structures for EhPFK3.

References

Bertoline, L.M.F., Lima, A.N., Krieger, J.E., Teixeira, S.K., 2023. Before and after AlphaFold2: An overview of protein structure prediction. Front Bioinform 3, 1120370. https://doi.org/10.3389/fbinf.2023.1120370

Chi, A., Kemp, R.G., 2000. The Primordial High Energy Compound: ATP or Inorganic Pyrophosphate?*. Journal of Biological Chemistry 275, 35677–35679. https://doi.org/10.1074/jbc.C000581200

Clark, C.G., Alsmark, U.C.M., Tazreiter, M., Saito-Nakano, Y., Ali, V., Marion, S., Weber, C., Mukherjee, C., Bruchhaus, I., Tannich, E., Leippe, M., Sicheritz-Ponten, T., Foster, P.G., Samuelson, J., Noël, C.J., Hirt, R.P., Embley, T.M., Gilchrist, C.A., Mann, B.J., Singh, U., Ackers, J.P., Bhattacharya, S., Bhattacharya, A., Lohia, A., Guillén, N., Duchêne, M., Nozaki, T., Hall, N., 2007. Structure and Content of the Entamoeba histolytica Genome, in: Advances in Parasitology. Academic Press, pp. 51–190. https://doi.org/10.1016/S0065-308X(07)65002-7

Dang, T., Angel, M., Cho, J., Nguyen, D., Ingram-Smith, C., 2022. The Role of Acetate Kinase in the Human Parasite Entamoeba histolytica. Parasitologia 2, 147–159. https://doi.org/10.3390/parasitologia2020014

Ehrenkaufer, G.M., Weedall, G.D., Williams, D., Lorenzi, H.A., Caler, E., Hall, N., Singh, U., 2013. The genome and transcriptome of the enteric parasite Entamoeba invadens, a model for encystation. Genome Biol 14, R77. https://doi.org/10.1186/gb-2013-14-7-r77

Loftus, B., Anderson, I., Davies, R., Alsmark, U.C.M., Samuelson, J., Amedeo, P., Roncaglia, P., Berriman, M., Hirt, R.P., Mann, B.J., Nozaki, T., Suh, B., Pop, M., Duchene, M., Ackers, J., Tannich, E., Leippe, M., Hofer, M., Bruchhaus, I., Willhoeft, U., Bhattacharya, A., Chillingworth, T., Churcher, C., Hance, Z., Harris, B., Harris, D., Jagels, K., Moule, S., Mungall, K., Ormond, D., Squares, R., Whitehead, S., Quail, M.A., Rabbinowitsch, E., Norbertczak, H., Price, C., Wang, Z., Guillén, N., Gilchrist, C., Stroup, S.E., Bhattacharya, S., Lohia, A., Foster, P.G., Sicheritz-Ponten, T., Weber, C., Singh, U., Mukherjee, C., El-Sayed, N.M., Petri, W.A., Clark, C.G., Embley, T.M., Barrell, B., Fraser, C.M., Hall, N., 2005. The genome of the protist parasite Entamoeba histolytica. Nature 433, 865–868. https://doi.org/10.1038/nature03291

Reeves, R.E., Serrano, R., South, D.J., 1976. 6-phosphofructokinase (pyrophosphate). Properties of the enzyme from Entamoeba histolytica and its reaction mechanism. Journal of Biological Chemistry 251, 2958–2962. https://doi.org/10.1016/S0021-9258(17)33484-1

Wilson, J.E., 2003. Isozymes of mammalian hexokinase: structure, subcellular localization and metabolic function. Journal of Experimental Biology 206, 2049–2057. https://doi.org/10.1242/jeb.00241

Zhang, Y., Lin, Z., Wang, M., Lin, H., 2018. Selective usage of isozymes for stress response. ACS Chem Biol 13, 3059–3064. https://doi.org/10.1021/acschembio.8b00767